UNIVERSITA' VITA-SALUTE SAN RAFFAELE

CORSO DI DOTTORATO DI RICERCA INTERNAZIONALE IN MEDICINA MOLECOLARE

Curriculum in Basic and Applied Biology and Immunology

Cutting-edge transcriptomics to identify leukemia-intrinsic and -extrinsic correlates of defined patterns of immune escape and post-transplantation relapse

DoS: Luca Aldo Edoardo Vago

Second Supervisor: Saar Gill

Tesi di DOTTORATO di RICERCA di Pier Edoardo Rovatti

matr. 017133

Ciclo di dottorato XXXIV°

SSD MED/15

Anno Accademico 2022/2023

RELEASE OF PHD THESIS

Il sottoscritto	Pier Edoardo Rovatti
Matricola	017133
Nato a	Verona
Il	02/08/1994

autore della tesi di Dottorato di ricerca dal titolo

Cutting-edge transcriptomics to identify leukemia-intrinsic and -extrinsic correlates of defined patterns of immune escape and post-transplantation relapse

- X AUTORIZZA la Consultazione della tesi / AUTHORIZE *the public release of the thesis*

- NON AUTORIZZA la Consultazione della tesi per …… mesi /DO NOT AUTHORIZE *the public release of the thesis for …… months*

  a partire dalla data di conseguimento del titolo e precisamente */ from the PhD thesis date, specifically*

  Dal / *from* ……/……/…… Al / *to* ……/……/…… Poiché /*because*:

  □ l'intera ricerca o parti di essa sono potenzialmente soggette a brevettabilità/ *The whole project or parts of it may be the subject of a patent application;*

  □ ci sono parti di tesi che sono già state sottoposte a un editore o sono in attesa di pubblicazione/ *Parts of the thesis have been or are being submitted to a publisher or are in the press;*

  □ la tesi è finanziata da enti esterni che vantano dei diritti su di esse e sulla loro pubblicazione/ *the thesis project is financed by external bodies that have rights over it and its publication.*

E' fatto divieto di riprodurre, in tutto o in parte, quanto in essa contenuto */ reproduction of the thesis in whole or in part is forbidden*

Data 02/11/2023 Firma /Signature ……

DECLARATION

This thesis has been:

- composed by myself and has not been used in any previous application for a degree. Throughout the text I use both 'I' and 'We' interchangeably.
- has been written according to the editing guidelines approved by the University.

Permission to use images and other material covered by copyright has been sought and obtained. For the following image/s (specify), it was not possible to obtain permission and is/are therefore included in thesis under the "fair use" exception (Italian legislative Decree no. 68/2003).

All the results presented here were obtained by myself.

All sources of information are acknowledged by means of reference.

ACKNOWLEDGEMENTS

Abstract

Allo-HCT provides a remarkable demonstration that immunotherapies can cure hematological malignancies, including AML. However, leukemic cells can enact multiple strategies to evade immune recognition and outgrow in clinical relapse, such as reducing antigen presentation or dampening effector responses through the expression of inhibitory checkpoint molecules. Increasing evidence suggests that leukemic cells actually weave a much broader net of interactions, involving several other immune cell types within the bone marrow microenvironment. Still, how this complex crosstalk between malignant cells and the bone marrow niche may shape the features of leukemia post-transplant relapse remains unknown.

By exploiting the high resolution provided by scRNA-seq, we provide a detailed insight of the human bone marrow immune microenvironment and the changes that arise following allo-HCT, both when disease reemergence is prevented, and when it occurs. Using cryopreserved BM aspirates, we profiled samples from N=25 adult AML patients at the time of disease relapse; N=5 post-transplant patients in complete remission (CR), each tested at two different timepoints (+90 and +365 days) and N=6 healthy controls (HC). ScRNA-seq allowed us to recapitulate known leukemia-intrinsic features of each relapse modality, such as HLA loss, down-regulation of HLA class II molecules and upregulation of inhibitory T cell ligands. Moreover, by focusing on malignant cells, we could highlight novel features of relapse. HLA loss relapses exhibited a more immature profile, hinting that the hematopoietic cell of origin impacts on the mechanism of post-transplantation relapse. Leukemic cells also featured a high inflammation-associated gene score (iScore), as also evident in non-malignant HSPCs from relapsed patients compared to HC and CR.

Focusing on specific BM immune compartments, we annotated a rare subset of immature $CD56^{bright}$ NK cells characterized by higher expression of IFN-related genes and NK exhaustion markers, which were enriched in patients with upregulation of T cell inhibitory ligands compared to other relapses, thus suggesting a shared mechanism of dysfunction signature between T and NK cell that may favor leukemia immune evasion. Further, we describe functional and compositional reshaping of the T cell compartment. In conclusion, we generated a comprehensive atlas of the BM immune microenvironment in AML post-transplantation relapses, showing that inflammation shapes immune subset composition and transcriptional profile in the BM, and that leukemia mechanisms of immune evasion are influenced by the surrounding milieu.

Table of Contents

ACRONYMS AND ABBREVIATIONS

aGvHd Acute graft versus host disease
Allo-HCT Allogeneic Hematopoietic Cell Transplantation
AML Acute Myeloid Leukemia
BCR B cell receptor
BM Bone Marrow
BMMCs Bone Marrow Mononuclear Cells
CBU Cord Blood Unit
cGvHD Chronic graft versus host disease
CM Central memory
CN-LOH Copy neutral loss of heterozygosity
CNV Copy number variations
CPM Counts Per Million
CR Complete Remission
CTL Cytotoxic T lymphocyte
DAMP Damage-associated molecular pattern molecule
DC Dendritic cell
DEG Differentially expressed gene
DLI Donor lymphocyte infusion
EM Effector memory
EMRA Terminally differentiated effector memory
Ery Erythroid progenitor
Ex Exhausted
FBS Fetal Bovine Serum
GEX Gene Expression (only for Chromium technologies)
GMP Granulocyte-monocyte progenitor
GO Gene ontology
GSEA Gene set enrichment analysis
GvHD Graft versus host disease
GvL Graft versus leukemia
HC Healthy Control
HLA Human Leukocyte Antigen
HS(P)C Hematopoietic Stem (and Progenitor) Cell
IFN Interferon
KIR Killer cell immunoglobulin receptor
LAIP Leukemia-associated Immune Phenotype

LSC Leukemic stem cell
LymP Lymphoid progenitor
mAb Monoclonal antibody
MAIT Mucosal-associated invariant T
MEP Megakaryocytic-erythroid progenitor
MHC Major Histocompatibility Complex
Mo month
Mono Monocytes
MPP Multipotent progenitor
mRNA Messenger RNA
NK Natural killer
PB Peripheral Blood
PBS Phosphate-Buffered Saline
PCA Principal Component Analysis
pDC Plasmacytoid dendritic cell
QC Quality control
scRNA-seq Single-cell RNA sequencing
TCR T cell receptor
Treg Regulatory T cell
(T)ME (Tumor) Microenvironment
TRM Transplant-related mortality
UMI Unique Molecular Identifier
UMAP Uniform Manifold Approximation and Projection
Y year

LIST OF FIGURES AND TABLES

1 Introduction

1.1 Hematopoietic cell transplantation

1.1.1 Definition

Hematopoietic cell transplantation (HCT) is a therapeutic treatment that aims at the restoring of the hematopoietic and immune system in patients whose bone marrow has previously been depleted by the use of chemotherapy and/or radiotherapy. Restoration of bone marrow function can be accomplished through the collection, and subsequent infusion, of hematopoietic stem and progenitor cells (HSPCs) either from the patient themselves (referred to as autologous HCT) or from a healthy donor (referred to as allogeneic HCT). Typically, HSPCs can be harvested from the bone marrow (BM), peripheral blood (PB), and cord blood units (CBU). These cells possess the ability to differentiate into all functional blood cells while retaining their self-renewal capability, ultimately aiming to rejuvenate the patient's hematopoietic and immune systems.

Since its first application in the 1960s, significant advancements in the HCT technique have contributed to make it a highly effective and reliable treatment option for many hematological malignancies, such as acute myeloid leukemia, lymphomas, and multiple myeloma. Furthermore, bone marrow transplantation has emerged as an efficacious therapeutic approach for the management of various pathological disorders outside onco-hematology. These encompass both inherited, such as hemoglobinopathies, inborn errors of metabolism, and congenital aplasia, as well as acquired conditions, including autoimmune diseases and solid tumors (Duarte et al. 2019). **(Figure 1)**

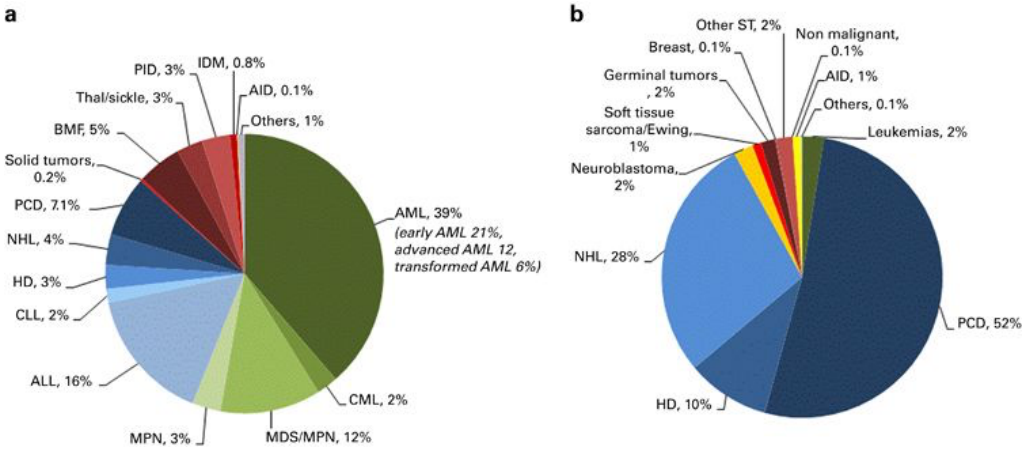

Figure 1. HCT indications.

Relative proportion of indications in Europe in 2015 for allogeneic (left) and autologous HCT (right) (Passweg et al. 2017).

In the context of autologous treatment, stem cells of the patient are collected and preserved prior to any myeloablative therapy, and later reintroduced into the patient's body with the aim of restoring hematopoietic function. This enables the use of chemotherapeutic agents with high toxicity levels, which would otherwise result in persistent aplasia of the bone marrow. Hence, autologous HCT is most effective when there is a direct correlation between chemotherapy dose and anti-tumor response, and when the major dose-limiting toxicity of the treatment is represented by myelosuppression. Autologous HCT, for its biological properties, offers the advantage of avoiding any immunological activation of the graft against healthy tissues, resulting in an overall good tolerance of the procedure (Du et al. 2021), (Copelan 2006).

However, within the realm of hematological malignancies, there exists a significant possibility of acquiring, during the process of HSPCs collection, malignant cells, and reintroducing them would ultimately contribute to disease reoccurrence.

In contrast, allo-HCT, by making use of donor cells coming from a family-related or an unrelated donor, adds to the therapeutic effect of the chemotherapeutic conditioning regimen, the active role played by the donor’s immune system in eradicating the disease (Copelan 2006). In fact, genetic differences between donor and recipient are responsible for the graft activation towards leukemia (GvL). Nonetheless, allo-HCT presents numerous challenges. First, a suitable donor might not always be available. Second, despite the beneficial effect of GvL, host-donor genetic disparities are also bearer of the most toxic side effect of the transplant, the graft-versus-host disease (GvHD), where host’s tissues are recognized as non-self, and attacked by the donor’s immune cells (Klepin, Rao, and Pardee 2014). Hence, because morbidity and mortality are more frequently associated to this process, patient’s health status at the time of transplant can heavily influence the transplant outcome and overall survival, independently of the underlying disease (Sorror 2005), (Michelis et al. 2015), (Hemmati et al. 2011).

1.1.2 Stem cell source

The term "stem cells" is frequently employed to describe a population of cells that possess the ability to remain in an undifferentiated state while simultaneously exhibiting the capacity for self-renewal and the potential to differentiate into a diverse array of specialized cell types, thereby contributing to the formation of a functional progeny. Thus, the fundamental attributes of hematopoietic stem cells (HSCs) reside in their inherent capacity for self-renewal and their potential to undergo

differentiation into all mature blood lineages (Bryder, Rossi, and Weissman 2006). HSCs can be collected for transplant from different sources: bone marrow (BM), peripheral blood (PB) and cord blood (CB).

The physiological origin of bone marrow renders it a highly desirable source for HSCs. Due to its inherent inclusion of stromal cells, which offer molecular-level support to the cells and facilitate optimal engraftment, BM represents the most "natural" source for HSCs. Moreover, the favorable ratio between stem and T cells contributes to a diminished susceptibility to acute and chronic GvHD (Pruszczyk et al. 2017). The harvesting process, however, is performed through an invasive procedure consisting in the aspiration of the marrow from both the posterior superior iliac crests, thus requiring either a general or an epidural anesthesia.

Mobilization of HSCs to the peripheral blood, on the other hand, has emerged as a progressively employed alternative to BM harvesting (**Figure 2**).

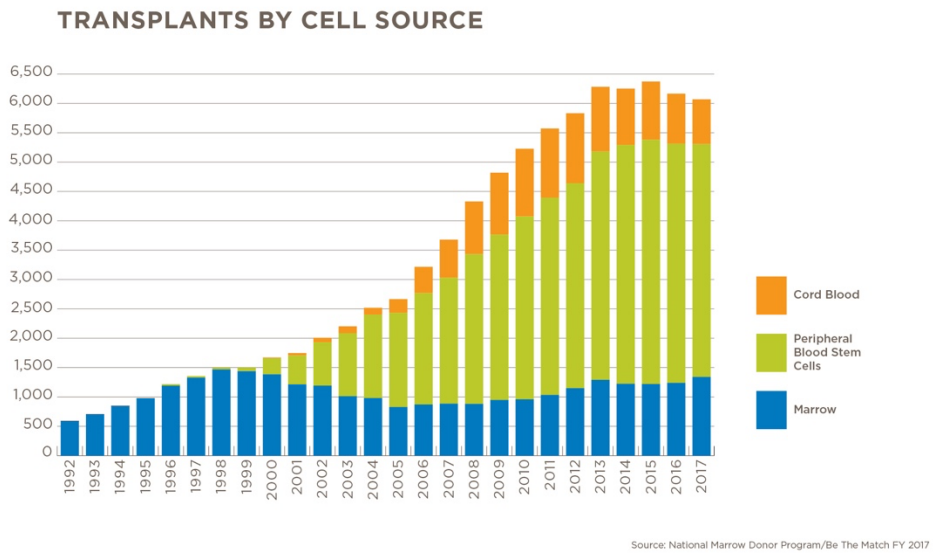

Figure 2. Number of transplants from unrelated donor.

Colored by cell source (1992-2017). Adapted from *https://bethematchclinical.org/.*

Indeed, transplantation of peripheral blood stem cells (PBSCs) represents a notably convenient approach from the perspective of the donor, as the leukapheresis process is a non-invasive procedure characterized by a high level of safety, similar to that of a simple blood draw. The presence of HSCs within the PB is a rare occurrence, as they usually make up for less than 0.1% of all circulating nucleated cells. The mobilization, and subsequent release into the circulatory system, of these HSCs from their specialized bone marrow microenvironment is obtained through the utilization of growth factors, such as G-CSF, and/or other pharmacological agents,

such as Plerixafor (a small molecule CXCR4 antagonist, which impedes the interaction between CXCR4 and SDF-1a9), which increase the quantity of HSCs present within the peripheral blood from 10 to 100-fold. Importantly, it is widely recognized that the use of G-CSF or other mobilizing agents is not linked to an increased risk of cancer development (Shaw et al. 2015). However, the acquisition of peripheral blood inherently entails the transfer of greater quantities of T cells in comparison to BM, thereby increasing the susceptibility to GvHD (Cutler et al. 2001), with no statistically significant difference in terms of overall survival compared to BM harvesting (Claudio Anasetti et al. 2012), (Cheuk 2013).

Umbilical cord blood is a relatively novel source of HSCs. Thanks to the establishment of cord blood banks where CBUs are stored and cryopreserved, it has become a valid alternative for patients that lack other donors. Moreover, CBUs present a decreased risk of GvHD, due to T cells being mostly immunologically naïve. Thanks to this, CBUs are also more permissive when it comes to HLA incompatibilities. On the other hand, CBUs usage is strongly limited by the reduced probability of engraftment, delayed immune reconstitution, unavailability of the donor for additional donations, and a generally low volume of blood available per unit, which often limits its usage for low weight hosts (<50kg), like children.

1.1.3 Choice of the donor and HLA matching

Donor choice and its compatibility with the host represents one of the major players in determining the outcome of allo-HCT. In fact, not only it affects BM repopulation, but it also has a crucial role in the two most frequent causes of transplant failure: GvHD and the underlying disease reoccurrence.

Donor compatibility is defined mostly by the alleles matching on the Major Histocompatibility Complex (MHC), a key part of the immune system controlled by genes located on the short arm of chromosome 6 (6p21.31). HLA stands for the human MHC and encodes extremely polymorphic cell surface molecules. This variability is explained by its fundamental immunological role: HLA molecules present antigenic peptides to T cells, educating the T cell to discriminate between "non-self" and "self" antigens, with subsequent elimination of cells expressing foreign peptides. In the context of transplant, where two foreign immune systems must coexist, being able to mitigate HLA natural functions is crucial.

According to the structure and function of proteins encoded, the HLA system is divided in three classes: class I, II, and III. While MHC class III includes genes without completely clarified functions, class I and II molecules are central in T cell

activation, which is achieved through recognition of antigens localized in the peptide-binding groove.

Class I molecules, composed of HLA-A HLA-B and HLA-C (HLA-classical antigens) and HLA-E, HLA-F and HLA-G (non classical antigens), are ubiquitously expressed by nucleate cells, and exploit their function by binding peptides mostly derived from processing of endogenous proteins. Proteins in the cytosol or nucleus of the cell are degraded by the proteasome and loaded on the newly assembled MHC class I heterodimer into the endoplasmic reticulum (ER) lumen. The peptide-MHC complexes are then exposed on the cell membrane through the Golgi, thus permitting the recognition of infected and/or defective cells (Klein and Sato 2000). Class I molecules are recognized by CD8 T cells through their T cell receptor (TCR) and by killer-like immunoglobulin receptors (KIRs) on the surface of NK cells. More in particular, while T cells recognize the peptide-HLA complex (HLA restriction), NK cells are believed to recognize the loss of expression of HLA class I molecules (missing self).

Class II molecules, coding for HLA-DP, HLA-DQ and HLA-DR proteins, are expressed mostly by antigen presenting cells (APCs) such as dendritic cells, macrophages, and B cells. However, in response to concurring conditions such as infections or inflammation, they can be expressed also in non-immune cells (Neefjes et al. 2011). CD4 T cells are the main "recipients" of class II processed peptides, and, in this case, the presented peptides are a part of the exogenous milieu, hence deriving from proteins degraded by the endocytic pathway. Although MHC class I and II are described as two separated entities, links between the two pathways such as cross-presentation allow DCs to expose extracellular peptides on MHC class I molecules and therefore enable the activation of CD8 T cells also against external microorganisms and tumors (Kurts, Robinson, and Knolle 2010). Likewise, autophagy among others have been shown to permit the presentation of intracellular peptides on MHC class II molecules (Neefjes et al. 2011).

As said before, the most unique characteristic of the MHC lies in the polymorphism of its genes. Allele variants mostly determine differences in the anchor residues to which the peptides dock, creating a unique bond between each binding groove and the antigen presented. Despite the high variability in the HLA system, all HLA genes, being encoded in a very small region of the DNA, are generally inherited together, due to linkage disequilibrium. Thus, one entire HLA locus is inherited from each parent determining the individual's haplotype and allowing the identification of compatible donors. Following a mendelian inheritance, two siblings have a 25% probability to be HLA identical, a 50% chance of being HLA haploidentical and a 25% chance to don't share any haplotype.

HLA incompatibilities, in the context of allogeneic HCT, are surely the main immunological barriers to transplant success. We can distinguish HLA matched transplants, where donor and recipient share identical haplotypes, or HLA mismatched transplants, among which we can find haploidentical transplantation, where donor and recipient only share one haplotype.

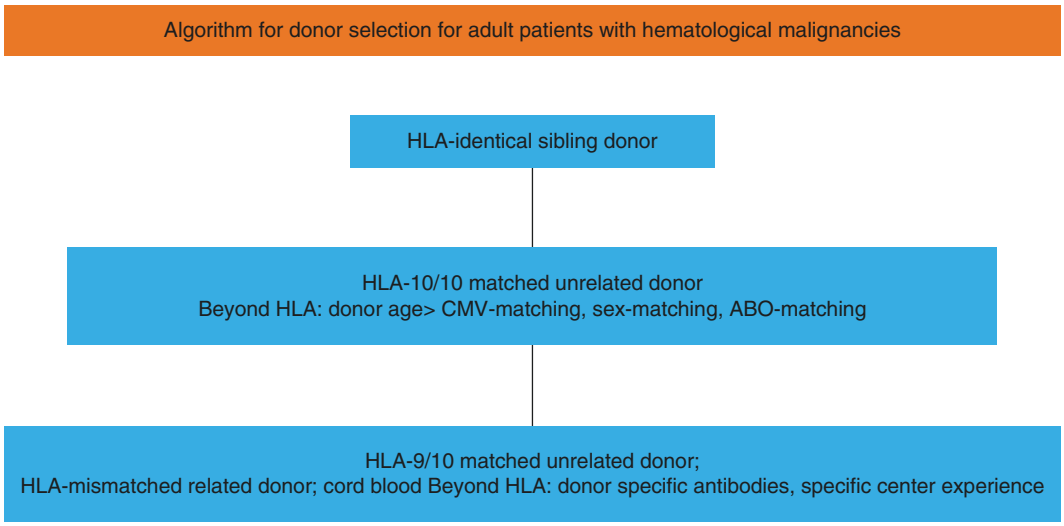

Figure 3. Algorithm for donor selection.

Adapted from EBMT Handbook, Enric Carreras et al., 2019.

Among HLA matched transplants, an HLA genotypically identical sibling donor represents the gold standard source of stem cells for allo-HCT (**Figure 3**). Indeed, the absence of HLA disparities allows a faster engraftment, a lower risk of developing GvHD and a rapid immune reconstitution. However, as family units become smaller with time, it has been calculated that only 30% of the population in need for a transplant actually has an HLA-matched sibling donor (C. Anasetti and Hansen 1994). The natural consequence is that alternative sources, such as CBUs, haploidentical-related donor, matched unrelated donor and mismatched unrelated donors are being increasingly used.

Matched unrelated donors (MURD) are characterized by a full match on HLA- A, -B, -C, DRB1, and DQB1 alleles (10/10). In this setting, similar outcomes regarding TRM and survival have been shown compared to HLA-identical transplants, hence representing the second choice when the latter is not available (Saber et al. 2012). Also with MURD, finding a compatible donor is not always simple, especially for ethnic minorities.

Mismatched unrelated donors (MUD) with a limited degree of mismatching (e.g., compatible HLA-A, -B, -C and -DRB1 phenotypes) are still associated with very good outcomes (Yakoub-Agha 2016) and ease the donor finding process. Indeed, nowadays, as more than 32 million potential unrelated donors have been enlisted in worldwide registries, the probability of finding a well-matched donor reaches approximately 75% for Caucasian patients, whereas the rate is much lower for ethnic minorities and mixed-race patients, due both to higher genetic diversity of HLA haplotypes and lesser availability (Gragert et al. 2014) (**Figure 4**). As incompatibilities between HLA systems grow, the outcome of HCT becomes poorer, as risk of GvHD and treatment-related mortality (TRM) grows, and engraftment of neutrophils and platelets takes more time.

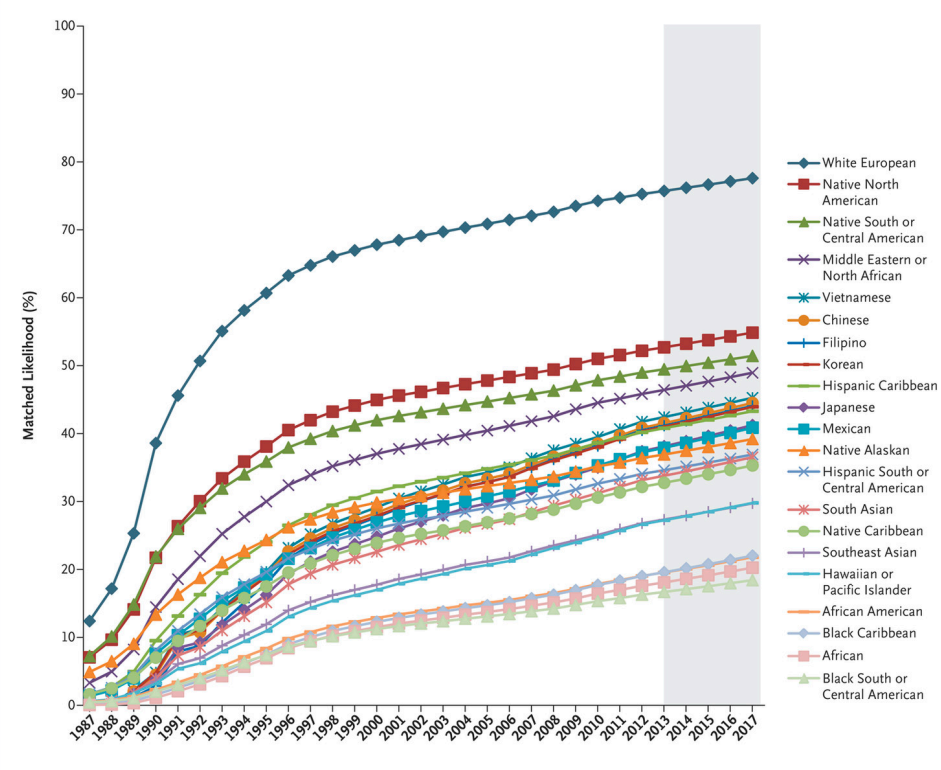

Figure 4. Likelihood of finding an 8/8 HLA match by year since 1987 to 2013.

Projected match likelihoods are also presented for 2013 through 2017 (shaded area). Adapted from Gragert L et al. N Engl J Med 2014;371:339-348.

Cord blood units (CBU) also represent a feasible alternative to matched transplants, as they are easier and faster to obtain. Moreover, CBU cells are 10-1000 times less alloreactive than adult peripheral blood cells, determining a lower risk of GvHD even with increasing number of HLA mismatches (Risdon et al. 1994).

Half-compatible family donor (haploidentical) transplant has been an issue in the transplantation community for years. The major challenge, historically, has been the strong graft-versus-host and host-versus-graft alloreactivity due to the several HLA incompatibilities. Hence, experience with haploidentical transplantation has been characterized by high rated of graft failure, GvHD and TRM.

Several efforts, have been made to finally develop a safe platform for haploidentical transplantation, which presents numerous advantages: first, almost every patient has at least one related haploidentical donor (either a parent, sibling or child) and being able to rely on this approach can be extremely helpful when a transplant is urgently needed, and sometimes allows the possibility to select among multiple donors the best match based on age, sex, and infectious status. Moreover, the lower cost in stem cell obtainment and the unnecessity of national registries can be especially useful in low-income nations.

Use of haploidentical donors for allo-HCT has been continuously growing in the latest years: since 2005, a 291% increase has been witnessed. The growing resort to this transplantation setting has been seen for all diseases, even if myeloid malignancies still represent the most important reason (Passweg et al. 2017).

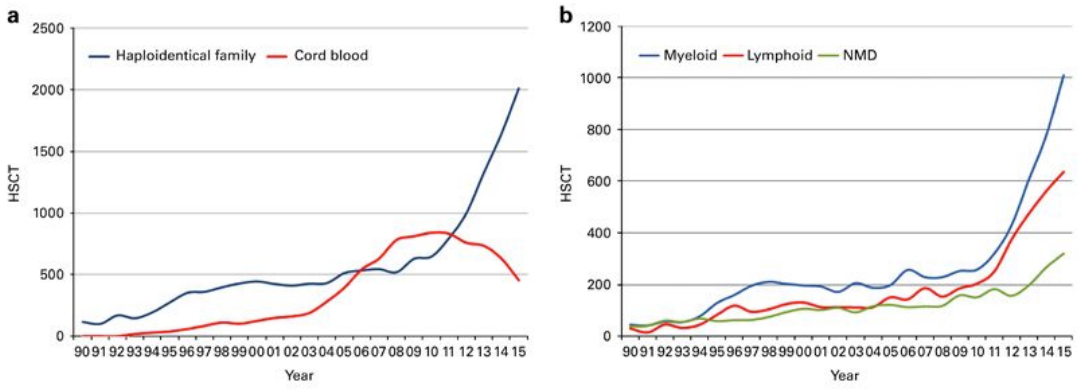

Figure 5. Trends in haploidentical HCT In Europe between 1990-2015.

Comparison with CBU transplantation (a) and among malignancies (b) (Passweg et al. 2017).

1.1.4 Graft-versus-Host Disease (GvHD)

GvHD is a major leading cause of death after transplantation, second only to disease relapse. It is caused by donor T cells that, following the encounter with foreign (non-self) antigens, in the presence of a pro-inflammatory environment, attack and destroy healthy recipient's tissues. It's a severe and often life-threatening condition, which affects many organs, in particular skin, gastrointestinal tract, liver and lungs (J. L. M. Ferrara et al. 2009). The likelihood and severity of the disease are

directly correlated to the number of HLA mismatches between donor and recipient. Nevertheless, other minor risk factors (including age of donor and recipient, gender disparity, multiparous female donors) can influence this condition (Nash et al. 1992), (Gale et al. 1987), (J. H. Antin and Ferrara 1992). Moreover, even in the context of HLA-identical transplantation there is a non-negligible risk of developing acute GvHD, due to the recognition of minor histocompatibility antigens (miHAgs), highly polymorphic peptides displayed by HLA molecules of recipient cells (Falkenburg et al. 2003), (Bleakley and Riddell 2004).

Traditionally, GvHD has been divided into acute and chronic, based on the time of occurrence after HCT, being it before or after 100 days (Sullivan et al. 1992),(Martin et al. 1990). However, this distinction cannot be taken too strictly, and profound differences that go beyond it make acute and chronic GvHD two distinct entities.

In acute GvHD, tissue damage determined by the underlying disease activity, combined with the conditioning toxicity, induces the release of DAMPs and pro-inflammatory cytokines, and increases the expression of HLA molecules, thus activating the donor's immune system. Moreover, activation and proliferation of effector T lymphocytes leads to a cytokine storm through the recruitment of additional mononuclear effectors, amplifying the process (Ghimire et al. 2017), (Joseph H. Antin and Ferrara 1992). Acute GvHD primarily targets skin, the gastrointestinal tract, and hepatic tissues. The extent of involvement of these three main targets decides the severity and thus the prognosis of aGvHD (J. L. Ferrara et al. 2009).

Chronic GvHD, presents a different pathophysiology, though donor immune cells are still largely responsible and can also arise from progression of the acute form.

Dysregulated T but also B-immunity plays a major role in its development and fibrosis usually is the final step of this process (Zeiser and Blazar 2017).

1.1.5 Graft-versus-Leukemia effect

Donor graft cells are not only responsible for the return to normal hemopoiesis following allo-HCT, but are also deemed major factors in the delivery of the anti-tumoral activity of the transplant. In fact, disparities between the donor and recipient's HLA, though being responsible of GvHD development, are also the main driver in the recognition and elimination of residual tumor cells by the donor's immune system (GvL), and in particular by T cells. The first evidence of such an effect was highlighted more than 50 years ago, when in murine models leukemia eradication was obtained after bone marrow engraftment without the use of other myelosuppressive agents (Barnes et al. 1956). The idea, once applied to humans,

led to the definition, for the first time, of the term "adoptive immunotherapy" when referring to transplant.

Another indirect proof of the GvL effect was given by the observation that recipient of syngeneic HCT have an higher risk of disease relapse than patients receiving allogeneic HCT (M. M. Horowitz et al. 1990), (Marmont et al. 1991). Moreover, T cell depletion from the graft is also associated with an increase in relapse incidence (**Figure 6**).

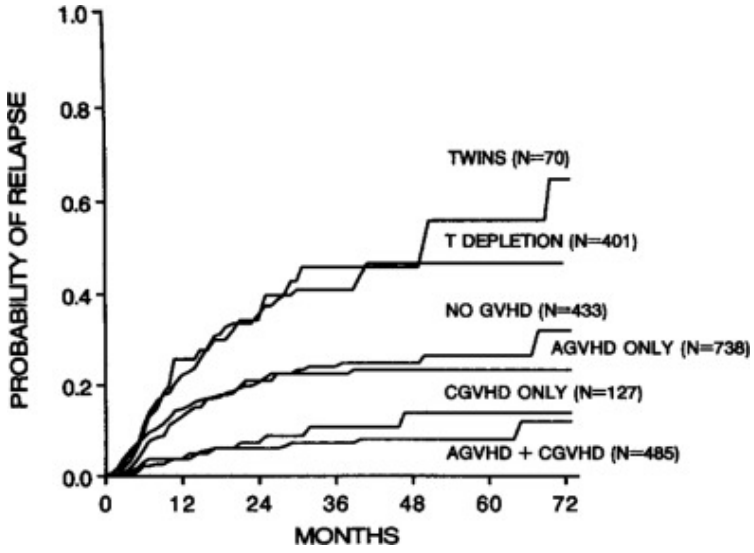

Figure 6. Probability of relapse after BMT.

Likelihood of relapse for AML according to type of graft and developement of GvHD (Horowitz et al., 1990)

The power of GvL is also shown by the clinical practice of donor-lymphocyte infusions to treat post-transplant relapse. DLIs are, indeed, able to induce remission in a high percentage of patients with chronic myeloid leukemia (CML) (Kolb et al. 2004), but are also effective in lymphoma, AML, myelodysplastic syndromes (Depil et al. 2004) and multiple myeloma, whereas rare responses are seen in acute lymphoblastic leukemia (ALL).

Clearly, the most common side effect of DLIs, involving up 40-60% of patients, is GvHD onset (Kolb et al. 2004),(Collins et al. 1997), although patients that suffer from GvHD are less exposed to disease relapse, meaning that the activation of the donor immune system is not limited to healthy tissues but also to dysfunctional ones.

Of note, also NK cells are involved in determining a GvL effect, and a proof of this can be derived from the persistence of a GvL effect even after complete T cell depletion of the graft. The major triggers for NK cell activation and subsequent release of perforin-granzyme and cytokines are the presence of killer cell

immunoglobulin receptor (KIR) ligand/KIR ligand incompatibilities between host and donor cells, where the absence of an MHC class I KIR ligand in the recipient, but not in the donor, prevents the inhibition of donor NK cell-mediated cytotoxicity (Nguyen et al. 2005), and the expression by leukemic cells of ULBPs and MIC-A/B, which are among the ligands for NK cell receptor NKGD2 activation (Bauer et al. 1999). In haploidentical settings, it has been observed that in the first months after transplantation NK cell reactivity is an important mediator of GvL when host cells lack of specific KIR ligands. This effect was even enhanced in T cell depleted graft, where the potent alloreactivity of T cells can mask this important feature of NK cells (Vago et al. 2008).

Considering that long term survival is dented by disease relapse, it is clear how the major curative intent of allo-HCT relies on GvL. Nevertheless, a delicate balance marks GvL and GvHD and strategies to enhance the first without aggravating the latter are crucial. In this prospective, donor selection can be guided by specific mismatches on HLA-DPB1. Some of these are in fact considered permissive, precisely because of their role in disease recognition which manifests a beneficial impact on relapse(Kawase et al. 2009). Moreover, minor histocompatibility antigens selectively expressed by hematopoietic cells, such as HA-1, HA-2, HB-1 and BCL2A1, or aberrantly expressed proteins due to molecular dysregulation can be actively targeted. In this context, donor T cells that recognize leukemic restricted antigens are isolated and expanded in vitro and then infused in the patient to establish a strong reaction against the cancer. The same approach can be used with NK cells, shown to have a wider role in GvL compared to GvHD. A number of pharmacological agents, such as tyrosine kinase inhibitors (TKIs), hypomethylating agents and checkpoint inhibitors have been or are currently being studied to increment the killing of tumoral cells without leading to GvHD(Y.-J. Chang, Zhao, and Huang 2018).

1.2 Relapse following allo-HCT

1.2.1 Acute Myeloid Leukemia

Acute myeloid leukemia is a rapidly progressing malignancy of immature myeloid cells that fail to undergo normal differentiation. The subsequent uncontrolled proliferation affects normal haematopoiesis and is responsible of multilineage cytopenia, eventually determining not only marrow but multi-organ failure. AML diagnosis speaks for 1.2% of all new cancer diagnosis, with an increased incidence in older adults. Despite major advances in the treatments, the outcome often remains

dire, and five-year survival doesn't reach 30% (Newell and Cook 2021). Many driver mutations promote clonal expansion, the most common ones being within FLT3, NPM1 and DNMT3A, though a wide variety of cytogenetic and molecular abnormalities are responsible for its heterogeneity.

General therapeutic strategy for AML is to induce disease remission through chemotherapy, mostly with cytarabine and anthracycline as the mainstay. If complete remission is achieved, consolidation therapy is essential and includes chemotherapy or allo-HCT. Choice between the two is mostly driven by the leukemic genetic-risk profile, treatment-related death scores and patient's performance status. Although maintaining a higher toxicity, allo-HCT is the strongest antineoplastic therapy since it leverages on high doses of chemotherapies in conditioning, and it allows a constant immune control over tumoral cells through the GvL effect.

1.2.2 Relapse

Despite substantial improvements in supportive-care treatments, diagnostics monitoring and graft manipulation, the major cause of treatment failure, eventually leading to death in up to 30% of all transplant settings (M. Horowitz et al. 2018) , is still represented by the reappearance of the initial disease, without consistent advances over the last 20-30 years (**Figure 7**).

Disease relapse is often expression of a more aggressive disease, and in the frame of transplant-related toxicities, the prognosis is poor, with little to no suitable salvage options. Indeed, overall survival is around 20% at only 1 year after relapse and is especially aggravated when relapse occurs within 6 months from transplant (Bejanyan et al. 2015).

The ability of donor-derived T cells to establish a proficient GvL following allo-HCT depends on a complex net of immunological interactions, whose balance is crucial in determining the effectiveness of transplant and abating the occurrence of clinical relapse, and it is becoming increasingly recognized that failure of allo-HCT and reappearance of the original disease in relapsed form are often the expression of mechanisms of tumor immune escape (Zeiser and Vago 2019), either dampening the activity of these donor-derived effector cells (Toffalori et al. 2019b; Noviello et al. 2019b) or rendering leukemic cells invisible to them (Christopher et al. 2018a; Toffalori et al. 2019b; Vago et al. 2009a).

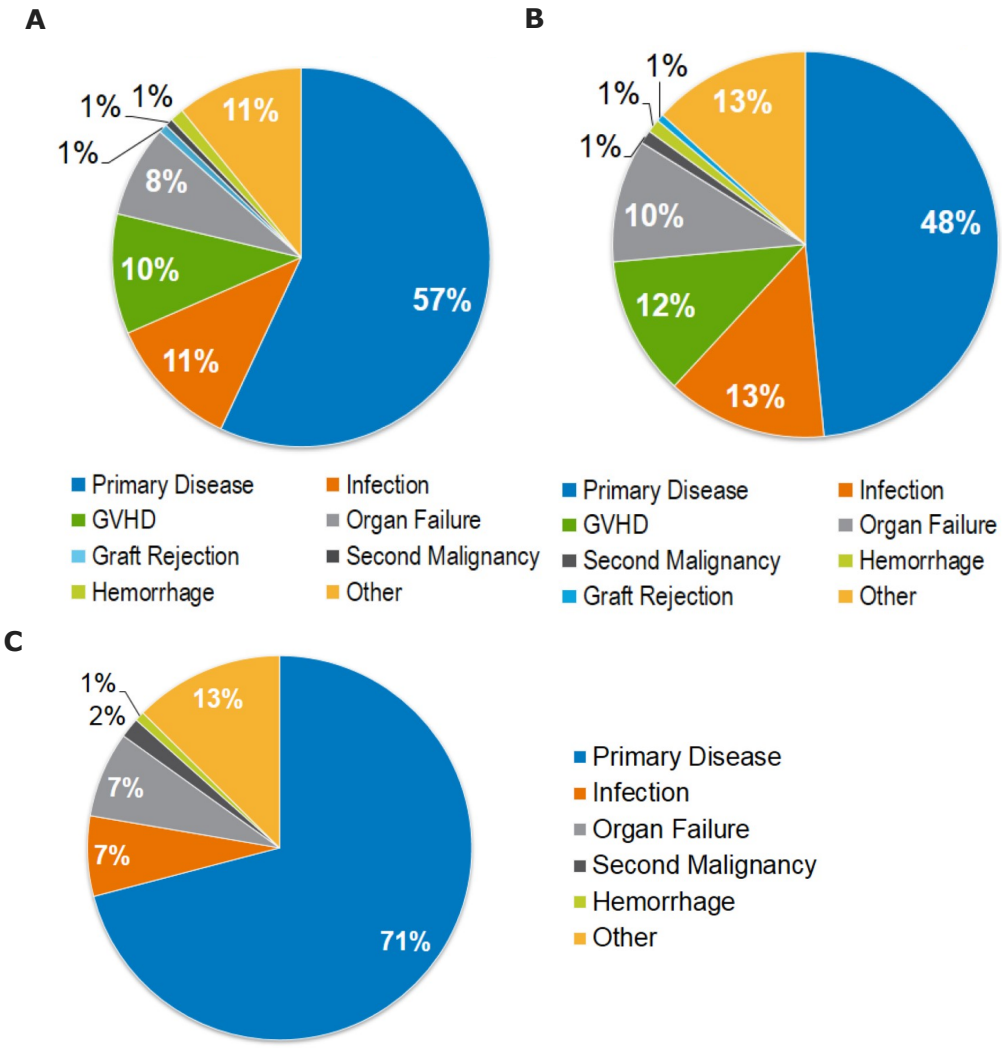

Figure 7. Causes of disease relapse following HCT.

A) Among HLA-matched sibling transplant recipients at or after 100 days, 57% of deaths are attributed to primary disease. B) Among unrelated donor allogeneic HCT, after 100 days, 48% of deaths are related to primary disease. C) After autologous HCT, 71% of deaths are due to primary disease. (D'Souza A, Fretham C., 2018).

1.2.3 Leukemia intrinsic mechanisms of relapse

1.2.3.1 HLA loss

Genomic loss of the mismatched (patient-specific) HLA haplotype through copy neutral loss of heterozygosity (CN-LOH) represented the first evidence of a recurrent modality through which leukemia evades immune recognition following allo-HCT (Vago et al. 2009a). CN-LOH, also known as uniparental disomy, is as a frequent genetic alteration in solid cancers (O'Keefe, McDevitt, and Maciejewski 2010; Tuna, Knuutila, and Mills 2009), although rarely described on hematological malignancies, and consists in the combination of a deletion of a genomic region, rapidly counterbalanced by duplication of its homologous region on the other chromosome, resulting in an acquired homozygous genotype for all genes encompassed in the

alteration, without alterations in gene content or expression levels (Mary Horowitz et al. 2018; Itzel Bustos Villalobos et al. 2010). In the setting of allo-HCT from haploidentical donors, CN-LOH events that encompass the entire HLA region lead to irreversible loss of the haplotype that encodes for the mismatched HLA, and to duplication of its homologue, thus rendering leukemic cells "invisible" to the donor immune system.

After HLA loss occurs, mutated subclones rapidly become the predominant population precisely because donor-derived T cells are no more able to recognize blasts, as the TCR-HLA interaction, the major driver of alloreactivity, is turned ineffectual (Vago et al. 2009b),(I. B. Villalobos et al. 2010). Moreover, since this mechanism allows malignant cells to retain a physiological copy number of HLA class I loci, NK cells will not receive their "missing self" activation signal. These observations are of crucial value, since they imply that the whole GvL effect derived from T and NK cells is lost, and DLI infusions are to be considered ineffectual, if not harmful, since the toxic effect of GvHD is preserved (Tsirigotis et al. 2016a).

This relapse modality accounts for approximately 30% of relapses after haploidentical HCT (Crucitti et al. 2015; Grosso et al. 2017; McCurdy et al. 2016), and while it has also been reported in other transplantation settings, in particular after well-matched unrelated donor HCT, it usually exhibits a lower incidence (Toffalori et al. 2012),(Waterhouse et al. 2011),(Stölzel et al. 2012), probably due to a lower alloreactivity that leukemic cells undergo in this transplantation settings. Interestingly, as opposed to what happens in haploidentical transplantation, HLA mismatches in MUD transplant are usually scattered between the two haplotypes, thereby turning ineffectual any attempt at escape from alloreactivity by losing one allele.

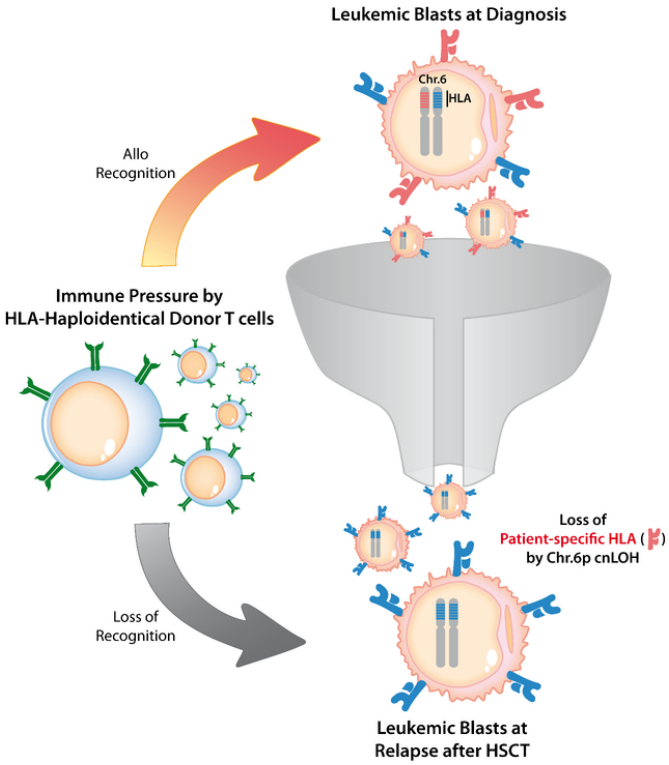

Figure 8. Loss of mismatched HLA in leukemic cells after haploidentical HCT.
Adapted from Horowitz et al., Bone Marrow Transplant., 2018.

A number of studies have investigated the features and risk factors for HLA loss, showing that this escape modality is more frequent in late relapses and when allo-HCT is performed in active disease (Vago et al. 2009a; Crucitti et al. 2015).

1.2.3.2 HLA class II downregulation

Several years after the HLA haplotype loss was described, two independent studies identified a different modality by which leukemia can alter its HLA asset, hiding from T cell recognition. By comparing paired patients' samples collected before and after transplantation, both studies evidenced abolished expression of HLA class II genes and of their master regulator class II major histocompatibility transactivator (CIITA) in up to 40% of AML post-transplantation relapses (Christopher et al. 2018a; Toffalori et al. 2019b). Of note, differently from its genetic counterpart, this mechanism was apparently not correlated with the number of donor-recipient incompatibilities and occurred with similar frequencies after HLA-compatible and -incompatible transplants.

Another, even more relevant, difference from the previously described HLA loss is that in these relapses sequencing of HLAs and their regulatory network revealed no

mutations that could explain the abrogated expression of class II, hinting toward a primarily epigenetic origin of this phenotype (Christopher et al. 2018a; Toffalori et al. 2019b). Lack of class II molecules expression can occur by different epigenetic-driven processes, such as downregulation of CIITA, linked to the hypermethylation of its promoters(Toffalori et al. 2019c),(Christopher et al. 2018b), and mutation in epigenetic regulators such as EZH2 (Ennishi et al. 2019). Several studies also reported HLA class II downregulation due to deletions and point mutation in HLA class II genes and of a recurrent fusion between CIITA and programmed death-ligands PD-L1 and PD-L2, leading to concurrent downregulation of HLA class II genes and upregulation of these inhibitory ligands (Steidl et al. 2011).

In the case of AML post-transplantation relapses, recent reports demonstrated the involvement of both transcription factors (IRF8, MYB, MEF2C, and MEIS1) (Eagle et al. 2022), and polycomb repressive complex 2 (PRC2) as key epigenetic driver of this immune escape modality, showing PRC2-mediated chromatin compaction at HLA class II and CIITA loci in leukemic blasts at the time of relapse (Gambacorta et al. 2022).

1.2.3.3 Upregulation of T cell inhibitory ligands

Alterations at the interface between T cells and leukemic blasts can lead to reduced immune recognition and become responsible of relapse in up to 40% of cases. It has been shown that costimulatory interactions, necessary for T cell activation against target cells, are significantly altered after allo-HCT. In particular, activator molecules such as CD11A and B7-H3 are downregulated, whereas expression of ligands that induce inhibition is increased. Of these, PDL-1 overexpression on blasts was shown to correlate significantly with relapse, and other molecules such as PVRL2 and CD80 were also implicated (Toffalori et al. 2019c).

Plenty are the molecular drivers of this relapse mechanism and most remain unknown. Activation of aberrant janus kinase (JAK), Myc oncogenic signalling and epigenetic alterations on its promoter have all been described as drivers of PD-L1 upregulation (Green et al. 2010), (Prestipino et al. 2018), (Casey et al. 2016). In addition, low levels of micro RNA-34a, involved in PD-L1 degradation, and post translational modifications are also implicated in its expression (X. Wang et al. 2015), (C.-W. Li et al. 2016). The frequency of changes in costimulatory molecules expression after transplant is not linked to compatibility between donor and host, similarly to downregulation of HLA class II molecules (Tsirigotis et al. 2016b).

Noticeably, T cells immunophenotypic changes at the time of relapse mirror those observed in leukemic blasts (Toffalori et al. 2019b; Noviello et al. 2019a). In fact, a

growing number of studies highlighted the co-expression of multiple inhibitory checkpoint receptors on donor-derived T cells and their association with post-transplantation relapse. In the context of HLA-matched transplants TIM-3 and LAG-3 have been shown to be overexpressed in leukemia antigen-specific T-cells (Jain et al. 2019). Coherently, PD-1^{high}/TIM-3^{+} PB T cells of transplanted patients showed functional exhausted features and accumulated before clinical diagnosis of relapse, indicating a strong association between PD-1^{high}/TIM-3^{+} T cells frequency and leukemia relapse (Y. Kong et al. 2015). Moreover, studies reported a higher frequency of $CD8^{+}$PD-1^{+}/TIM-3^{+} and PD-1^{+}/LAG-3^{+} T cells in the bone marrow(BM) of AML relapsed patients (Williams et al. 2019).

1.2.4 Leukemia extrinsic mechanisms of post-transplantation relapse

Though very different, the mechanisms described above all share the abrogation of T cell recognition of leukemia cells as the main gateway to relapse. Nonetheless, the interaction between leukemia and T cells is not the only element to be taken into consideration. Malignant cells not only adapt to become more aggressive and less detectable by the immune system, but they can also modify their environment to support disease spread (Baryawno et al. 2019). This interaction between cancer cells and their environment is well-studied in solid tumors, and it's increasingly being examined in blood diseases as well. After an allo-HCT procedure, this relationship gets even more intricate, due to the combination of elements from both the donor and the recipient.

1.2.4.1 Metabolism-related mechanisms

Recent studies have reported the key importance of metabolic rewiring as a new hallmark of AML onset, progression, and relapse after allo-HCT (Uhl et al. 2020; Mishra, Millman, and Zhang 2023) (Vallet et al. 2022)

In particular, hypoxia and competition for nutrient availability are two major forces able to drive immunosuppression in the TME. In fact, both tumor cells and T lymphocytes rely on glycolytic metabolism, which results in an increase of lactate (lactic acid, LA) as a byproduct of ATP production. Alterations in the energetic interplay in the TME inevitably determine an increase in LA, and a consequent increased acidosis of the TME, which directly hampers effector functions of different immune subsets (e.g NK cells, monocytes, dendritic cells, macrophages, Tregs and T effector cells), and thus GvL responses (Z.-H. Wang et al. 2021). In line with these findings, lactic acid (LA) production by tumor cells has been shown to have a suppressive effect towards cytotoxic T lymphocyte (CTLs) activity by obstructing

lactate efflux and subsequently altering T cell metabolism (Fischer et al. 2007) (C.-H. Chang et al. 2015).

Importantly, a number of studies, although carried out mainly in solid tumors, showed that targeting T cell glucose, amino acid, and lipidic metabolisms in the TME with anti-PD-1/PD-L1 and CTLA4 antibodies (Staron et al. 2014; Ho and Liu 2016), Imatinib (Gottschalk et al. 2004) Acyl-coenzyme A: cholesterol O-acyltransferase-1(ACAT-1) (W. Yang et al. 2016) and idoleamine 2,3 dioxygenase-1 (IDO) inhibitors (GDC-0919, INCB024360) (Nayak-Kapoor et al. 2018, 1) can be exploited as novel anti-cancer therapeutic strategies, leveraging the reprogramming of the metabolic asset of tumor and effector cells.

Lastly, some reports have described an increased level of oxidative markers and altered anti-oxidant balance in the serum of patients undergoing allo-HCT, fostering the common hypothesis by which the conditioning regimen can induce oxidative stress (Sari et al. 2008; Sabuncuoğlu et al. 2012). The main cause of oxidative stress is the altered regulation of reactive oxygen species (ROS) levels in the cells, which culminate in a high degree of oxidative DNA damage and dramatically hamper proper T cell activation (H. Kong and Chandel 2018).

1.2.4.2 Immunomodulatory role of the BM microenvironment

Although in the non-transplant setting, several studies highlighted that leukemic cells can reprogram the TME by producing different immunosuppressive enzymes, such as idoleamine 2,3 dioxygenase-1(IDO-1) (Munn et al. 2005), arginase (Mussai et al. 2013), the ectonucleotidase CD73 (Serra et al. 2011), the ectonucleoside triphosphate dyphosphohydrolase-1 CD39 (Dulphy et al. 2014), known to support tumor escape. Recent evidences, highlighted that malignant cells can also evade GvL effects by secreting anti-inflammatory cytokines (IL-4, IL-10, TGF-b), reducing the expression of pro-inflammatory and growth factors (IL-15, G-CSF, IFN-γ), in a sort of paracrine pathway that ultimately involves and co-opt all surrounding cells in the TME.

1.2.4.3 Inflammation-mediated remodeling of the BM

One of the major hallmarks of cancer is inflammation (Hanahan and Weinberg 2011). While its correlation to different solid cancer types (Greten and Grivennikov 2019) has been largely demonstrated, its contribution to AML relapse has only been hypothesized in the light of leukemic and T cells interactions. Outside of the transplantation realm, increased activity in inflammatory pathways has been correlated to the progression of AML from myelodysplastic syndromes (Barreyro,

Chlon, and Starczynowski 2018), to reduced EFS (Stratmann et al. 2022), and has been reported to control HSCs and accelerate the development of AML in animal models via cytokine production (Carey et al. 2017). Moreover, an increased IFN-γ gene signature has been shown to be predictive of poor response to chemotherapy and, in relapsed/refractory AML, to targeted immunotherapy (Vadakekolathu et al. 2020).

Finally, a recent report highlighted how inflammation is able to remodel entirely the TME of adult and pediatric AML patients, both by expanding atypical B cell population, GMZK+ precursor T cells, and T regulatory cells (Lasry et al. 2023).

1.3 Single cell technologies to unveil cellular diversity

Since the first bulk RNA library sequencing in the late 00s leveraging NGS techniques, RNA-seq has become one of the most valuable and extensively used tool in cancer research. While previously used technologies like RT-PCR and microarray-based assays allowed only quantification of a known pool of transcripts, RNA-seq enabled for the first time the sequencing of the whole transcriptome, opening the gates to a series of previously unreachable data: sequencing of non-model organisms whose genome was unknown, detection of gene isoforms, gene fusions, sequence variations (SNP), and many other features.

Despite revolutionizing our understanding of biology, RNA-seq from bulk tissue and/or dissociated cells presents an important limit, as it cannot resolve specific cell types, which is often critical to understanding the deepest and more complex layers of biological systems. Bulk sequencing is, in general, cheap and not time-consuming, both from the pre-analytical and the computational standpoint. However, by providing only cell-averaged profile expression, sample heterogeneity can't be assessed (although methods to estimate the abundance of cell types in mixed populations have shown promising results (Chen et al. 2018). To uncover rare cell populations, and answer to more complex biological questions, such as tracing developmental trajectories, gene expression must be assessed at the single-cell level.

scRNA-seq was first introduced in 2009 (Tang et al. 2009), and, since then, its applications, and the laboratory and computational methods available, have advanced at an unprecedented pace. Each scRNA-seq method basically follows the same steps required for bulk RNA-seq, like solid tissues dissociation, cell lysis, reverse transcription, amplification, and sequencing. However, scRNA-seq protocols requires the two additional steps of cell isolation and labeling. These are also the steps that vary the most across different pipelines.

1.3.1 scRNA-seq "wet" pipelines

scRNA-seq pipelines can be essentially divided based on the different techniques used for cell isolation and cDNA synthesis.

Regarding cell isolation, plate-based techniques leverage single cell isolation and library preparation in individual wells of a plate. This allows for higher read depths per cell, though at the cost of a lower cellular output (Kashima et al. 2020). Most commonly used protocols include SMART-seq2 (Picelli et al. 2014), MARS-seq (Keren-Shaul et al. 2019), QUARTZ-seq (Sasagawa et al. 2013), and SRCB-seq (Soumillon et al. 2014). Droplet-based techniques, on the other hand, while able to process a significantly higher number of cells, have generally lower read counts. Moreover, gene information from droplet-based approaches can only be obtained either at the 5' or 3' end of each transcript, whereas plate-based methods can generate reads from whole transcripts (Griffiths, Scialdone, and Marioni 2018) (**Figure 9**). Most commonly used microfluidic-based protocols include Drop-seq (Macosko et al. 2015) and 10X genomics Chromium (Zheng et al. 2017).

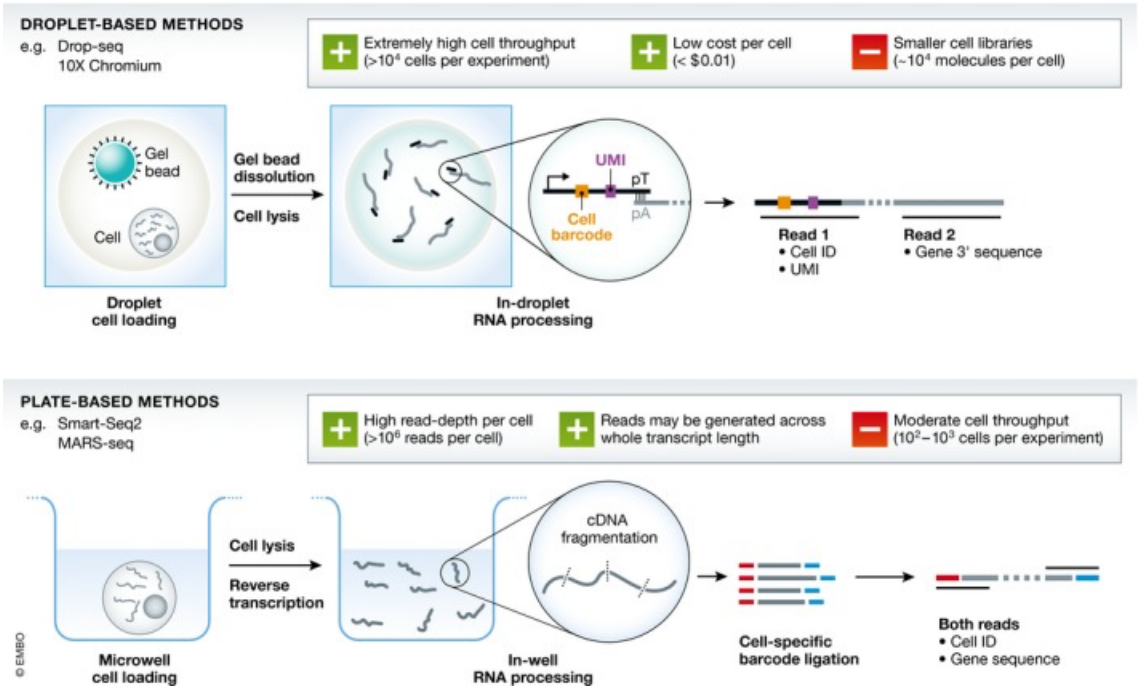

Figure 9. Different cell isolation methods for single cell pipelines.

(Griffiths, Scialdone, and Marioni 2018)

cDNA synthesis from mRNA transcripts is another critical step: main protocols are divided into UMI-based (or tag-based), where a unique molecular identifier is incorporated in the initial reverse transcription step along with the barcode, allowing more reliable read counts, and protocols that leverage template-switching mechanisms, enabling generation of full-length cDNAs (Picelli et al. 2014).

Lately, to enhance the depth and precision of scRNA-seq techniques in capturing the intricate regulatory mechanisms underlying cellular functions and signaling, significant strides have been taken to assess other aspects at a single-cell level, including chromatin accessibility (Baek and Lee 2020), surface proteins (Stoeckius et al. 2017), TCR/BCR sequences (Han et al. 2014), and spatial transcriptomics (Larsson, Frisén, and Lundeberg 2021), which can even be combined into single experiments to produce multi-omic single cell datasets.

1.3.2 scRNA-seq computational pipelines

Experimental innovation has been accompanied by the development of several computational tools to analyze this newly generated data. As of 2023, scRNA-tool, a database used to catalogue software packages for the analysis of scRNA-seq data, had collected approximately 1600 bioinformatic tool, comprising mostly visualization (~40%), dimensionality reduction (~25%), clustering (~23%), and integration (~18%) software, as well as pre-processing, data acquisition and differential expression pipelines. Notably, between 2018 and 2023, the number of available tools witnessed a 5-fold increase, and if the trend continues at this rate, it is expected to reach, by the end of 2025, at least 3000 available packages (Zappia and Theis 2021) (Zappia, Phipson, and Oshlack 2018). A number of comparison and benchmarking studies have been performed in the last few years, covering almost every step of a standard single-cell analysis pipeline (Vieth et al. 2019; Cole et al. 2019; Dal Molin, Baruzzo, and Di Camillo 2017; Soneson and Robinson 2018), at the point that even studies comparing these studies have started to come out (Germain, Sonrel, and Robinson 2020).

Despite the availability of all these tools, three main "ecosystems" have emerged as the most popular and widely used: R based Bioconductor (Huber et al. 2015) and Seurat (Hao et al. 2021a), and Python based scverse (Virshup et al. 2023). Furthermore, best-practices workflows have also been presented (Heumos et al. 2023), in an attempt to standardize computational workflows employed.

2 AIM OF THE WORK

Allo-HCT represents the most successful therapeutic option for many patients suffering from AML. Nevertheless, leukemic cells often find means to evade control from the donor-derived immune system and re-emerge. To date, three alternative and frequent mechanisms by which AML cells modify their features and escape immune control have been described: genetic loss of the mismatched HLA haplotype (HLA loss), downregulation of HLA class II molecules and upregulation of inhibitory ligands, all ultimately leading to abolished leukemia recognition by T lymphocytes.

Nonetheless, a sizable portion of disease recurrences are still unaccounted for. Many other immune cell types weave a canvas of interactions with leukemic clones in the bone marrow niche, where AML originates, and this complex tumor microenvironment (TME) has already been demonstrated to play a role in anti-tumor immunity in other settings.

In the present study, by leveraging 10x Genomics Single Cell Immune Profiling solution, our aim is to map by scRNA-seq the transcriptomic changes that occur in the bone marrow of patients who experience AML relapse after allo-HCT, with the ultimate goal of improving our understanding of how leukemic cells exploit their TME to escape immune surveillance and identify new vulnerabilities to be exploited for personalized therapeutic approaches.

More specifically, we first initiate by closely examining leukemic cells, with the primary objective of identifying known leukemia-intrinsic features of post-transplantation relapse, and uncover how these changes influence and shape the surrounding TME.

We subsequently turn our attention towards the primary TME populations that play pivotal roles in post-transplant immunity, NK and T cells. Exploiting the high resolution provided by scRNA-seq, we dissect these immune cell subsets to uncover intricate molecular signatures, differential expression patterns, and potential interplay with leukemia cells that may offer insights into relapse mechanisms and immune evasion strategies.

To conclude, our in-depth exploration of the bone marrow environment in post-transplantation relapses, combined with our focus on leukemia and immune cell dynamics, contributes on the understanding of how the BM niche could be exploited to find novel vulnerabilities in AML relapses.

3 RESULTS

3.1 Study design and patient characteristics

We retrospectively reviewed clinical and epidemiological data from a non-consecutive cohort of N=36 patients, of which N=25 with a diagnosis of AML who underwent allo-HCT and later experienced disease relapse at our institution between 2009 and 2022, N=6 HC, and N=5 patients with a diagnosis of AML who, following allo-HCT, remained in CR for at least 1 year. **Table 1** summarizes patients' characteristics.

Patients from our AML relapse cohort were characterized by different mechanisms of leukemia relapse, including downregulation of HLA class II (N=5), upregulation of inhibitory ligands (N=4), genomic loss of incompatible HLAs, "HLA loss" (N=10), and unknown mechanisms of relapse (N=6).

3.2 scRNA-seq data pre-processing

3.2.1 Cell Ranger

Cell Ranger software comprises a set of informatic pipelines with the ultimate function of processing Chromium scRNA-seq outputs. Here, we used it to align reads, generate feature-barcode matrices and perform initial clustering and QC.

Median estimated number of cells was 7,648 (range 438-25,480), median number of reads per cell (sequencing depth) was 42,630 (14,893-279,683), median number of captured genes 1,667 (480-4,423), median percentage of reads mapped confidently to the transcriptome 72% (40-82). Notably, intronic reads retention significantly improved the number of reads mapped confidently to the transcriptome (Wilcoxon rank sum test, p-value<0.001), median genes per cell (0.007), reads mapped antisense to gene (<0.001), and total genes detected (<0.001).

Relevant summary statistics are shown in **Table 2**.

3.2.2 Cell-free mRNA correction and doublets removal

The 10X Chromium platform that was used in this work is a droplet-based technology. Droplet-based scRNA-seq strictly depends on the assumption that within each droplet, where UMI and barcode tagging and reverse transcription take place, only mRNA from a single cell is present. Nonetheless, violations of this principle are very common, even in high quality datasets, and may interfere with following biological interpretation of scRNA-seq data (Zheng et al. 2017).

A well-known, and non-negligible, phenomenon that often occurs is the formation of empty droplets, and/or droplets where, other than a cell, a mixture of cell-free

RNA ("ambient" RNA) from the initial cell suspension is present, which leads to sequencing of exogenous RNAs that mainly derive from dead cells, and that will be assigned to a cell's native RNA during library construction. A common consequence of high ambient RNA contamination can be cell-type mislabeling, as the presence of cell-type-specific markers might blend different cell populations together and interfere with correct clustering.

Here, we used SoupX (Young and Behjati 2020), a method that, by analyzing mRNA expression profiles from empty droplets, estimates the cell-specific contamination fraction and produces a count matrix with corrected expression profiles of native mRNA. In our cohort, only one sample returned an estimated contamination fraction >20%. Of note, this was a sorted leukemia sample, and we therefore speculate that the absence of cluster-specific genes influenced SoupX results. To avoid subtracting too much signal, a default 5% contamination fraction was set for this sample. Median ambient RNA percentage was 2.5 (range 1-10.1%) (**Figure 10A**).

Among the most frequent genes whose expression became zero in a larger fraction of cells after correction, we notably found *HBB,* and several *TRB* and *IGHV* chains, along with other cell-type-specific markers such as *CST3*, *LYZ*, and *AZU1*. Among those genes whose expression became lesser, but not necessarily zero, we found a prominence of mitochondrial genes (i.e. *MT-CO1, MT-CO2, MT-ND1, MT-ND2*). These results suggest that the use of SoupX in our dataset allowed us to increase the ability to discern different cell-types, both by removing cell-specific markers from clusters where those markers are not expected and correcting signal coming from dying or distressed cell, which are typically associated with mitochondrial content leakage. (**Figure 10B**). SoupX modified counts were used for all downstream analysis.

Another important single-cell artifact that can strongly alter downstream analysis consist in the capture, in a single reaction volume (in our case, a droplet) of two or more cells, which will then be sequenced as a single cell (doublets or multiplets).

Depending both on cell density at the moment of sample loading and the absolute number of cells captured, the proportion of doublets in single-cell experiments can reach 20% of estimated cells, making accurate doublet detection, and removal, trivial. Here, we leveraged scDblFinder (Germain et al. 2021), a method that, similarly to other doublet-detection tools, generates artificial heterotypic doublets from the given dataset and a kNN network to build a cell-level predictor matrix.

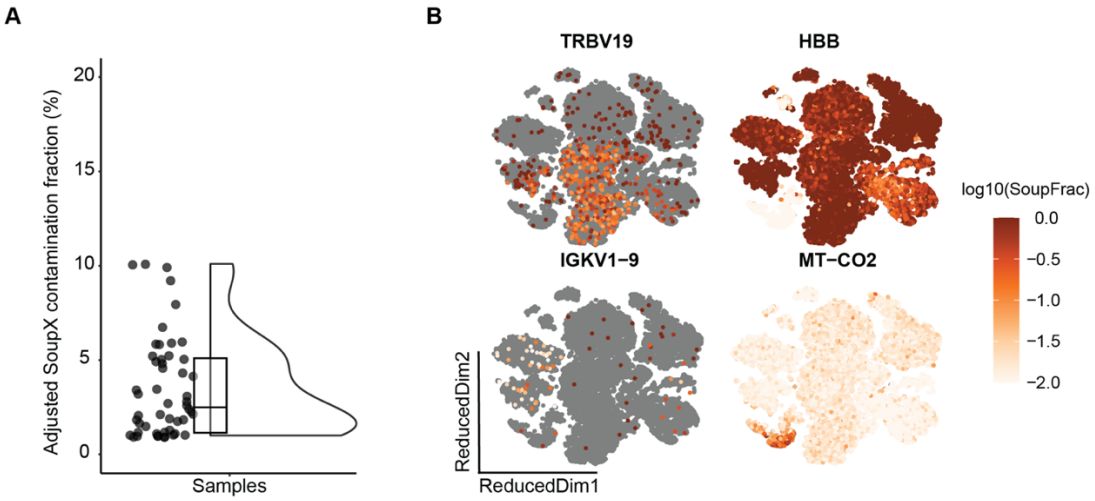

Figure 10. Cell-free mRNA removal with SoupX.

A) Raincloud (Allen et al. 2021) plot displaying adjusted SoupX contamination fraction values for each sample. Dots indicate individual values; boxplots show median, interquartile range (IQR) and highest and lowest values (whiskers) excluding outliers; half-violins provide an explicit representation of the distributions. B) t-SNE plots of sample GEXV49, showing, for four exemplary genes, the log10 of the fraction of observed counts that are identified as contamination for each cell.

Briefly, by clustering real cells and artificial doublets together, scDblFinder identifies as doublets those cells that share similar properties to artificial doublets.

In our dataset, median percentage of estimated doublets was 6.9% (range 0.7-18.5).

Results from scDblFinder were also combined with those from souporcell (Heaton et al. 2020). Souporcell uses minimap2 to remap raw readings to a reference genome, freebayes to identify candidate variations, and vartrix to quantify the number of cell alleles supported by each cell. Cell allele counts are then subjected to sparse mixture model clustering to identify doublets and determine the genotypes of each cluster.

Leveraging the presence of two different genotypes in most of our samples, we were able to increase our sensitivity in doublet detection by identifying cross-genotype doublets, which in some cases might have highly similar transcriptional profiles (homotypic doublets), therefore precluding detection only by their transcriptional profile (**Figure 11**).

With souporcell, median fraction of estimated doublets was 2.9% (range 0.05-34.4).

Collectively, median percentage of doublets (on the whole dataset, prior to low-quality cell removal) was 9.7% (range 0.7-40.4).

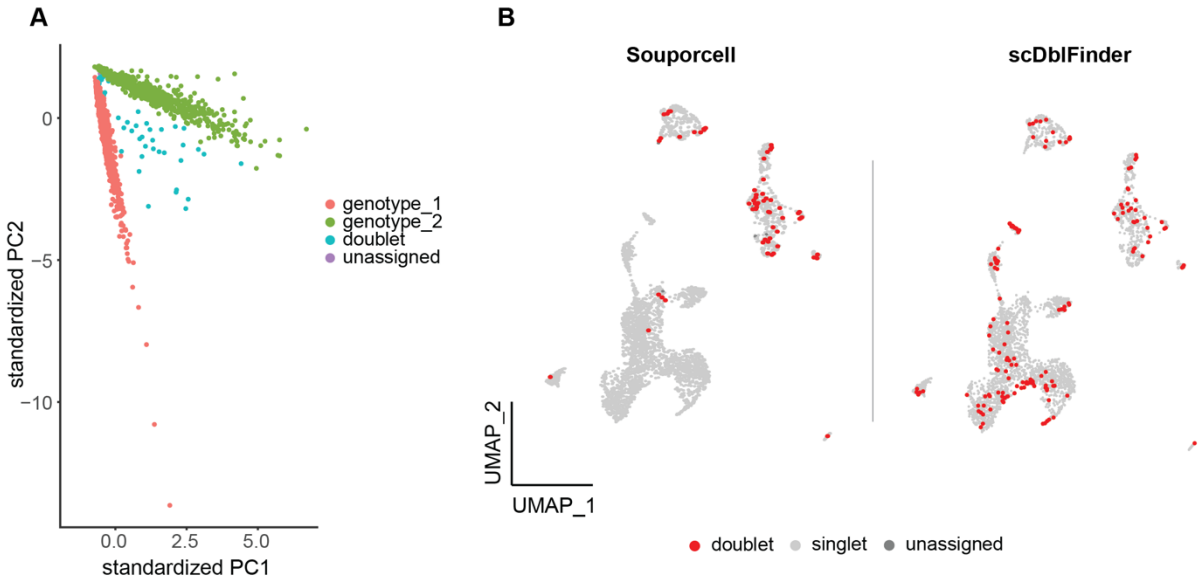

Figure 11. Doublet identification results in a sample (GEXV15).

A) PCA of cells based on genotype assignment loss metrics. The log loss for each genotype provides a quantitative measure of the certainty (or uncertainty) associated with each cell's assignment to the respective genotype. Cells that cluster "in the middle" of the two genotype are predicted to be cross-genotype doublets. B) UMAP of doublets identified by souporcell (left) and scDblFinder (right). While there is some degree of concordance (for this sample, 15% of total doublets), combining the two methods allows for better doublet isolation.

3.2.3 Low-quality cells filtering

scRNA-seq library preparation protocols require a suspension of viable single cells, and to obtain high-quality data, minimizing the presence of cellular aggregates and dead cells is critical. Despite pre-processing steps to ensure sample's integrity, such as dead cell removal or FACS sorting, low-quality sequenced cells are a common finding, and several methods and metrics are available to filter data to only retain cells that are of high quality.

Cell QC is usually performed on the following three QC covariates: the number of counts per barcode (count depth), the number of genes per barcode, and the fraction of counts from mitochondrial genes per barcode. In our dataset, since we started from BMMCs and we expected RBC contamination to some extent, we also calculated the fraction of counts from ribosomal and hemoglobin genes to be added to our QC metrics, to identify and exclude erythrocytes from downstream analysis. In our dataset, RBCs were also characterized by a generally low read depth, number of genes expressed and mitochondrial content (**Figure 12A**).

In cell QC, covariates are usually filtered via thresholding. Cells that show a low count depth, few detected genes and a high fraction of mitochondrial reads might reflect cells with ruptured membranes, whose cytoplasmic mRNA has leaked out and therefore only the mRNA in the mitochondria is still present.

Nonetheless, it is crucial to consider the three QC covariates jointly when thresholding decisions are made. A higher fraction of mitochondrial counts might characterize a cell that is undergoing several respiratory processes, whereas cells with low or high read counts might correspond to quiescent cell populations or cells larger in size, respectively. In our dataset, for example, samples are characterized by a mixed population of blasts (large cells with a high transcriptional activity) and lymphocytes (small cells in a relatively quiescent state).

In our QC pipeline, we first removed genes characterized by high "dropout" events, causing them to be expressed in less than 10 cells per sample. These genes, characterized by 0-counts, can dramatically reduce the average expression for a cell and influence downstream analysis. For low-quality cell detection and filtering, we both used manual thresholds, as recommended by single-cell analysis guidelines (Luecken and Theis 2019), and sample-wise automatic filtering based on the number of median absolute deviations (MAD) (McCarthy et al. 2017). For the latter, instead of focusing on the single covariates for outlier detection, we used a combined approach that takes into account read counts, number of genes, and mitochondrial and ribosomal reads fraction together. This allowed us to avoid filtering of cell populations characterized by a single outlying characteristic (i.e. small subsets of rapidly proliferating cells with higher read counts) and true detection of low-quality cells (**Figure 12B**).

In total, median fraction of low-quality cells was 8.9% (range 5.8-20.8). Median number of cells per sample that were kept following low-quality filtering and doublets removal was 4382 (range 361-14282).

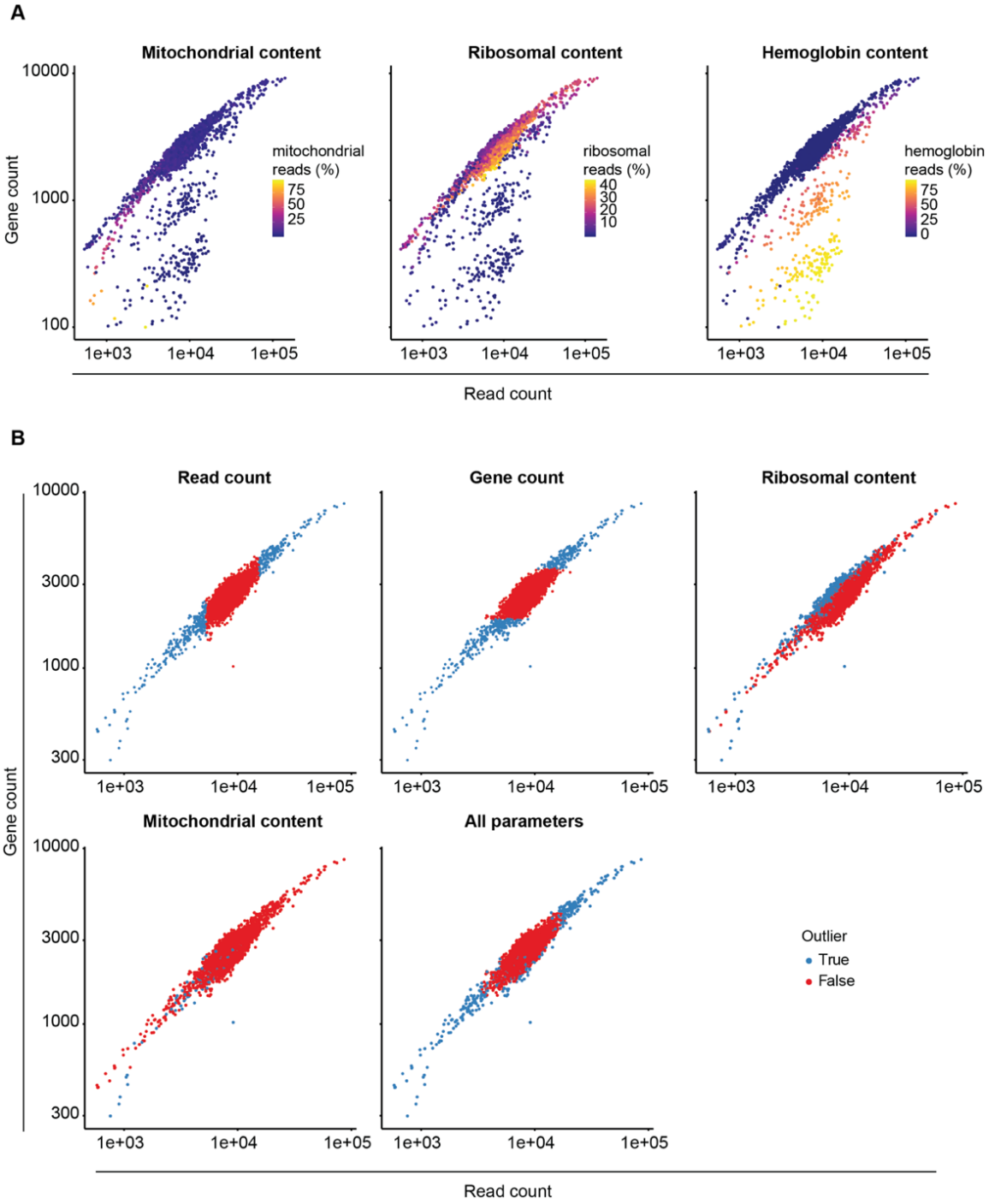

Figure 12. Low-quality cell identification and removal.

A) Scatter plots of sample GEXV05, characterized by an RBCs population. The x-axis and y-axis depict number of reads and genes, respectively. Color gradient indicates the fraction of mitochondrial (left), ribosomal (middle) and hemoglobin (right) reads per cell. RBCs are characterized by a low number of reads, mitochondrial and ribosomal reads percentages, and a high hemoglobin genes content. B) Scatter plots of GEXV05 following erythrocytes filtering. Blue dots represent cells defined as outliers with different criteria. From left to right and top to bottom: read counts, number of genes, ribosomal content, mitochondrial content and all of the previous parameters combined.

3.2.4 Cell annotation

Possibly the most crucial part of all scRNA pre-processing pipelines consists in defining the cellular identity of each cell in a given dataset. Here, we used a three-steps approach:

The first step, automated, classifier-based cell-type annotation, was performed leveraging the SingleR R package (Dvir Aran, Aaron Lun, Daniel Bunis, Jared Andrews, Friederike Dündar n.d.), both in cell- and cluster-modes. SingleR is a computational tool designed for unbiased cell-type annotation, that leverages reference data sets of pure cell types sequenced by microarray or bulk RNAseq. While this annotation method is fast, unbiased and automated, it mainly relies on single references, and this can lead to inaccuracy when cell types in "query" and "reference" datasets are not well matched (i.e. from different organs) or in the presence of poorly characterized and rare cells (Abdelaal et al. 2019) (Pasquini et al. 2021).

To partially make up for this limit, we then used a personalized reference-mapping method (see Methods section). Briefly, we first calculated gene average expression for each cluster at different resolution. Then, low-expressed genes were filtered from cluster-average expression values based on CPM, and cluster-gene matrices were rescaled. Finally, rescaled values were used to calculate a module score for each cell type in our reference datasets, and each cell was then assigned to the population with the highest value.

Similar to classifier-based approaches, the reliability of this method depends on the quality of the reference data. However, the possibility to filter low-expressed genes and manually curate gene signatures from references allowed us to better tune our annotations.

Finally, exploiting the `FindMarkers()` function embedded in Seurat, we examined the most significant up- or down-regulated genes in each cluster at different resolutions, and performed manual annotation of clusters combining gene expression profiles and information from previous annotation methods (**Figure 13**).

This step was necessary, as clusters showed variable degrees of ambiguity among automatic annotation methods. In particular, for most samples this was necessary for the distinction between CD8 and CD4 T cells and between CD8 T and NK cells. At this point of the analysis, our aim was to obtain a broad cell type characterization in order to exclude low-quality clusters and have a general outline of each sample.

Clusters that couldn't be characterized by either method or that exhibited a strong enrichment in mitochondrial genes were excluded from further analysis.

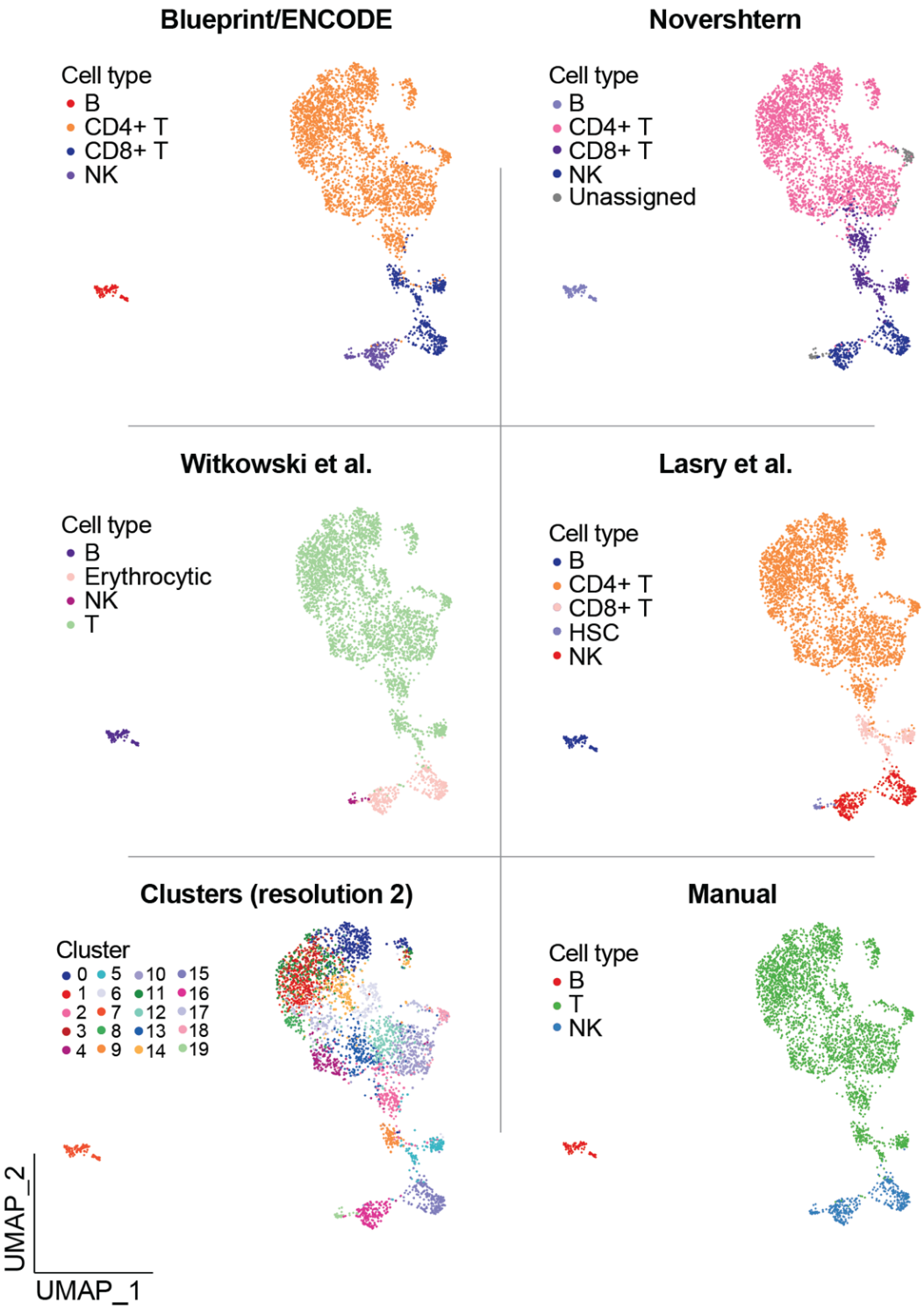

Figure 13. Cell annotation on GEXV05 (HC) sample.

Cell type assignation was performed leveraging SingleR (top panels, here are showed annotations obtained via analysis by-cluster with two different reference datasets), reference atlases (middle panels), and manual marker analysis (bottom). Despite a high degree of concordance, some discrepancies can be observed, especially in CD4/CD8 T and CD8 T/NK cell discrimination.

3.3 BM landscape of AML relapses following allo-HCT

Following cell-type annotation, our next step was to effectively integrate our dataset, to unveil a comprehensive atlas of the BM microenvironment of post-transplantation AML relapses. An integrated approach presents several advantages, including the possibility to increase our statistical power, especially important when dealing with rare cell populations, or cell types and states that might be exclusive to certain patient subsets. Furthermore, a collective view can also be both time and cost-efficient, by circumventing the process of individual analyses followed by post hoc comparisons.

Following samples merging, counts were re-normalized and scales, and dimensionality reduction and cluster calculation were performed. We applied again our cell-annotation workflow, this time leveraging also previous annotations for individual samples. While mostly overlapping, re-clustering in a merged dataset allowed us to also correct some cell type assignation.

In total, we obtained 263,606 annotated BM cells. Among these, 189,892 (72%) cells were from AML patients, 43,653 (16.6%) from CR patients, and 29,991(11.4%) from HC.

By looking at the UMAP projection it is already possible to highlight some degree of BM microenvironment remodeling, with some clusters being populated both by AML and control patients, and other clusters dominated almost exclusively by AML samples (**Figure 14A**). As expected, clusters that were leukemia patient-specific were particularly enriched in myeloid immature cell populations, whereas myeloid mature and lymphoid populations were distributed more evenly across experimental groups (**Figure 14B**). More in detail, AML patients showed increased percentages of some specific subsets of hematopoietic stem (HSC) and progenitor (MEPs and MPPs) cells, while mature myeloid populations, in particular monocytes and pDC, were depleted in AML patients. Lymphoid populations were largely unchanged, except for a decrease in B cell percentages in AML patients (**Figure 14C**). Interestingly, while a certain degree of BM remodeling was somewhat expected in these patients, CR and HC samples were largely overlapping, hinting that, following immune-reconstitution, the BM of patients that undergone a procedure of allo-HCT is able to return to a condition of normal hemopoiesis even after a short period of time.

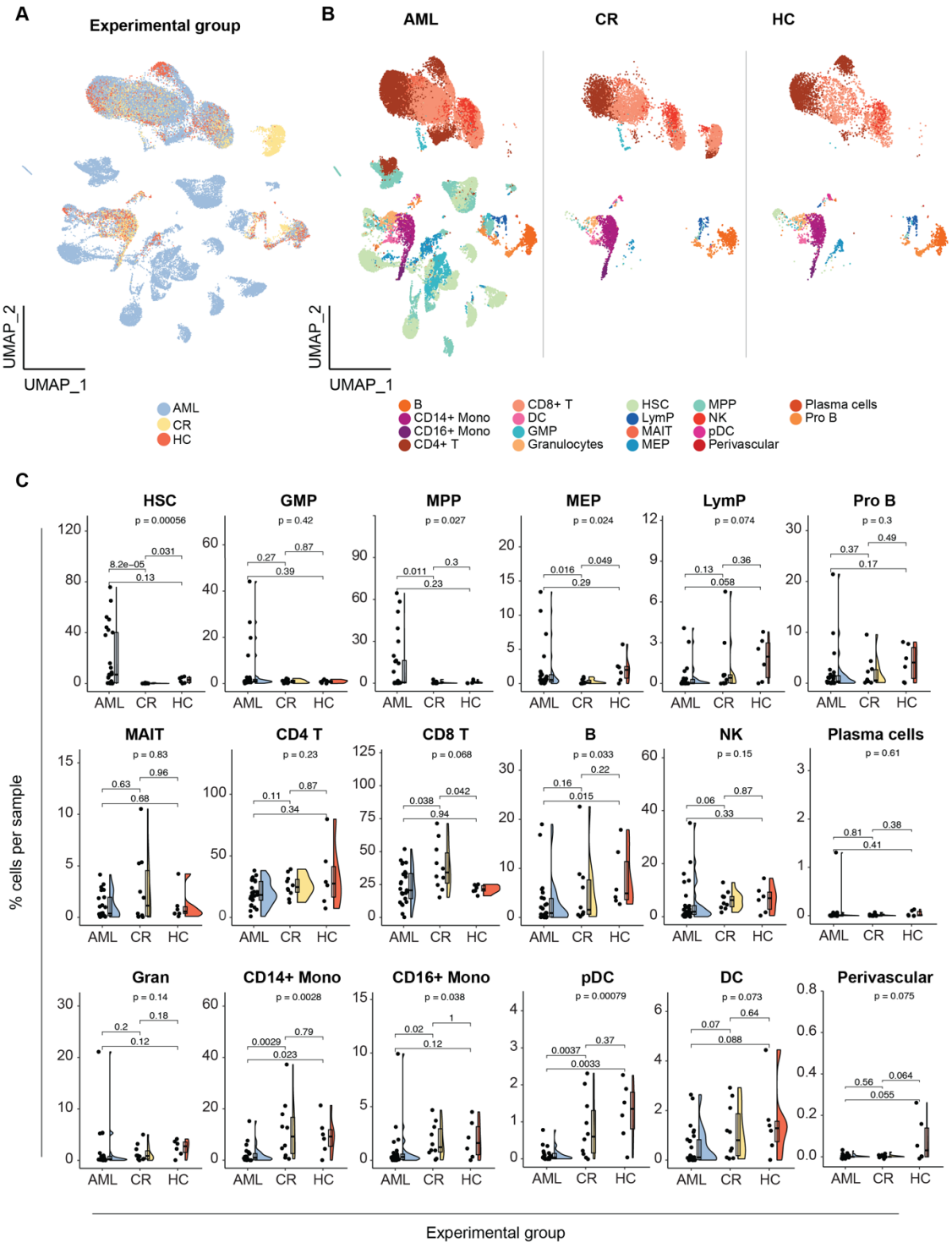

Figure 14. BM landscape of AML relapses following allo-HCT.

A) UMAP of merged dataset colored by experimental group. B) UMAP of merged dataset, grouped by experimental group and colored by manual annotation. C) Raincloud plots showing the percentage of immature (upper panels), lymphoid mature (middle panels), myeloid mature (lower panels), and perivascular (lower right panel) cells among the different experimental groups. P values were calculated by Wilcoxon Rank-Sum test for pair-wise comparisons, and by Kruskal-Wallis test for global comparisons.

3.3.1 Malignant and microenvironment separation

To better assess how leukemia relapses remodel the BM microenvironment, we first sought to separate malignant cells from their healthy counterparts.

To identify leukemic blasts, we started from three observations: first, malignant cells have already been shown to form patient-specific clusters in solid tumors (Darmanis et al. 2017) (Jerby-Arnon et al. 2021). We therefore hypothesized that the clusters mainly occupied by AML samples that we observed might be mainly composed of leukemic populations. This would also be in concordance with the fact that these clusters were mainly constituted by HSPCs. The second observation comes from clinical routine in hematological patients: allo-HCT in the context of hematological malignancies involves the replacement of the patient's diseased hematopoietic system with that of a healthy donor. Successful transplantation results in complete donor chimerism, where recipient's blood and immune cells are entirely donor-derived. Monitoring chimerism is a vital and common procedure, as it can offer insights into the graft's stability, potential complications, and the risk of disease relapse. An increase in the host-derived fraction (Lindahl et al. 2022) often signals an impending disease relapse, indicating that the patient's original, diseased hematopoietic cells are starting to repopulate the system. In our dataset, AML patients were characterized by a clinically overt relapse, and their BM was therefore populated by two genotypically distinct populations.

Last, we employed inferCNV (Timothy Tickle and Itay Tirosh, n.d.) to discern cells with copy number variations (CNVs) within our dataset. Traditionally, AML isn't associated with a high prevalence of chromosomal aberrations. We therefore validated this approach both by specifically applying it only on those patients where documented evidence of chromosome gains or losses was present, and by comparing results with those coming from patient-specific clusters and genotype inference.

3.3.2 Patient-specific cluster assessment

We observed that not only AML samples had the tendency to cluster together, but that most of these clusters were also patient-specific (**Figure 15A**).

Following an already validated approach and using high resolution clustering information, we calculated, for each cluster, an "occupancy score" (Lasry et al. 2023), that would reflect the degree of patient-specificity of this cluster (see Methods section) (**Figure 15B**). As expected, higher scores were assigned to cells in HSPC clusters, which have been shown to be mainly patient-specific. Based on score distribution, we chose a threshold of 70% of sample abundance to define a cluster as patient-specific, and therefore malignant (**Figure 15C-D**). Malignant clusters

mainly consisted of HSPCs, erythrocytic precursors and myeloid cells, with a small fraction of T and NK cells, which surprisingly clustered in a patient-specific fashion and that were all derived from a single patient (PZ170136) (**Figure 15E**).

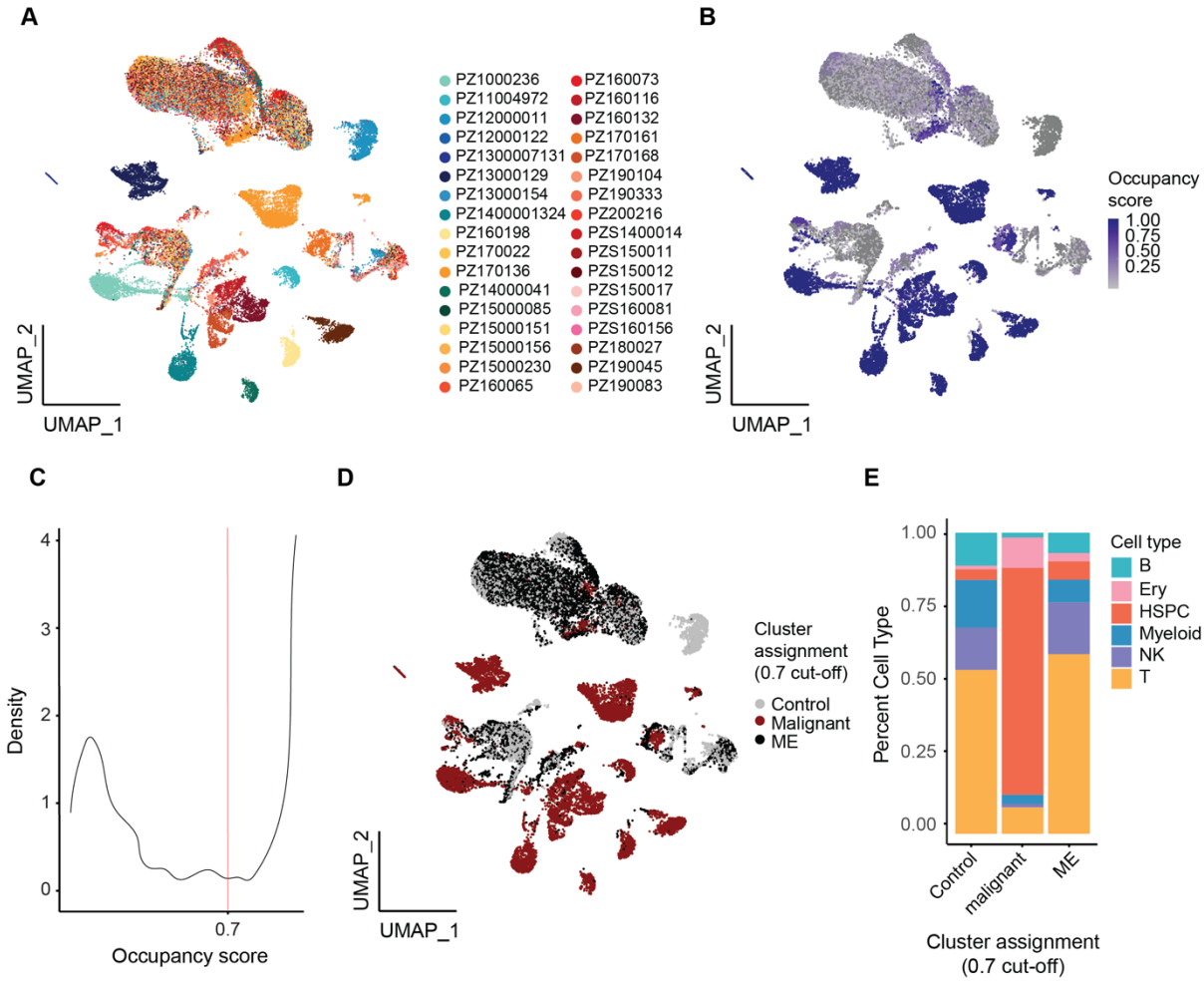

Figure 15. Occupancy score calculation.

A) UMAP showing the merged dataset, colored by patient code 3. B) UMAP showing occupancy score values for each cell. C) Density plot showing occupancy score distribution. It is possible to observe a slight bimodal distribution, with most cells either having a very low occupancy score and a peak after 0.7. D) UMAP showing malignant and ME assignment based on a cut-off of 70% between single patient and control cells ratio. Control cells are labelled in grey. E) Barplot displaying broad cell type distribution across different groups, as defined by a 70% cluster occupancy cut-off.

3.3.3 Souporcell genotype assessment

Initially, we used souporcell to better discriminate, and get rid of, doublets and multiplets. Here, we leveraged the possibility to use transcriptomic data to infer host-donor chimerism to identify malignant and TME cells.

We first validated this approach by exploiting two patients' sorted samples (see Methods). By running souporcell after merging TME and leukemia samples in both

patients, we could show that the majority of cells that were assigned to donors' genotype were assigned to lymphoid populations, including T, B, and NK cells, and a small percentage of mature myeloid cells, whereas host-assigned cells were mainly composed of HSPCs and had a tendency to populate patient-specific clusters. (**Figure 16A-B**). To further confirm that souporcell is a suitable method to discriminate AML blasts from their surrounding, donor-derived, TME, we show that souporcell-assigned host genotype corresponded in large part to the sorted leukemic samples, while donor genotype matched with TME samples (**Figure 16C**). For TME_1 and TME_2, donor-genotype percentage were 95.3% and 94.9%, respectively, while for LK_1 and LK_2 0.2% and 0.1%, respectively.

Following validation of this approach, we applied this analysis to our whole cohort (except for HC, CR, and sorted samples) (**Figure 16D**). Except for a small, unexpected, population of host-derived lymphoid cells (8% of all host cells), most of B, T and NK cells were assigned to a donor origin, while host-derived cells mainly comprised HSPCs and erythrocytic precursors, Interestingly, we also found a small proportion of myeloid mature cells of host origin, that may suggest some residual or retained functionality of the host's original hematopoietic system. (**Figure 16E**).

By examining host-derived lymphoid populations, we found out that most of these cells pertained to sample GEXV11 (PZ13000129) and were also previously marked as malignant by occupancy score analysis. In this latter case, it is possible that, due to lower coverage, souporcell was not able to correctly discern the two genotypes.

3.2.4 CNV assessment with inferCNV

Our patient cohort included a number of patients that harbored chromosomal gains or losses (see **Table 3**). To further confirm that patient-specific clusters and host-derived cells were correctly labeled as malignant, we leveraged inferCNV, a bioinformatic method that can be used to identify copy number alterations by analyzing expression levels of genes across different positions of the genome in comparison to a set of reference "normal" cells. We applied this analysis to each sample individually, when clinical data was available.

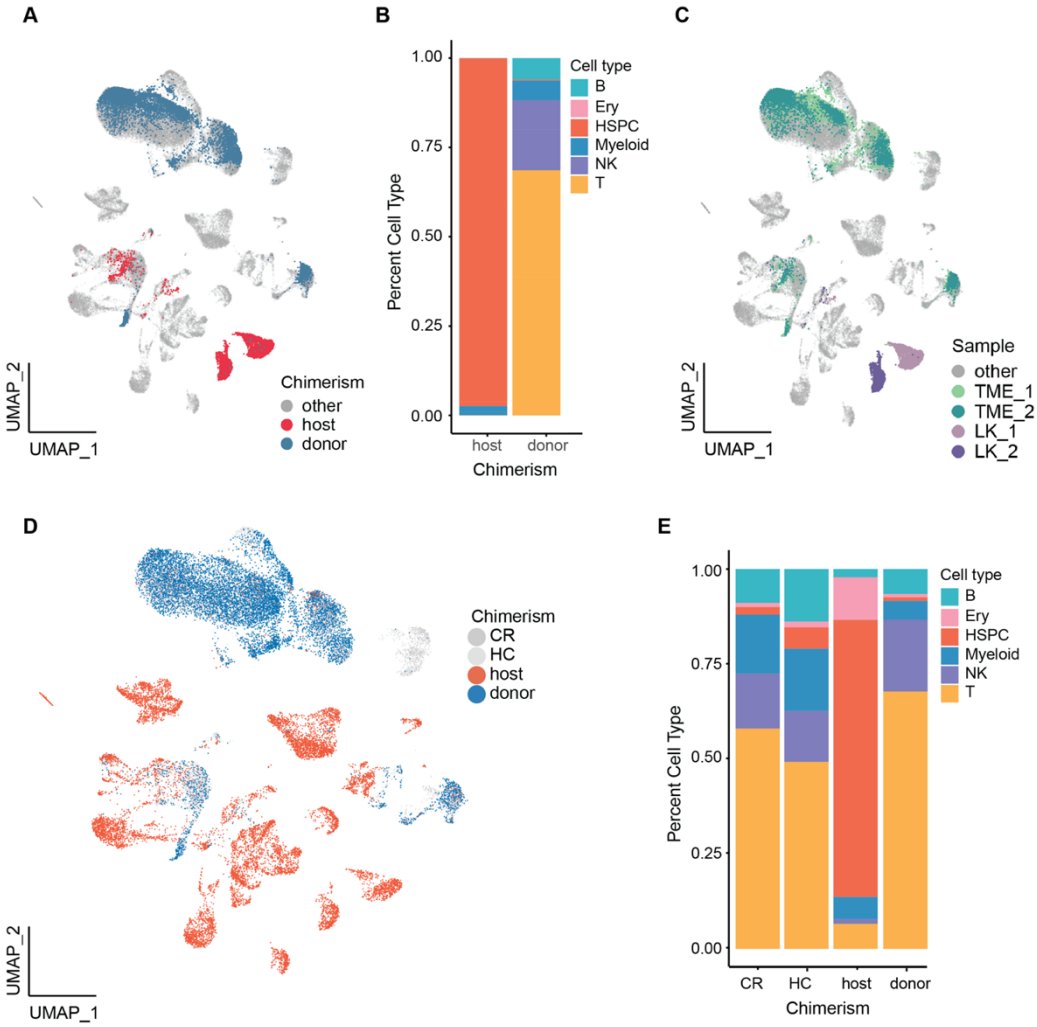

Figure 16. Souporcell benchmarking.

A) UMAP showing host and donor assignment for sorted samples. Grey cells represent other samples. B) Barplot showing cell type of host and donor-derived cells. C) UMAP showing cells from sorted samples. D) Global UMAP showing host and donor assignment for each AML sample. E) Barplot showing cell type fraction of host, donor, HC and CR cells.

InferCNV was able to detect large scale chromosomal aberrations, such as deletion of chromosome 7 in PZ190045 (**Figure 17A**). Recapitulating our previous findings, CNV+ cells were mainly located in patient-specific clusters, while CNV- cells corresponded to lymphoid-cell populated clusters (**Figure 17B**). By combining results from each sample (**Figure 17C**), we could highlight that CNV+ cells were mainly constituted of HSPCs, erythroid progenitors and myeloid mature subsets, while CNV- cells were mainly annotated as T, NK, and B cells (**Figure 17D**). Interestingly, for some patients we detected CNV+ across lymphoid lineages, suggesting that, in these cases, CNVs occurred at early stages of hematopoietic development.

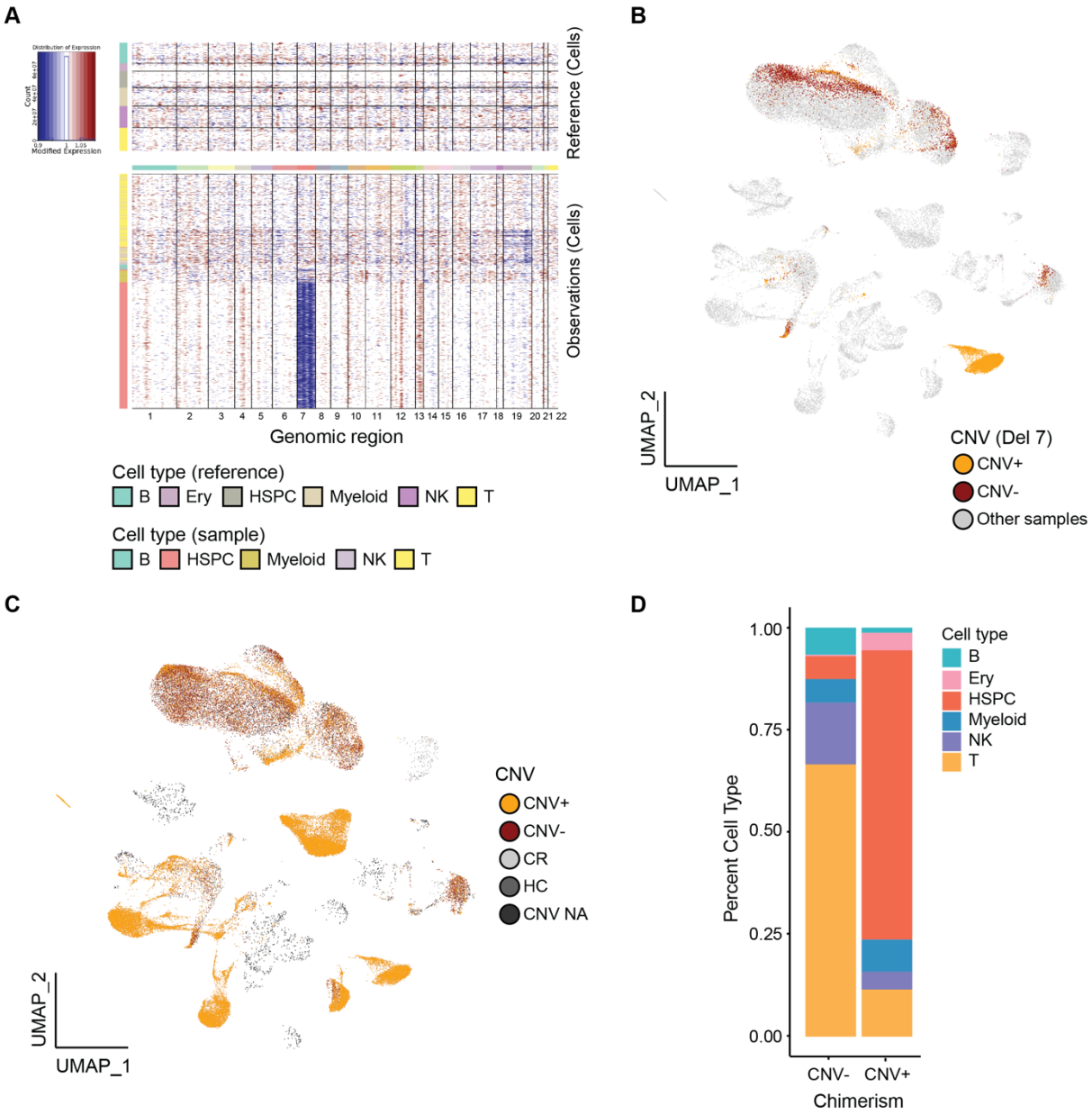

Figure 17. InferCNV to detect large chromosomal aberrations.

A) InferCNV-generated heatmap for PZ190045. It is possible to note the presence of the deletion of the entire chromosome 7 in HSPCs. B) UMAP of merged dataset showing inferCNV results for patient PZ190045. Yellow indicates CNV+ cells, red CNV- cells, and grey cells pertaining to other samples. C) InferCNV results for all samples in our cohort. Yellow and red are CNV+ and CNV- cells, respectively. Black, dark grey, and light grey show cells from samples without clinically-annotated CNV data, HC and CR. D) Bar plot showing broad cell type distribution across CNV+ and CNV- cells.

3.2.5 Malignant-ME separation

Results from occupancy score calculation, souporcell analysis, and inferCNV were combined and examined (**Figure 18A**). For those samples where CNV data was available, 71% of cells were concordantly defined as "malignant" by all three

methods, while 11% by 2/3 and 17% by only one method. Given this, we decided to consider these methods as "complementary" in malignant cell definition, rather than applying a consensus criterion. A total of 106,812 (40.5% or the whole dataset) cells were classified as malignant by either method (**Figure 18B**). Malignant populations mainly consisted of HSPCs and myeloid progenitor and mature cells, with a small fraction of B, T and NK cells (**Figure 18C-D**). Thanks to these three methods, we were able to confidently split malignant and microenvironment cells in 24 out 25 AML patients. PZ13000129, with an incomplete split, was excluded from further analysis.

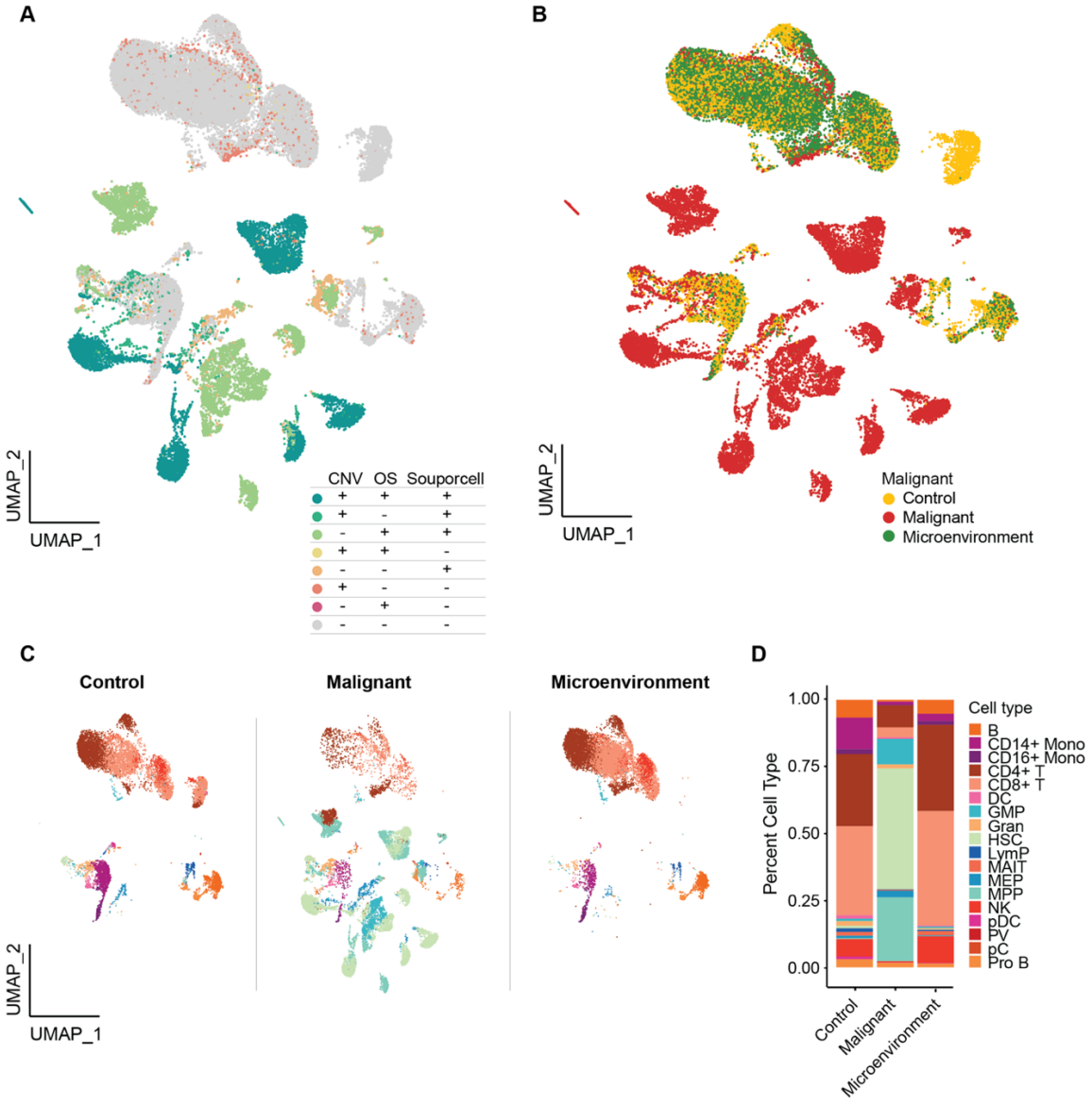

Figure 18. Malignant-ME separation.

A) UMAP of merged dataset. Cell are colored based on which method assigned them as malignant. B) UMAP showing malignant (red), ME (green) and control (yellow) cells, based on the three methods mentioned above. C) UMAP of merged dataset, colored by fine cell type annotation, split by malignant assignment. D) Barplot showing cell type proportion among the different groups.

3.2.6 Dataset split and Harmony integration

Following separation of malignant cells from the TME we sought to investigate at a higher resolution cell type populations, to better comprehend how the BM microenvironment is influenced by leukemia relapses.

We therefore split our dataset based on broad cell types (NK, T, B, myeloid mature and immature). For each broad cell type object, except for immature myeloid cells, we applied Harmony integration prior to analysis. In fact, when integrating multiple samples from different sequencing runs and library preparations, confounding factors can arise. A relevant challenge is represented by differences in expression levels of certain molecules that are the result of a different cell handling among samples, or "batches". A very common batch effect can be seen among different sequencing runs, or library preparations. In our dataset, a very strong batch effect was represented also by the employment of different chemistries and protocols across samples, and by the use of FACS sorting during sample preparation.

To account for technical variation while retaining real biological variation, numerous data integration methods exist. Harmony (Korsunsky et al. 2019), a linear-embedding model, is a well suited tool for simple integration tasks (Tran et al. 2020) (Chazarra-Gil et al. 2021). Harmony operates in a reduced-dimensional space, typically a PCA space, and considers each dataset (batch) separately to pull together cells that exhibit a similar transcriptional profile though an iterative process.

To show an example of how batch correction performs, we first tested Harmony on our whole dataset. Without batch correction, when projected onto a UMAP space, it is possible to note that cells pertaining to a specific batch tend to cluster together (**Figure 19A**). This was particularly relevant for batch #1, which was prepared with a 3' sequencing technology. Interestingly, while T and NK cells tended to suffer less from this type of confounding variable, in the case of batch 1 we could highlight a complete segregation even within these cell types. By applying Harmony correction, batch effect was notably decreased, with a more even cluster occupation (**Figure 19B**). Batch effect correction also almost eliminates patient-specific clusters and is particularly evident when looking at the more immature cell populations (**Figure 1C-D-E-F**).

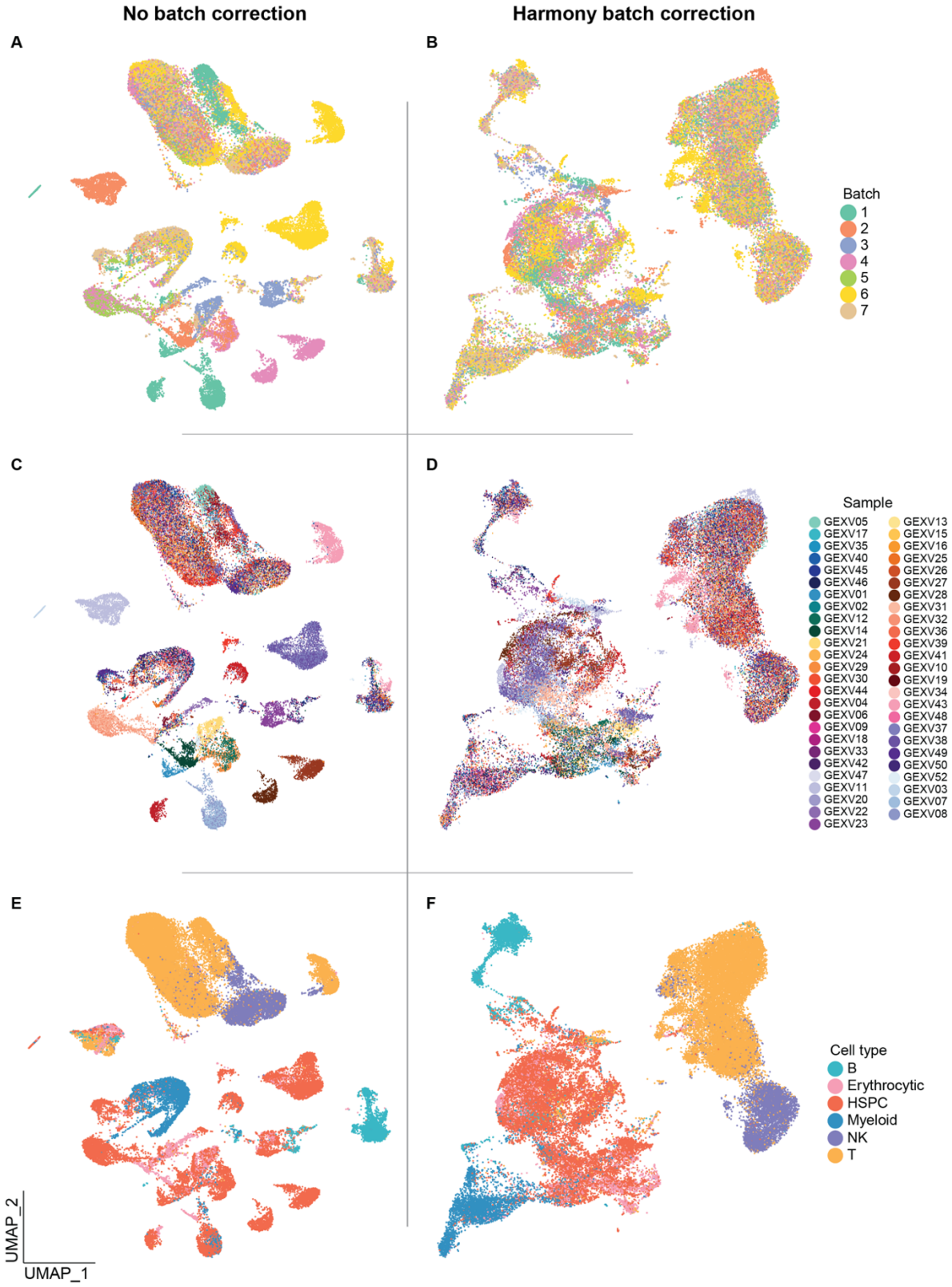

Figure 19. Effects of Harmony batch-effect correction.

On the left side, merged dataset without Harmony correction, colored by batch (upper panel), sample (middle), and cell type (lower). On the right side, UMAP with Harmony integration.

3.3 ScRNA-seq recapitulates known leukemia-intrinsic features of relapse

We obtained a total of 82,254 HSPC, of which 96% were classified as malignant by previous analysis. Following re-clustering, we aimed at exploring this major population and, by focusing on the different experimental groups, at better characterizing the different leukemia-intrinsic features of relapse. Interestingly, while HLA loss relapses, those characterized by upregulation of inhibitory ligands, and those with an unknown pattern of relapse had a tendency to distribute more evenly across the UMAP, relapses characterized by downregulation of MHC-II clustered closely, underscoring a robust transcriptional similarity among them. The tight clustering suggests that the gene expression profile found in these leukemic blasts overrides other potential differences, such as cell type or differentiation level (**Figure 20A**). We examined expression of known de-regulated genes across post-transplantation relapses (Toffalori et al. 2019b), both related to MHC-II surface expression and co-stimulatory/inhibitory molecules, to investigate whether at the single cell transcriptomic level we could confirm their mechanism of relapse. Downregulation of MHC-II patients exhibited, indeed, downregulated expression of most MHC-II genes, thereby validating the accuracy of this categorization. HLA loss patients showed a more diverse pattern of expression, with heterogeneous, but generally high, levels of expression of both MHC-related genes and costimulatory and immune checkpoint molecules. Both other relapses and those defined by upregulation of inhibitory molecules showed high expression of all sets of genes, hinting that they might have exploited common pathways to evade immune control. Moreover, strong expression of MHC-II related genes hints at the possibility that these cells were residing in a ME characterized by high levels of inflammation (**Figure 20B**). To further combine these gene expression profiles, we calculated an immune activation score measuring the capacity of a given cell to present antigens and modulate T cell responses (**Figure 20C-D**). As expected, relapses defined by upregulation of inhibitory ligands and other relapses had a higher score, compared to those with HLA loss and, more evidently, those with MHC-II downregulation. Interestingly, one patient classified as inhibitory ligands upregulation showed a very low score. This might be due to the fact that, except for HLA loss relapses, the relapse classification we used here has been validated by comparing bulk RNA-seq expression profiles at the time of relapse and diagnosis. Therefore, it is possible that, while effectively upregulating costimulatory and inhibitory molecules at the surface of these blasts

compared to the time of diagnosis, this patient's relapse might be linked to other, still unknown, pathways.

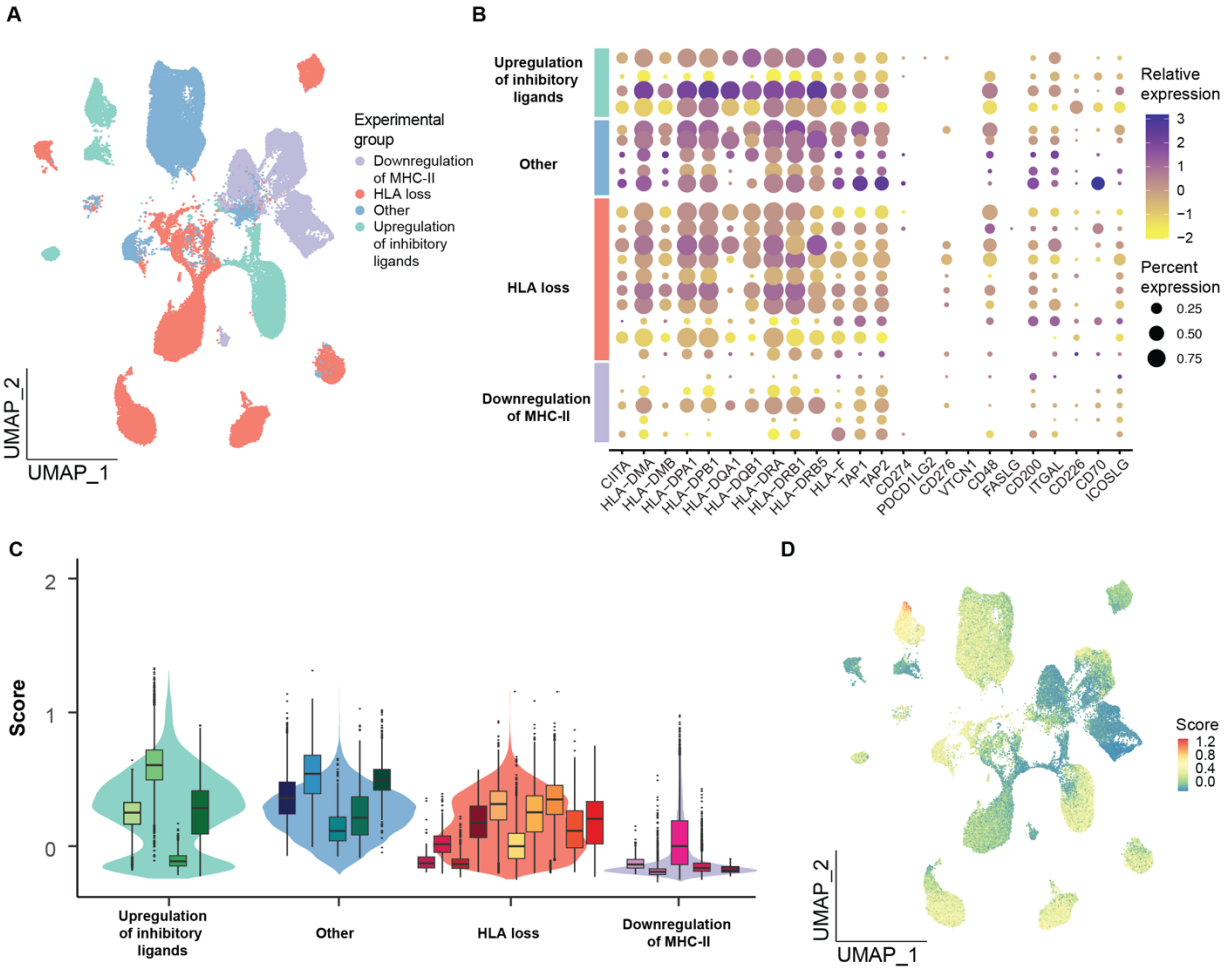

Figure 20. Overview of malignant cell population in our cohort.

A) UMAP of all malignant cells, colored by experimental group. B) Dotplot showing, for each patient in the different AML relapse groups, mean relative expression and percent of cell expressing genes related to class II antigen presentation and costimulatory/inhibitory molecules. C) Violin plots showing immune activation score of each cell, grouped by different mechanism of relapse. Box plots show values for each individual patient within the experimental group. D) UMAP showing immune activation score for each cell. Highest scores are in red, whereas lower scores are colored light blue.

To further characterize these different relapses, we looked at the distribution of leukemic cells among different cell types.

Interestingly, HLA loss relapses were characterized by a higher fraction of HSCs, while other experimental groups showed a mixed population of both early, and late progenitors (**Figure 21A-B**), suggesting that HLA loss relapses may have their origin, or main drivers, in less differentiated cells. Concordant to this finding, HLA loss showed an higher LSC17 (Ng et al. 2016) compared to other relapses (**Figure 21C**). Of note, besides defining cell stemness, the LSC17 score represents a clinical

prognostic factor that predicts resistance to commonly used first-line chemotherapy regimens and correlates with poor outcome.

To delve deeper into this observation and also evaluate the potential interplay with the ME, we implemented the iScore analysis (Lasry et al. 2023). This score provides information about inflammation-related pathways de-regulated in AML cells, and has been demonstrated to correlate with BM microenvironment "architecture" alterations, especially in T and B cell populations. Moreover, iScore has prognostic value, and can be used to stratify AML patients. Indeed, similar to LSC17, a higher iScore has been associated to poor outcomes.

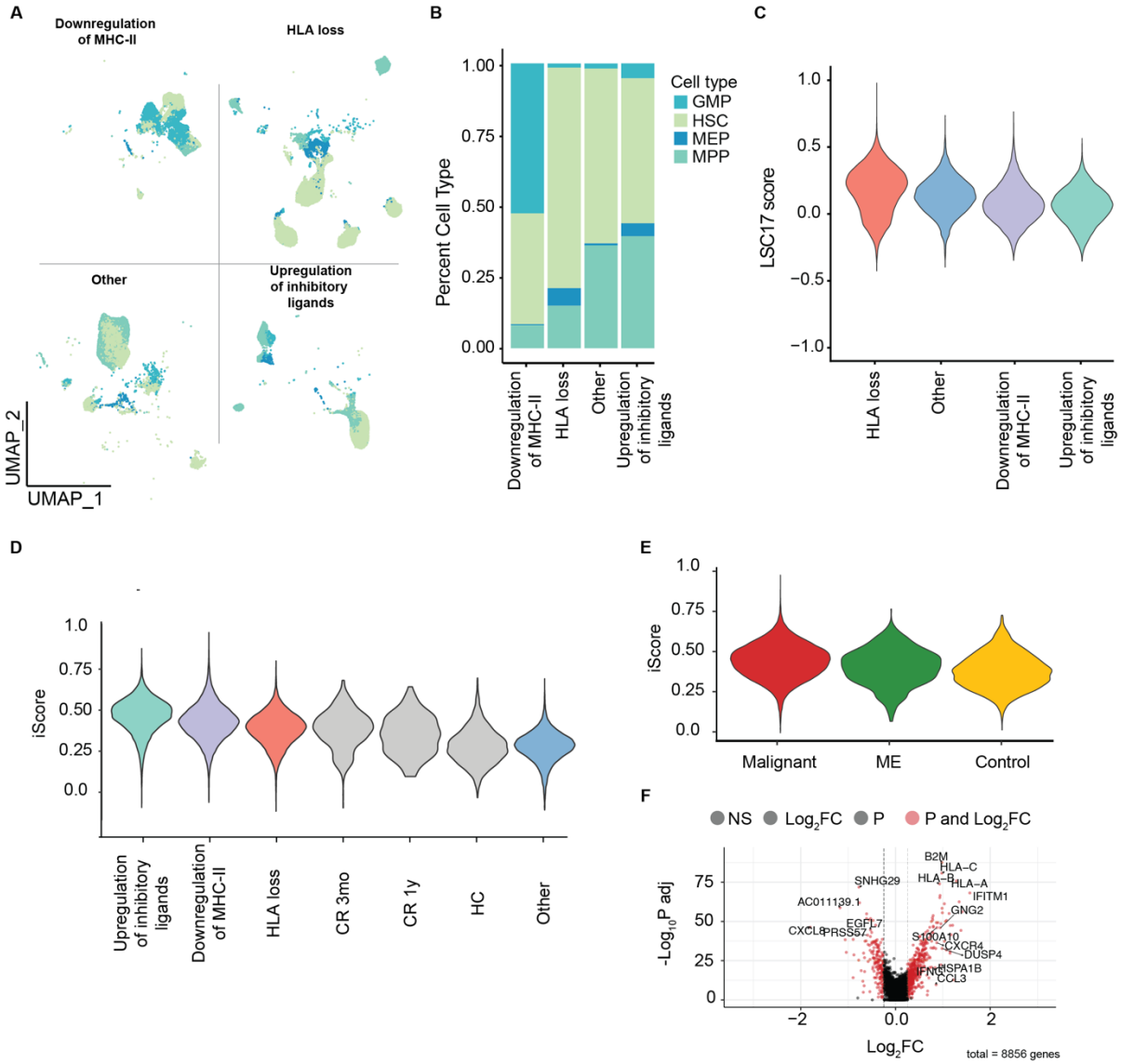

Figure 21. Leukemia stemness and inflammation scores.

A) UMAP of malignant cells, colored by cell type and split by experimental group. B) Bar plot showing relative proportion of hematopoietic precursors among different experimental groups. C-D-E) Violin plots of LSC17 score (C) and iScore. iScore was calculated both on experimental groups (D) and among malignant, microenvironment and control cells (E) F) Volcano plot showing DEGs between healthy HSPCs (microenvironment) and control HSPCs.

In our cohort, in line with previous observations, relapses characterized by upregulation of inhibitory ligands presented a higher iScore, underlining that a likely cause of immune cell dysfunction in these patients might be related to a strong pro-inflammatory BM ME.

Even more interestingly, yet uncharacterized relapses showed a lower iScore. Following our previous reasoning, we might hypothesize that while the phenotype of these relapses resembles that of patients with high immunological activation, the upstream mechanism that initiated leukemia immune evasion might not be linked to inflammation (**Figure 21D**). Last, we compared iScore also considering the immature ME. While a certain degree of difference was expected between malignant cells and ME and/or controls, we surprisingly found out that also healthy HSPCs from AML patients showed a distinctly high inflammation score compare to control cells (**Figure 21E**). By examining DEGs among these two cell subtypes, we highlight an increased expression in ME of several immune-related markers (*IFNG, IFITM*, HLA class I genes) (**Figure 21F**). These results might further reinforce the hypothesis that AML cells co-opt their TME to favor proliferation and survival.

3.4 Dynamics of NK cells in AML relapses

A total of 26,264 NK cells were isolated and reclustered.

Fine annotation was performed leveraging cluster-defining DEGs at 0.5 resolution, which returned 8 different clusters (**Figure 22A**). Based both on canonical lineage-defining markers (*NCAM1, IL7R, SELL, KLRC1, CD44, XCL1, FCGR3A, GZMK, XCL2,* and *CD160*) and published scRNA-seq NK datasets (C. Yang et al. 2019), we confidently identified three major clusters of $CD56^{bright}$, $CD56^{dim}$ and transitional NK cells (**Figure 22B**). Moreover, we identified a small population of $CD56^{bright}$ cells, that clustered separately from the rest of the cells, that we renamed as "inflamed" NK. Indeed, by looking at DEG in this group of cells, we could highlight a significant upregulation in interferon-stimulated genes compared to other NK cells. Among those with the highest log_2FC, in particular, we found *IFIT2*, *IFIT3*, *OASL* and *ISG15* (**Figure 22C**). We performed GSEA on the GO classification to characterize the functional roles and biological processes associated with the identified genes. GSEA results revealed a significant enrichment of terms related to IFN-γ response, IFN-α response, and TNF-α signaling via NFκB (**Figure 22D**). Lastly, we selected a panel of genes related to interferon and TNF signaling to be able to separate these cells from other NK cells on a transcriptomic level (**Figure 22E**). Following our refined annotation (**Figure 22F**), by looking at relative proportion of these subsets among different

post-transplantation relapses, we found a slight increase in the inflamed NK cluster in patients with upregulation of inhibitory ligands (**Figure 22G**). This increase was confirmed also when analyzing the percentage of inflamed cells across the four relapse groups and controls. Mean percentage was 5.42%, versus a mean 0.74% among all other groups, although we could observe that only in 2/4 patients with upregulation of inhibitory ligands this subtype was markedly elevated (**Figure 22H**). However, the presence of these cells within this kind of relapse sparks some interest, as it might suggest that prolonged activation and the presence of an IFN-rich inflammatory ME cause both T and NK cells to undergo processes of exhaustion, which may ultimately favor leukemia immune evasion.

Finally, we focused our attention on the relationship between NK cells and HLA loss relapses. HLA loss patients, while losing the major target of T cell-mediated alloreactivity, are still, in principle, subjected to NK cell control. The LOH mechanism does not alter overall surface expression of HLA class I molecules, thus circumventing the "missing self" NK pathway (Mace 2023), but the loss of HLA alleles might result in the loss of ligands for inhibitory KIRs, thus triggering NK cell alloreactivity (Barrett and Blazar 2009). To begin to understand the mechanisms underlying NK cell failure to respond to HLA loss relapses, we focused on the $CD56^{dim}$ cluster. These cells, in fact, are believed to be a direct progeny of $CD56^{bright}$ NK cells (Freud, Yu, and Caligiuri 2014), and are characterized by a far greater cytotoxic capacity (Cooper, Fehniger, and Caligiuri 2001). HLA loss are generally late relapses (Crucitti et al. 2015). In our cohort, median time from transplant to HLA loss relapse was 517.5 days (range 124-1186), similar to that of unknown relapses (median 693 days, range 56-1093), while both relapses characterized by downregulation of MHC-II and upregulation of inhibitory ligands had significantly shorter time to relapse (**Figure 23A**).

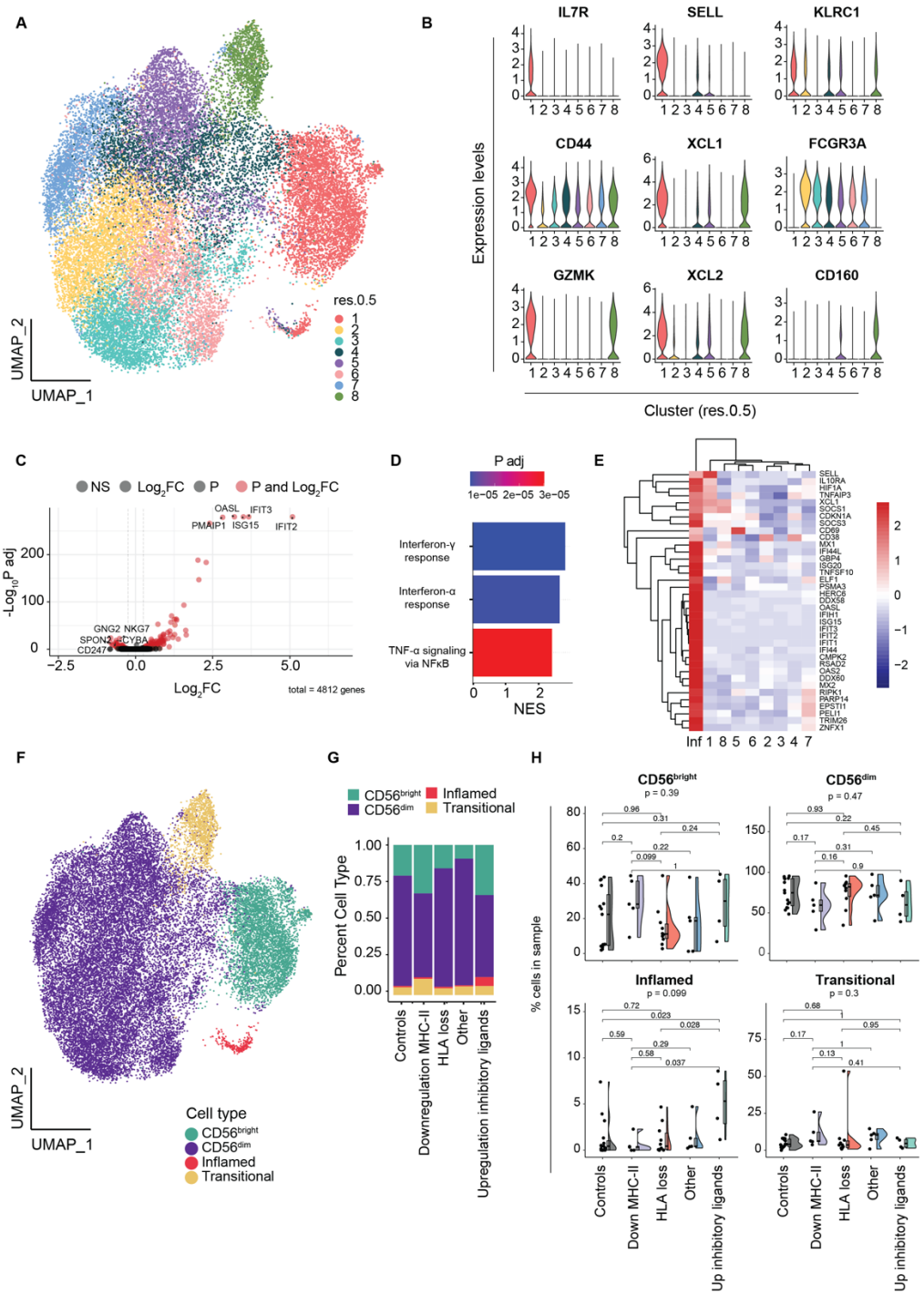

Figure 22. NK subtypes characterization.

A) UMAP of all NK, colored by clusters calculated at resolution 0.5. B) Violin plots showing canonical markers used for refined cell annotation. Cluster 1, not expressing FCGR3A, was classified as CD56bright. Cluster 8, which showed an intermediate gene expression profile between CD56bright and the other clusters, was assigned as transitional NK. Remaining clusters shared very similar gene expression profiles, and were therefore annotated as CD56dim. C) Volcano plot of inflamed NK versus all other NK cells. Red dots depict significantly de-regulated genes. D) Bar plot showing enriched GO terms obtained from GSEA of DEGs in inflamed NK versus other NK. E) Heatmap of selected IFN- and TNF-related genes that characterize inflamed NK cells. F) UMAP of all NK, colored by refined annotation. G) Bar plot showing NK subtypes relative proportions across experimental groups. (continues)

H) Raincloud plots depicting each NK subtype percentage across experimental groups. Dots represent individual patients. Global p values for each graph were calculated via Kruskal-Wallis non-parametric test, whereas multiple pair-wise comparisons were performed with Wilcoxon Rank sum test.

Given the later onset of HLA loss relapses, we hypothesized that the CD56^{dim} subset would assume a more dominant role over its CD56^{bright} counterpart. As a matter of fact, we observed a steep decline in CD56^{bright} proportion over time to transplant ($R = -0.61$, $p < 0.001$), also supporting the theory that these cells are immature precursor to CD56^{dim} NK (**Figure 23B**). Last, using recently published gene signatures of NK cell activation markers (Ni et al. 2020) (Crinier et al. 2021) (Duault et al. 2021) (L. Li et al. 2023), we generated a module score to test the functional properties of CD56^{dim} NK cells in our cohort. While, expectedly, HC exhibited a low score, CR samples showed a much higher activation profile, similar to that of upregulation on inhibitory ligands relapses. Interestingly, HLA loss relapses showed a very low score, providing evidence that NK cells in these relapses are, in fact, unable to counteract leukemic cells (**Figure 23C**).

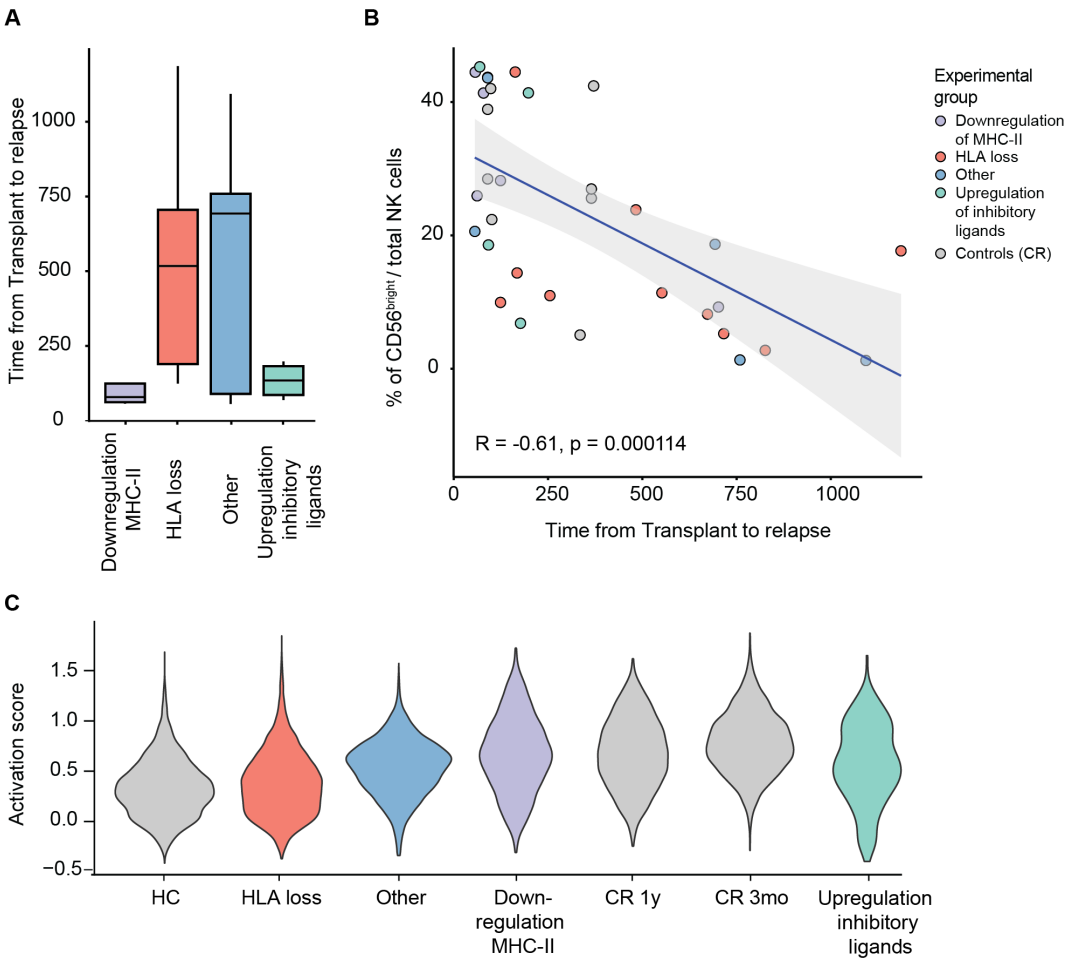

Figure 23. Dynamics of different subset of NK cells in AML relapses.

A) Box plot showing time to relapse in each experimental group. B) $CD56^{bright}$ percentages over time following transplantation. Dots indicate each patient and are colored by experimental group. Regression line was calculated using a linear regression model. Gray area shows confidence intervals. C) Violin plots showing NK activation score for each cell in our different experimental groups.

3.5 T cell responses in AML relapses

Following reclustering, we isolated 93,062 T cells. T cells were annotated and separated into major subtypes, including, for both CD4 and CD8, T_{EMRA} (terminally differentiated effector memory), T_{EM} (effector memory), T_{CM} (central memory) and $T_{naïve}$ (naïve). Moreover, we were able to define a population of MAIT (mucosal-associated invariant T) cells, T regulatory cells (Treg) and a subset of CD8 T_{EM} cells enriched in inhibitory receptors, in particular *TNFRSF9, TIGIT, VCAM1, CTLA4, LAG3, TOX, PDCD1,* and *CD38*, and that was therefore defined as $T_{EM.EX}$ (effectory memory exhausted) (**Figure 24A**). We compared T cell subset distribution across different experimental groups. Among CD4 subsets we observed an expected higher fraction of $T_{naïve}$ cells in HCs, although not reaching statistical significance. Among CD8 subsets, relapses with MHC-II downregulation were enriched in T_{EM}, while relapses with upregulation of inhibitory ligands had an increase in $T_{EM.EX}$ cells. Although differences were not statistically significant, Tregs were higher in patients in CR at 3mo, in agreement to the fact that these are the T cell subset to reconstitutes earlier in the post allo-HCT setting (Dekker et al. 2020) (**Figure 24B-C**).

Finally, we leveraged scRepertoire (Borcherding, Bormann, and Kraus 2020) to delve into clonotype analysis of T cells. ScRepertoire allows processing of data derived from 5' TCR immune profiling and integration with Seurat gene expression analysis. First, we looked at the clonotypic frequencies of T cells. We observed a marked clonal expansion of CD8 T cells, in particular sustained by T_{EM} and T_{EMRA}, while CD4 T cells mainly consisted of rare clones (**Figure 25A-C-D-E**).

By analyzing the interconnection between different T cell subsets, we could also highlight that T_{EM} and T_{EMRA} share a large part of their clonotypes, suggesting that T_{EM} cells that undergo expansion following leukemic cell recognition might subsequently differentiate into T_{EMRA}, generally characterized by a higher cytotoxic capacity. The low degree of clonotype sharing between CD4 and CD8 T cells corroborates our subset annotation.

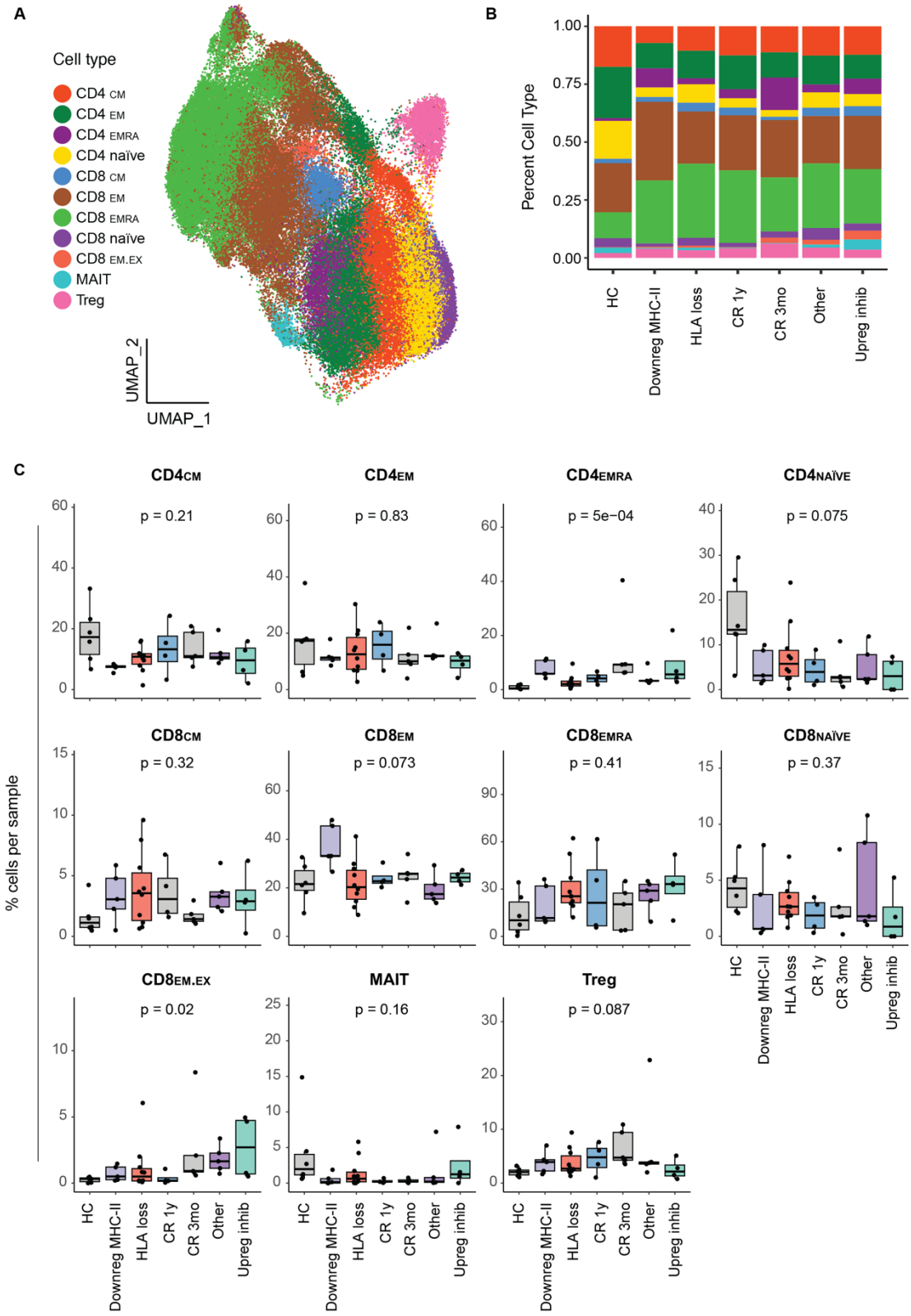

Figure 24. Distribution of T cell subsets

A) UMAP projection of T cells, colored by subset. B) Bar plot showing relative proportion of T cell subsets across experimental groups. C) Box plot of relative percentages of each T subset across experimental group.

Looking in detail at clonotype quantification, we first observe that, in our dataset, T_{EMRA} and T_{EM} consisted mostly of hyperexpanded (> 100 cells) and large (> 20 cells) clones (**Figure 25C**), with less than 20% and 40% rare clones, respectively (**Figure 25D**). Accordingly, both of these T cell subtypes were also characterized by the lowest values of Shannon and inverse-Simpson indices. The latter are measures of diversity that take into account both richness (number of clonotypes) and evenness (how evenly are cells distributed across the different clonotypes). More in general, we see that CD8 T cells feature more expanded clonotypes than CD4 T cells, similar to what observed in a different AML cohort (Apostolova et al. 2023).

Interestingly, $T_{EM.EX}$ were largely composed of rare cell clones, possibly indicating that exhaustion and shrinkage of this T cell population is an early event in the pathogenesis of AML relapse

Last we analyzed TCR repertoire across different experimental groups (**Figure 26)**. Relapses characterized by MHC-II downregulation were characterized by a larger proportion of hyperexpanded and large clones, with only 30% unique clonotypes. This finding was also reflected by lower values of Shannon and inverse Simpson indices. On the other hand, relapses with upregulation of inhibitory ligands showed a higher percentage of unique clonotypes, and were mainly composed of rare and small TCR clone types, and as a consequence a higher value of both Shannon and inverse Simpson indices. This latter finding is in agreement with the proposed immune escape mechanism, where leukemia recognition by the immune system is stunned by IR expression, and T cell activation and expansion is prevented.

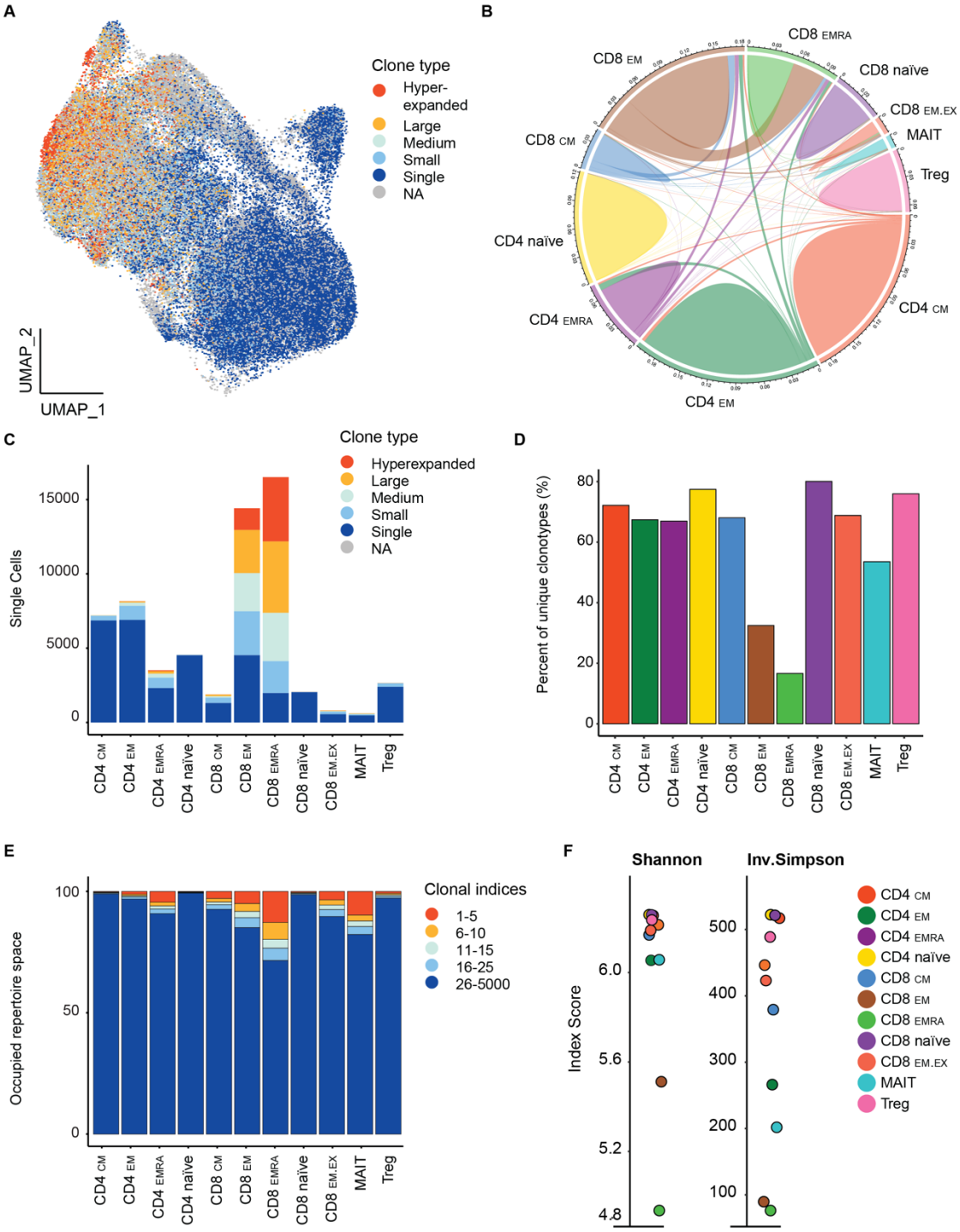

Figure 25. Clonotype analysis on T cell subsets with scRepertoire.

A) UMAP projection of T cells, colored according to the size of the TCR clone they belong to (clone type: hyperexpanded (100 <X <= 10000), large (20 < X <= 100), medium (5 < X <= 20), small (1 < X <= 5), single (X = 1)). B) Chord diagram representing shared TCRs among different T subsets. Each fragment of the outer part of the circle represents a T subset. Size of the arc is proportional to the number of shared TCRs. C)Bar Plot showing absolute numbers of T cells for each subset, colored according to clone type. D) Percent of unique (single) clonotypes for each T subpopulation. E) Fraction of T cell belonging to a specified clone type bin, grouped by T subset. For example, in CD8 T_{EMRA} the first 5 more abundant cell clones account for approximately 15% of the total cells. F) Dot plot showing Shannon and inverse Simpson index scores for each T subtype.

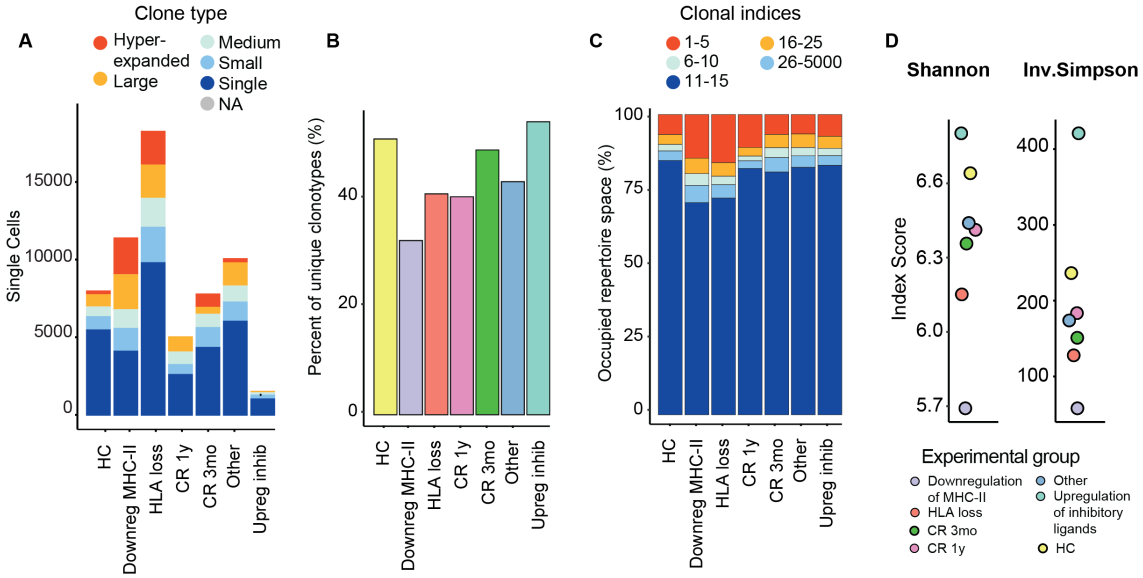

Figure 26. Clonotype analysis on experimental groups with scRepertoire.

A) Absolute numbers of T cells for each experimental group, colored according to clone type of pertinence. D) Percent of unique clonotypes for each experimental group. E) Fraction of T cell belonging to a specified clone type bin, separated by experimental group. F) Dot plot showing Shannon and inverse Simpson index scores for each experimental group.

4 DISCUSSION

Allogeneic hematopoietic cell transplantation (allo-HCT) currently represents the most effective treatment for high-risk malignancies such as acute myeloid leukemia (AML). Despite the advances in the clinical management of patients, and the increasing understanding of the biology underlying allo-HCT success, its efficacy is dramatically hampered by disease relapse. As of today, despite the increasing availability of potentially promising therapeutic options, prognosis for patients that experience disease recurrence is dismal, with a 2-year survival<15% (Webster, Luznik, and Gojo 2021).

Several factors complicate the already difficult management of AML relapses following allo-HCT. In particular, a previously unappreciated layer of complexity is related to the recent observation that post-transplantation relapse may occur through a number of alternative and largely mutually-exclusive modalities, each obeying to a different biology and, possibly, requiring a different therapeutic approach (Toffalori et al. 2019a; Vago 2019).

The epicenter of the attention, when trying to understand how to fight back AML relapses, has so far been the interaction between blasts and T cells. Graft versus Leukemia (GvL) effect, in fact, is strictly linked to the presence of donor's T lymphocytes, which recognize incompatible MHC molecules, minor histocompatibility antigens, and tumor-associated antigens on the surface of leukemic blasts and eliminate them (Dickinson et al. 2017).

Nonetheless AML develops, and is sustained by, a specialized bone marrow (BM) microenvironment, that comprises a number of immune cell subsets together with mesenchymal stromal cells, vascular endothelial cells, osteoblasts, sympathetic nerve fibers, and non-myelinating Schwann cells (Morrison and Scadden 2014). How this rich microenvironment collaborates with or adapts to the selective immune pressure driven by the transplant, and why it fails to enact measures to counteract leukemia immune escape, is still largely unknown.

Single-cell technologies are rapidly revolutionizing almost every field of biomedical research. Since their first applications, the development of droplet-based techniques and, in parallel, the refinement of computational tools has significantly expanded our ability to interrogate cellular heterogeneity at an unprecedented resolution. Rather than observing the average behavior of a multitude (bulk) of cells, it is now possible to dissect the intricacies of individual cells. This granular approach has paved the way for the generation of comprehensive human cell atlases, providing a detailed roadmap of cell types, states, and interactions, offering invaluable insights into

human biology, and, importantly, disease (Sikkema et al. 2023) (Regev et al. 2017) (Snyder et al. 2019).

In this work, we aimed at generating comprehensive atlases of the bone marrow of different post allo-HCT relapses, with the ultimate goal of providing insights into how the leukemia microenvironment undergoes dynamic changes in response to allo-HCT and how these alterations may contribute to its resurgence according to different mechanisms.

Understanding the interplay between the diverse cellular components of the BM is of paramount importance. Not only does it provide a snapshot of the local environment during relapse but also sheds light on the potential protective or permissive roles these cells play in the context of disease progression. Moreover, exploring the unique transcriptomic signatures of individual cell populations within the BM can illuminate the molecular pathways that are activated or suppressed within AML post-transplantation relapses.

In the present study, we leveraged a droplet-based 3’ and (for most patients) 5' sequencing platform to profile BM samples from a diverse cohort comprising 36 patients. Of these, 25 patients, previously diagnosed with AML and having undergone allo-HCT, experienced disease relapse, while 5 patients maintained a stable complete remission (CR) for a minimum of one year post-transplantation, providing insights into the BM landscape that characterizes a successful therapeutic response. To further reinforce the validity of our findings, we incorporated samples from healthy controls (HC). Cells from this latter control cohort represent the “normal” bone marrow ME, free from the complexities of AML or post-transplant alterations.

Alongside capturing whole transcriptomic data, the 5' sequencing approach also allowed us to simultaneously sequence the T-cell receptors (TCRs) and B-cell receptors (BCRs) of our patients, which potentially enables analysis of diversity, clonality, and antigenic targets of the adaptive immune cells present in a dataset (Singh et al. 2019).

Despite its advantages, scRNA-seq presents many challenges, especially related to its heavy computational component (Lähnemann et al. 2020). Sparsity of data (Bouland, Mahfouz, and Reinders 2023), batch effects, dealing with doublets or multiplets, reproducibility (Gibson 2022), ambiguity in cell type annotation, and large datasets handling are just a few of the problems that might complicate distinguishing real biological variation from technical artifacts.

To account for this, our first efforts have been aimed at developing a robust pipeline that entailed the utilization of multiple tools to generate a reliable dataset (at the cost of parting with quite a few cells along the way).

We first relied on soupX (Young and Behjati 2020) for ambient mRNA contamination correction. For doublet and multiplet removal, we used two methods, scDblFinder (Germain et al. 2021) and souporcell (Heaton et al. 2020), which allowed us to notably improve our droplet assignment. In line with current best practices (Luecken and Theis 2019), the processed data then underwent quality control using Scater (McCarthy et al. 2017), that allowed us to control for multiple QC variables at once.

Following QC procedures, we delved into the equally critical and intricate task of cell annotation. Assigning accurate cellular identities is paramount in scRNA-seq pipeline, and more than 200 bioinformatic tools have been developed for this purpose (https://www.scrna-tools.org/). Incorrect or imprecise annotations can misguide downstream analyses and interpretations. To account for this challenge, we implemented a three step approach: first, we used SingleR's automated framework (Dvir Aran, Aaron Lun, Daniel Bunis, Jared Andrews, Friederike Dündar n.d.) While singleR allows for quick cell type annotation for multiple samples in parallel, it remains an unsupervised approach, applied to a dataset that, although "cleaned" of low-quality cells, is still extremely complex. Moreover, an inherent limit of this method is the reliance on single references, that, especially when dealing with heterogeneous samples or rare cell types, might lead to misclassification. We partially solved this problem by incorporating a gene set score approach: using published scRNA-seq data of AML BM samples, we built our own reference dataset (see Methods section), and calculated average expression of selected genes across cells that cluster together (and that are, therefore, similar at a transcriptomic level), to identify those that shared a more similar expression to that of the reference. While this model allowed us to incorporate more BM-specific subtypes in our classification, it raised an important question: how personal can, or should, reference-mapping be? The risk with this kind of approaches, indeed, is to confound tailoring with overfitting. To account for this, we combined these two approaches with manually curated marker analysis.

Following quality control and annotation procedures, we obtained a merged dataset that offered a comprehensive view of the bone marrow immune landscape in AML relapses. By looking at cell type distribution, we observed a shift in the bone marrow composition during AML relapses, indicative of the dynamic interplay between malignant cells and the surrounding microenvironment. Apart from an expected increase in myeloid progenitors, we also saw a significant decrease in the B cell fraction. Although humoral immunity has traditionally less relevance than T cell-mediated immunity in the context of allo-HCT, recent reports have highlighted a

contribution of certain B cell subsets in determining poor prognosis in AML (Lv, Wang, and Liu 2019), and CLL (DiLillo et al. 2013). Moreover, a similar decrease in B cell fraction in the BM, with a relative increase in the proportion of atypical pre-B and pro-B cells has been shown to promote a suppressive milieu in the microenvironment in AML patients (Lasry et al. 2023). We next sought to separate malignant AML cells from their immune ME. To do so, we used three different methodologies. First, we took advantage of the observation that leukemic cells' distinctive transcriptional signature inherently led them to cluster separately, allowing for an intrinsic differentiation from their immune counterparts. Next, we borrowed the concept of mixed chimerism from the clinics: transplanted patients, indeed, present the unique feature of hosting cells from two different organisms, where long-lived, stromal, and malignant cells are of recipient origin, while most immune cells are of donor origin (Deeg 2021). We resorted to souporcell (Heaton et al. 2020), first by successfully validating this method by exploiting the presence in our dataset of sorted samples from two different patients. Last, we applied CNV analysis with inferCNV (Timothy Tickle and Itay Tirosh, n.d.), first validating this method by comparing our results with clinical data, and then identifying malignant cells that carried large chromosomal aberrations.

Upon re-clustering the major population of HSPC, distinct patterns emerged regarding leukemia-intrinsic features of relapse. We highlighted a pronounced clustering of relapses with MHC-II downregulation, pointing to a specific transcriptional profile that trumps other cellular differences. This dominant clustering might suggest a more "clonal" structure of AML cells compared to other types of relapses (at least from a transcriptomic point of view), where all blasts share the same mechanism of immune evasion. Therapeutic targeting of these clones might thus potentially lead to eradication of AML in MHC-II downregulation relapses, which account for up to 50% of all relapses following allo-HCT (Toffalori et al. 2019b). Recent reports have used different strategies to rescue MHC class II surface expression, enabling CD4+-mediated leukemia recognition, either by pharmacologic inhibition of PRC2 subunits (an important epigenetic driver of this immune escape modality) (33), or leveraging T cell immunotherapies to induce local release of IFN-γ (34).

Importantly, we were also able to validate both downregulated MHC-II expression and upregulation of inhibitory ligands at the single-cell level, underscoring the robustness of this rather recent AML relapse categorization. This seems of particular relevance as, so far, these relapses were defined by their relative down or upregulation compared to paired pre-transplant samples. Validating these definitions

independently of a diagnosis' sample, holds promise for swifter and more effective therapeutic interventions, tailored specifically to the relapse profile.

Additionally, the immune activation score we defined offered a more nuanced functional perspective on malignancy characteristics in different relapse types. Relapses characterized by upregulated inhibitory ligands presented higher immune activation scores, indicating a heightened capacity to modulate immune interactions. While elevated expression of these molecules confirms their dependency on this mechanism for immune evasion, it also possibly hints at their vulnerability towards, for example, immune checkpoint inhibitors (ICIs). ICIs, following their success in solid tumors, have recently been tested in the post allo-HCT setting (Apostolova et al. 2023; Albring et al. 2017; Köhler et al. 2021), yielding inconsistent results. While the so far limited success of ICIs in AML post all-HCT underscores once again the complexity of immune evasion mechanisms in AML, it might also indicate that a more tailored therapeutic strategy aimed specifically at patients who suffer relapse driven by upregulation inhibitory ligands, may lead to better outcomes.

It should be noted, however, one outlier patient in our cohort exhibited a low immune activation score despite inhibitory ligand upregulation, emphasizing once again the complexity of relapse mechanisms and the potential existence of yet unidentified pathways influencing relapse.

We then examined the cellular composition across the different leukemia relapses. Notably, HLA loss relapses were shown to be predominantly characterized by Hematopoietic Stem Cells (HSCs), suggesting that these relapses may originate from a more immature cell, while other experimental groups showed a more mixed population, further suggesting that not all relapses are driven by the same cellular mechanisms or originate from the same progenitor cells. While it has already been demonstrated that AML relapses can arise from cells at different stages of hematopoietic maturation, ranging from more hematopoietic stem/progenitor cell phenotypes to immunophenotypically committed leukemia cells (Shlush et al. 2017), these findings may suggest a correlation between mechanism of relapse and leukemia cell of origin. Moreover, cells at different stages of maturation not only possess distinct molecular signatures but also exhibit diverse functional roles, influencing their interaction with the tumor microenvironment, response to therapy, and potential to drive disease progression (Galen et al. 2019). This multifaceted genetic backdrop necessitates a tailored therapeutic strategy. Especially in cases of less differentiated AML, the therapeutic aim should not be limited to eradicating the predominant tumor cells but also include efficient targeting of cancer stem cells.

To further confirm our findings, we evaluated the LSC17 metric (Ng et al. 2016). The elevated LSC17 scores associated with HLA loss relapses underscore not only the inherent "stemness" of this mechanism of relapse, but also add prognostic value, given the established association of the LSC17 score with resistance to frontline chemotherapeutic regimens.

Building on this, we also calculated the iScore (Lasry et al. 2023) on our different experimental groups, focusing on perturbed inflammation-associated pathways. The observed higher iScore in relapses characterized by upregulated inhibitory ligands further confirmed the strong relationship between immune cell dysfunction and a heightened pro-inflammatory BM ME. Interestingly, uncharacterized relapses exhibited a lower iScore, contradicting our previous hypotheses based on the immune activation score, and suggesting a mechanism of relapse that seems detached from established inflammatory pathways. The data thus underscores the importance of a comprehensive investigation into these uncharacterized relapses to bridge the knowledge gap. Finally, we compared iScore metrics between the healthy HSPC counterpart of AML patients and our CR and HC controls. Strikingly, these BM ME cells exhibited an enriched inflammatory signature, as evident both by the iScore value and DE analysis, indicating that the ME is intricately involved in the inflammatory process. However, whether it is the AML that initiates this inflammation in the ME or rather it is a pre-existing inflammatory state of the ME that contributes to the onset of AML remains unknown.

In the next section of our work, we focused on the BM ME lymphoid populations.

Starting from NK cells, we were able to identify a small subpopulation of $CD56^{bright}$ cells that exhibited a different transcriptional profile compared to the other $CD56^{bright}$. At a closer examination, these cells showed a pronounced upregulation of IFN-stimulated genes in contrast to their counterparts, in particular *IFIT2, IFIT3, OASL*, and *ISG15*. To unravel the underlying biological pathways these genes might influence, we performed GSEA analysis. Our findings highlighted a pronounced enrichment in processes associated with IFN-γ response, IFN-α response, and TNF-α signaling via NFκB, leading us to identify them as "inflamed" NK. Interestingly, by looking at NK subtype distribution among experimental groups, we could highlight an increase in inflamed NK especially in those cases marked by the upregulation of inhibitory ligands. On average, the inflamed subtype constituted 5.42% of total NK in this experimental group as opposed to a 0.74% mean across other groups. Yet, it's noteworthy that this marked increase was observable in only 2 out of 4 patients with upregulation of inhibitory ligands. Interestingly, this NK cell subtype has already been described in another study (C. Yang et al. 2019), where it was found in the BM

of a healthy donor. The presence of these inflamed NK cells in this specific relapse type, coupled with the previous observation of an elevated immune activation and iScore, may suggest that sustained immune activation, coupled with an IFN-rich inflammatory ME, might steer both T and NK cells towards an exhaustion trajectory. This exhaustion can potentially play into the hands of leukemia, facilitating its immune evasion mechanisms.

Although the role of NK cells alloreactivity in the allo-HCT setting has not yet been clarified, they're the first lymphoid compartment to reconstitute, and their successful recovery is associated to protection against relapse. In particular, the role of NK cells might be pivotal in the prevention of HLA loss relapses. Here, we delved deeper into the dynamics of NK cell subsets, especially the relationship between $CD56^{bright}$ and $CD56^{dim}$ cells. Our findings further support the prevailing hypothesis that $CD56^{dim}$ cells are the direct progeny of $CD56^{bright}$ NK cells. We observed a consistent decline in $CD56^{bright}$ proportion with time after transplant. This transition, which we observe both in experimental and control groups, could be indicative of a maturation process rather than representing a response to specific environmental cues during immune reconstitution. Finally, focusing on $CD56^{dim}$ NK functional characteristics, we leveraged previously published data to formulate a score to gauge their activation status. Strikingly, HLA loss relapses showed a lower activation score, suggesting functional impairment of this subset. This reduced functionality could be a critical factor contributing to the inability of the immune system to effectively combat HLA loss relapses. Further research would be essential to decipher the exact mechanisms behind this functional impairment and its implications for patient outcomes.

Lastly, we analyzed the dynamics of T cell responses in AML relapses. We were able to confidently characterize major subsets for both CD8 and CD4 T cells, including Tregs, T_{EMRA}, T_{EM}, T_{CM}, and $T_{naïve}$. Of particular interest, we annotated a subset of CD8 T_{EM} cells that exhibited an exhausted phenotype ($T_{EM.EX}$), characterized by upregulation of *TNFRSF9, TIGIT, VCAM1, CTLA4, LAG3, TOX, CD38* and PDCD1.

Notably, relapses characterized by upregulation of inhibitory ligands exhibited a pronounced enrichment in this T cell subset. Interestingly, supporting previous evidence that the relapse mechanisms here described are mutually exclusive (Toffalori et al. 2019b), $T_{EM.EX}$ were not observed in other experimental groups. We also observed an enrichment in T_{EM} in relapses characterized by MHC-II downregulation.

Finally, we exploited 5' TCR immune profiling data to characterize the TCR repertoire in the BM of AML relapses. Examination of clone distribution showed a pronounced clonal expansion within CD8 T cells, predominantly driven by T_{EM} and T_{EMRA}. In

contrast, CD4 T cells largely comprised of rare and small clones. Further examination of expanded clones, unveiled a large overlap in T_{EM} and T_{EMRA} clonotypes, implying a potential differentiation trajectory where T_{EM} cells, following leukemic cell recognition and subsequent expansion, might mature into T_{EMRA} cells, with an enhanced cytotoxic potential. Interestingly, $T_{EM.EX}$ were predominantly composed of rare clones, supporting the possibility that the strong pro-inflammatory milieu that features relapses with upregulation of inhibitory ligands (found enriched in this subset) impede these T cells from effectively recognizing and responding to leukemia antigens in their early stages of activation.
Assessment of clonotype frequencies across experimental groups revealed unique immune responses in AML. Relapses with MHC-II downregulation were characterized by large and hyperexpanded clones. Conversely, AML relapses showing upregulated inhibitory ligands presented a diverse and even TCR repertoire, supporting the evidence that this mechanism of relapse hinders T cell activation and proliferation.

In conclusion, in the present work we leveraged single cell technology to characterize the BM microenvironment of a vast cohort of leukemia post-transplantation relapses. We successfully described different mechanisms of leukemia relapse at the single-cell transcriptomic level, including upregulation of inhibitory ligands and downregulation of MHC-II, and provided insights into how these different mechanisms are intertwined to the surrounding milieu. We highlight an important, and previously unreported, role of inflammation in shaping the transcriptional profile of leukemia relapses, and provide indirect proof that different relapses may arise from progenitor cells at diverse stages of hematopoietic maturation. Last, we describe how the immune BM populations are reshaped following disease recurrence and allo-HCT, both in terms of cell composition, and functional remodeling.

Overall, while an in depth understanding of whether leukemia relapse is caused by an inflamed microenvironment, or *vice versa*, might only be achieved through longitudinal sampling from patients before and after transplant, our results here exemplify how the BM niche could be exploited to find novel vulnerabilities in AML relapses, and inform future therapeutic strategies.

5 MATERIALS AND METHODS

5.1 Ethical regulation

This study complies with all relevant ethical regulations and was approved by the San Raffaele Ethic Committee.

5.2 Human patient samples

5.2.1 Frozen human BM mononuclear cell preparation

Cryopreserved, anonymized BM aspirates from patients were collected upon signing off a written informed consent for banking and research use of these specimens, in agreement with the declaration of Helsinki and in accordance with the regulations of the institutional review boards of our institute (protocol HLALOSS, approved by the San Raffaele Ethic Committee on 2019). All samples were freshly processed to isolate mononuclear cells and stored in liquid nitrogen in the Ospedale San Raffaele Center for Biological Resources (protocol "Banca Neoplasie Ematologiche", approved by the San Raffaele Ethic Committee on October 6, 2010; latest amendment of June 14, 2012).

Frozen samples were thawed and transferred into nonpyrogenic, nontoxic, low-protein binding 15ml conical tubes (Falcon®) with a solution containing 1X PBS + 2% FBS + Benzonase (1:10.000 dilution). Cell suspensions were then centrifuged at 300g for 6 min at room temperature and the supernatant was discarded. Samples were then kept at 37°C for 15 min in the same solution as above, and, following centrifugation, supernatant was discarded and cells were resuspended in 1-2 ml ACK lysing buffer for 5 min on ice to allow red blood cell lysis. To quench the lysis reaction and dilute out the cytotoxic components of the ACK buffer, PBS was added at a volume 10-fold the amount of ACK buffer used. Following another centrifugation at 300g for 5 minutes, the supernatant was discarded, and cells were resuspended in PBS for downstream applications. Samples were subjected to dead cell depletion using Dead Cell Removal Kit (Miltenyi Biotec, 130-090-101), following manufacturers' instructions, and were resuspended in 1X PBS + 0.04% weight/volume BSA and kept on ice until GEM generation. Median cell vitality, assessed by automated cell-counting with Trypan Blue, was 89% (range 44-99).

5.2.2 FACS sorting

Based on prior knowledge about malignant/non-malignant ratio in the sample, prior to dead-cell removal samples from patients PZ190045, PZ160198, PZ160132, and PZ160116, were resuspended in 1X PBS + 2% FBS, labeled with antibodies and

sorted via flow cytometry using a FACS ARIA Fusion (BD Biosciences) cell sorter, in order to obtain two separate samples, one for the malignant and one for the non-malignant population. In detail, samples were labeled with the mixture of antibodies at 4°C for 20 minutes. Following incubation, samples were washed in 1X PBS + 2% FBS and resuspended in IMDM added with 10% FBS, 1% L-glutamine and 1% Pen/Strep and kept on ice until sorting.

The complete list of mAbs used in the study is provided in **Table 4**.

For sorting, a first logical gate was based on forward scatter area and height to exclude doublets, a second gate on forward and side scatter area followed by a gate on Annexin V negative cells, to exclude cells undergoing apoptotic processes. Subsequently, a gate based on patient-specific LAIP was applied to separate leukemic cells from ME cells.

Samples were sorted into 5-ml poly-propylene tubes containing 300 µl ice-cold PBS + 2% FBS. Following cell sorting, samples were centrifuged at 350g for 5 min at 4 °C.

5.3 Single-cell RNA-seq pre-processing

Except for the initial Cell Range pipeline, all downstream analysis was performed using the Seurat R package (v.5)(Hao et al. 2021b).

5.3.1 Library preparation

Libraries for samples GEXV01 to GEXV08 were prepared using Chromium Next GEM Single Cell 3' Kit v3.1. All other libraries were prepared using Chromium Single cell 5’ Immune Profiling kits (v1.1, 10x genomics) following manufacturer’s instruction and were sequenced on an Illumina NovaSeq 6000. Target cell recovery was 10,000 for each sample. For samples sequenced with a 5’ chemistry, we also performed V(D)J sequencing for paired TCR and BCR receptors.

5.3.2 Cell Ranger

Read alignment, filtering, feature-barcode matrices generation, UMI counting and initial clustering (used for SoupX) were performed using Cell Ranger v7.1.0 (10X Genomics)(Zheng et al. 2017). For each sample, `cellranger mkfastq` was run on the Illumina BCL output folder to generate FASTQ files. Then, for libraries processed with Chromium Next GEM Single Cell 3’ chemistry and for those processed with a 5’ chemistry that belonged to sorted leukemic samples, we used `cellranger count` to generate single cell feature counts, whereas for libraries processed with a

5’ chemistry that featured also TCR and BCR profiling we used `cellranger multi`, which enables simultaneous sequence assembly and paired clonotype calling on the V(D)J repertoire, and generation of GEX data.

More in detail, the `cellranger multi` pipeline, by discarding cells in the V(D)J dataset that are not also called in the corresponding 5’ GEX library, decreases overcalling issues that typically arise in V(D)J data, mainly due to background contamination caused by dead cells or cell-free DNA, resulting in a more consistent cell calling between these two. Both `cellranger count` and `cellranger multi` were launched with and without intronic read retention.

5.3.3 Souporcell

Cellranger outputs were used as input for souporcell, which was run on the same reference genome that was used for count matrix generation. Souporcell command for each sample followed software developer’s instruction, and the number of clusters to be identified by souporcell was set to 2, corresponding to the number of expected genotypes in each sample.

```
singularity exec -B $parentdir/souporcell souporcell_latest.sif souporcell_pipeline.py -i BAM_file_from_cellranger -b barcode_file_from_cellranger -f genome.fa -t 8 -o output_k2 -k 2
```

5.3.4 SoupX

Raw feature-barcode matrix, and Cellranger clustering information were used to run automated contamination fraction estimation for each sample. First, a `SoupChannel` object was created by supplying the table of droplets, the table of counts and clustering information from Cellranger output.

```
sc = SoupChannel(tod=mtx,toc=mtx_filt,metaData = mDat)
```

Then, `autoEstCont` function was used to estimate the level of background contamination, and `adjustCounts` function was used to remove the calculated contamination fraction from original table of counts.

```
sc1 = try(autoEstCont(sc))
out = adjustCounts(sc1)
```

5.3.5 scDblFinder

`scDblFinder` function was used using default settings. Since this method relies on the generation of artificial doublets by combining random cells and/or pairs of non-identical clusters, we first removed empty droplets and cells with low coverage (i.e. erythrocytes, see QC and filtering section). Moreover, to better account for homotypic doublets detection in our dataset, we first normalized and scaled counts, and performed PCA clustering on each individual sample. Note that these PCA coordinates were only used for doublet detection with scDblFinder.

5.3.6 QC and filtering

Mitochondrial, ribosomal and hemoglobin genes fraction was calculated leveraging the `PercentageFeatureSet` function included in the Seurat R package in the following way:

```
obj[["percent.mt"]] <- PercentageFeatureSet(obj, pattern = "^MT-")
obj[["percent.ribo"]] <- PercentageFeatureSet(obj, pattern = "^RP[SL]")
obj[["percent.hb"]] <- PercentageFeatureSet(obj, pattern = "^HB[^(P)]")
```

Our first QC filtering step was RBCs removal, which were not the focus of our analysis.

As RBCs commonly shed ribosomes during their maturation and are not involved in protein synthesis processes (Moras, Lefevre, and Ostuni 2017), after carefully reviewing each individual sample before QQC processing, we defined as RBCs cells that surpassed 1% hemoglobin genes count and did not reach 5% ribosomal count and filtered them out.

“Canonical” thresholds were a minimum of 400 genes and a maximum of 8000 genes detected per cell, and a maximum 25% of mitochondrial reads per cell.

When using MAD-based filtering, we need to account for the fact that the definition of “outlier” in our datasets can be highly influenced by sample composition (i.e. for samples with a high fraction of leukemic cells, T cells might be incorrectly classified as low-quality cells due to their relatively low number of reads and genes). To do so, we first used the `adjOutlyingness` function (from the robustbase R package(Maechler et al. 2023)) to compute the "outlyingness" for each cell based on four quality metrics: percentage of mitochondrial reads, percentage of ribosomal reads, log10 of read counts and log10 of detected genes. This function assesses how different each cell's metrics are from the "typical" cell, considering both the absolute

value of the metrics and any potential skewness in their distribution, and returns a numerical value (the outlyingness score).

Then, with the `isOutlier` function (scater R package (McCarthy et al. 2017)), we identified cells that were outliers based on their outlyingness scores. In this case, we used a value of MADs=2, which is a relatively strict threshold when defining an outlier. Cells were defined as low-quality if they didn't satisfy all the following criteria:

- All QC metrics within the "canonical" range
- Not an outlier based on MADs
- Defined singlet by scDblFinder
- Successful genotype assessment by souporcell (except for control and sorted samples)

5.4 Analysis of scRNA-seq data (individual samples)

Samples were first processed and analyzed individually. For each library, after filtering (see above), RNA expression data were normalized by total expression, multiplied by a scaling factor of 10,000 and log-transformed. Such normalization is crucial because raw counts often exhibit significant variability, even among identical cells. This variability primarily stems from inherent sampling effects. Specifically, raw counts are influenced by the capture, reverse transcription, and sequencing of individual RNA molecules, with each step introducing significant variability.

Then, for clustering and visualization purposes, we first chose a subset of genes characterized by highest cell-to-cell variation in our dataset. Focusing on genes with such variability has been shown (Brennecke et al. 2013) to enhance the ability to detect meaningful biological patterns in single-cell data. `FindVariableFeatures` function, implemented in Seurat, was used with "vst" (variance-stabilizing transformation) method, and 2,000 features per sample were kept. By using the "vst" method, we modelled the relationship between the variance and the mean of gene expression values across cells. Genes that exhibited notably different variance from what's expected in the model were defined as "variable".

These features were also subjected to subsequent linear transformation, with each gene's expression scaled to a mean of 0 and a standard deviation of 1. This is a pivotal step in single-cell data analysis, as it ultimately renders the expression levels of distinct genes directly comparable and allows the use of dimensionality reduction techniques like PCA, t-SNE or UMAP, since these methods are inherently sensitive to data scales.

Contextual to the scaling process, we also regressed out the percentage of mitochondrial reads, number of reads per cell, and the difference between the G2M and S phase scores, which are commonly labelled as unwarranted sources of variation. This preparatory step is particularly beneficial for clustering algorithms, ensuring they aren't influenced by a subset of non-biologically significant variables. Of note, we decided against adjusting for the S and G2M cell cycle scores individually. While these scores capture most of the cell cycle-related signals, regressing them out entirely in our dataset, which includes both quiescent hematopoietic stem cells and actively proliferating differentiated cells, might blur differences between these cell types. Instead, we used the differential scores between the G2M and S phases. This approach ensures that the distinction between non-proliferating and proliferating cells remains intact, while minimizing the influence of phase-specific variations within the proliferating cell population, which are not the focus of our investigation.

These processes were integrated in a custom function (see Appendix).

5.4.1 Dimensionality reduction and clustering

Single-cell datasets suffer from the so-called "curse of dimensionality" (Bellman and Bellman 1957). Despite having numerous dimensions in the number of genes, most of them are not informative, and rather add more noise and redundancy, making data analysis complex and biological signals ambiguous. We already reduced the dimensionality of the data with feature selection. To further reduce data complexity and for visualization, principal-component analysis (PCA) was performed on scaled data, and a k-nearest-neighbor (KNN) graph using the Leiden algorithm (Traag, Waltman, and van Eck 2019), an improved version of the Louvain algorithm (Duò, Robinson, and Soneson 2020), was constructed using 30 nearest neighbors and different resolutions to better explore the dataset.

Finally, we ran the UMAP algorithm (Becht et al. 2019) on the first 30 principal components with 30 nearest neighbors defining the neighborhood size and a minimum distance of 0.3.

5.4.2 Automated cell annotation with SingleR

Four different reference atlases were downloaded from celldex (Aran et al. 2019) R package: the Blueprint/ENCODE reference (Martens and Stunnenberg 2013), (The ENCODE Project Consortium 2012) and Monaco Immune data (Monaco et al. 2019), consisting of bulk RNA-seq data for pure stroma and immune cells, and sorted immune cell populations, respectively; and the Human Primary Cell Atlas (HPCA), (Mabbott et al. 2013) and the Novershtern reference (Novershtern et al. 2011),

composed of microarray datasets derived from human primary cells and sorted hematopoietic cells, respectively.

Both "main" and "fine" cell annotations were calculated with each reference dataset, and both per-cell and per-cluster profiles were obtained and compared.

5.4.3 Reference atlas-based manual cell annotation

For broad cell type annotation, gene signatures generated from scRNA-seq analysis of B-ALL bone marrow immune microenvironment by Witkowsky et al. (Witkowski et al. 2020) were used. For "fine" cell annotation, we leveraged gene signatures and cell type annotations from Lasry et al. (Lasry et al. 2023), which were obtained from scRNAseq analysis of 52 BM samples of healthy donors (N=10), and pediatric (N=20) and adult (N=22) AML patients.

For each cell-type in the reference dataset, the ten genes with the highest log2 fold change, and detected in at least 20% of the cells, with an average log2 fold-change > 0.2, and adjusted p-value < 0.001, were used as cell type specific gene signatures. Mitochondrial and ribosomal genes were also filtered.

For gene-set score calculation, among previously selected cell type-specific genes, only those in our dataset with a cluster average expression > 10 CPM were kept. Cluster-gene matrices were then rescaled by dividing each gene's expression value by its highest value across different clusters. This step was necessary to ensure that the analysis is not disproportionately influenced by very high or very low expression values of certain genes.

Finally, for each cell-type, we calculated a score by averaging the rescaled expression of the genes in the module for that cell-type and for each cluster the highest cell-type module was used for annotation. All these processes were integrated into a custom function (see Appendix)

5.4.4 Marker-based manual cell annotation

Cluster marker genes were determined by performing differential expression analysis. Seurat's `FindAllMarkers()` function was used with the MAST (Finak et al. 2015) package, which is suited for scRNAseq datasets and their characteristic sparsity. This function compares each of the clusters to the cells outside of that cluster, and identifies positive and negative markers. Only genes detected in at least 10% of the cells, and with, on average, at least a 0.25 log-fold difference between the two clusters were retained.

5.5 Analysis of scRNA-seq data (merged samples)

Following cell annotation and further sample purification by removal of low-quality clusters, we integrated data from all samples into a single dataset.

SoupX-corrected matrices and metadata were first pooled together, and normalization, variable features selection, scaling and PCA were performed as described above. Cells were re-annotated following previous methods, also leveraging previous results on individual samples.

5.5.1 Malignant and microenvironment separation

To evaluate cluster occupancy score, we used clusters defined at resolution 3 in our merged dataset, and for each of the 51 samples and 63 clusters we calculated the ratio between the number of cells from the patient and the sum of that patient and control cells. If occupancy score exceeded a threshold of 70%, we defined that cluster as patient specific, with a high probability of it being a malignant cells cluster.

Next, we used souporcell to discriminate between cells from either host or donor origin. First, leveraging the presence in our dataset of sorted samples, we benchmarked the accuracy of souporcell in identifying distinct genotypes.

We used samples from two patients whose LAIP allowed us to isolate by FACS sorting their leukemic and microenvironment populations, and to sequence both parts individually. We merged this patients' sequencing files, ran souporcell, and calculated the overlap between genotype assignment and sample provenience.

Following this approach validation, we applied this analysis to our whole dataset. As souporcell only calculates the probability of a cell of being either in genotype 1 or 2 and doesn't have information about cell origin, we manually assigned genotypes to host and donor values based on their relative frequencies in broad cell types. If a genotype was particularly predominant in a cell type that is typically of donor (i.e. T cells) or of host (i.e. HSPCs for AML patients) origin, we assumed that this would be the donor or host values, respectively.

Next, for patients with clinically annotated karyotype aberrations (**Table 3**), we ran inferCNV (Timothy Tickle and Itay Tirosh, n.d.) to identify malignant cells. InferCNV v1.3.3 was run on each AML patient sample individually. SoupX-corrected expression matrix was provided, and the annotation file required for the software was constructed by supplying broad cell type information annotation (HSPCs, erythrocytic, myeloid, T, NK and B cells). Samples from HC were used as controls for each patient.

Tu run InferCNV, we used cutoff = 0.1, min_cell_per_gene = 10, de-noise = TRUE, HMM = TRUE and analysis_mode = 'subclusters'.

5.5.2 Harmony

Following dataset split into different broad cell types, before UMAP and cluster calculation, Harmony was used to correct for batch effects. We ran Harmony using default settings, and using the different sequencing runs as integration variable.

```
harmony::RunHarmony(object = seurat_obj, group.by.vars = 'batch')
```

The first 30 dimensions of Harmony embeddings were kept for UMAP generation with 30 nearest neighbors. Clustering was performed using the Leiden algorithm at different resolutions (0.5, 1, 1.5, 2, 3).

5.6 Granular annotation of cell subsets

5.6.1 DE analysis

DE analysis was performed using `FindMarkers()` and the package MAST (Finak et al. 2015), as implemented in Seurat.

```
FindMarkers(object = s_obj,
                      min.pct = 0.1,
                      logfc.threshold = 0.25,
                      only.pos = FALSE,
                      min.cells.group = 10,
                      test.use = "MAST",
                      return.thresh = 1e-06)
```

5.6.2 AML cells

Immune activation score, iScore, and LSC17 were calculated using the `AddModule()` function in Seurat. This function calculates the average expression levels an input gene list on for each cell in a Seurat object, subtracted by the aggregated expression of a randomly generated control gene set. We used N=1000 control genes.

Genes used for immune activation score were: CIITA, HLA-DMA, HLA-DMB, HLA-DPA1, HLA-DPB1, HLA-DQA1, HLA-DQB1, HLA-DRA, HLA-DRB1, HLA-DRB5, HLA-F, TAP1, TAP2, CD274, PDCD1LG2, CD276, VTCN1, CD48, FASLG, CD200, ITGAL, CD226, CD70, and ICOSLG.

Genes used for iScore: ALOX5, AP2S1, ATP2B1, ATP8B4, CAPZB, CD38, CD79A, CST3, CTSG, CXCL2, CYBA, FCN1, FGR, FYB1, FYN, GSTP1, HOMER3, IRAK3, KMT2E, MEF2C, MPO, PSMA6, PSME1, RGCC, SAMHD1, SLC11A1, SLC2A3, TFPI, TMEM176B, TNFRSF1B, TYROBP, VSIR, CHMP4B, CCL7, EIF2AK2, HMOX1, PABPC1, RETN.

Genes used for LSC17: ADGRG1, AKR1C3, CD34, BEX3, EMP1, SMIM24, SOCS2, CPXM1, CDK6, FAM30A, DPYSL3, MMRN1, LAPTM4B, ARHGAP22, NYNRIN, ZBTB46, DNMT3B.

5.6.3 NK cells

Annotation of NK cell subsets, following reclustering, was obtained through differential expression analysis between cells within each cluster against all other cells. A resolution of 0.5 was used, resulting in 8 different NK clusters.

NK activation score was calculated with the following genes: *IFITM1, XCL2, IFITM3, TNFSF9, LINC02446, CXCR3, IL32, CD276, PDCD1, XCL1, XIST, MTRNR2L8, S100A10.*

5.6.4 T cells

To isolate T cells, we leveraged gene expression of canonical markers (*CD2, CD3E, CD3G, CD4, CD8A*). Moreover, TCR sequencing, available for samples processed with the 5' immune profiling solution, allowed us to validate gene expression data by comparing manually annotated T cells and barcodes associated to TCR sequences.

For refined subset annotation, we used resolution 3, which generated 43 different clusters and `FindMarkers()` function as implemented above. We compared gene signatures from a scRNA-seq atlas of CD8 TILs of hepatocarcinoma patients (Zhou et al. 2020) and a scRNA-seq dataset of CD4 T cells isolated from the PB of HC (Cano-Gamez et al. 2020) with our data, and annotated clusters based on similarity of gene expression profiles.

For TCR analysis, we used scRepertoire R package following author's vignette.

6 BIBLIOGRAPHY

Abdelaal, Tamim, Lieke Michielsen, Davy Cats, Dylan Hoogduin, Hailiang Mei, Marcel J. T. Reinders, and Ahmed Mahfouz. 2019. "A Comparison of Automatic Cell Identification Methods for Single-Cell RNA Sequencing Data." *Genome Biology* 20 (1): 194. https://doi.org/10.1186/s13059-019-1795-z.

Albring, J. C., S. Inselmann, T. Sauer, C. Schliemann, B. Altvater, S. Kailayangiri, C. Rössig, et al. 2017. "PD-1 Checkpoint Blockade in Patients with Relapsed AML after Allogeneic Stem Cell Transplantation." *Bone Marrow Transplantation* 52 (2): 317–20. https://doi.org/10.1038/bmt.2016.274.

Allen, Micah, Davide Poggiali, Kirstie Whitaker, Tom Rhys Marshall, Jordy van Langen, and Rogier A. Kievit. 2021. "Raincloud Plots: A Multi-Platform Tool for Robust Data Visualization." *Wellcome Open Research* 4 (January): 63. https://doi.org/10.12688/wellcomeopenres.15191.2.

Anasetti, C., and J. A. Hansen. 1994. "Effect of HLA Incompatibility in Marrow Transplantation from Unrelated and HLA-Mismatched Related Donors." *Transfusion Science* 15 (3): 221–30. https://doi.org/10.1016/0955-3886(94)90134-1.

Anasetti, Claudio, Brent R. Logan, Stephanie J. Lee, Edmund K. Waller, Daniel J. Weisdorf, John R. Wingard, Corey S. Cutler, et al. 2012. "Peripheral-Blood Stem Cells versus Bone Marrow from Unrelated Donors." *New England Journal of Medicine* 367 (16): 1487–96. https://doi.org/10.1056/NEJMoa1203517.

Antin, J. H., and J. L. Ferrara. 1992. "Cytokine Dysregulation and Acute Graft-versus-Host Disease." *Blood* 80 (12): 2964–68.

Antin, Joseph H., and James L. M. Ferrara. 1992. "Cytokine Dysregulation and Acute Graft-Versus-Host Disease." *Blood* 80 (12): 2964–68. https://doi.org/10.1182/blood.V80.12.2964.2964.

Apostolova, Petya, Stefanie Kreutmair, Cristina Toffalori, Marco Punta, Susanne Unger, Ann-Cathrin Burk, Claudia Wehr, et al. 2023. "Phase II Trial of Hypomethylating Agent Combined with Nivolumab for Acute Myeloid Leukaemia Relapse after Allogeneic Haematopoietic Cell Transplantation-Immune Signature Correlates with Response." *British Journal of Haematology* 203 (2): 264–81. https://doi.org/10.1111/bjh.19007.

Aran, Dvir, Agnieszka P. Looney, Leqian Liu, Esther Wu, Valerie Fong, Austin Hsu, Suzanna Chak, et al. 2019. "Reference-Based Analysis of Lung Single-Cell Sequencing Reveals a Transitional Profibrotic Macrophage." *Nature Immunology* 20 (2): 163–72. https://doi.org/10.1038/s41590-018-0276-y.

Baek, Seungbyn, and Insuk Lee. 2020. "Single-Cell ATAC Sequencing Analysis: From Data Preprocessing to Hypothesis Generation." *Computational and Structural Biotechnology Journal* 18: 1429–39. https://doi.org/10.1016/j.csbj.2020.06.012.

Barnes, D. W. H., M. J. Corp, J. F. Loutit, and F. E. Neal. 1956. "Treatment of Murine Leukaemia with X Rays and Homologous Bone Marrow." *British Medical Journal* 2 (4993): 626–27.

Barrett, John, and Bruce R. Blazar. 2009. "Genetic Trickery — Escape of Leukemia from Immune Attack." *New England Journal of Medicine* 361 (5): 524–25. https://doi.org/10.1056/NEJMe0903177.

Barreyro, Laura, Timothy M. Chlon, and Daniel T. Starczynowski. 2018. "Chronic Immune Response Dysregulation in MDS Pathogenesis." *Blood* 132 (15): 1553–60. https://doi.org/10.1182/blood-2018-03-784116.

Baryawno, Ninib, Dariusz Przybylski, Monika S. Kowalczyk, Youmna Kfoury, Nicolas Severe, Karin Gustafsson, Konstantinos D. Kokkaliaris, et al. 2019. "A Cellular Taxonomy of the Bone

Marrow Stroma in Homeostasis and Leukemia." *Cell* 177 (7): 1915-1932.e16. https://doi.org/10.1016/j.cell.2019.04.040.

Bauer, S., V. Groh, J. Wu, A. Steinle, J. H. Phillips, L. L. Lanier, and T. Spies. 1999. "Activation of NK Cells and T Cells by NKG2D, a Receptor for Stress-Inducible MICA." *Science (New York, N.Y.)* 285 (5428): 727–29. https://doi.org/10.1126/science.285.5428.727.

Becht, Etienne, Leland McInnes, John Healy, Charles-Antoine Dutertre, Immanuel W. H. Kwok, Lai Guan Ng, Florent Ginhoux, and Evan W. Newell. 2019. "Dimensionality Reduction for Visualizing Single-Cell Data Using UMAP." *Nature Biotechnology* 37 (1): 38–44. https://doi.org/10.1038/nbt.4314.

Bejanyan, Nelli, Daniel J. Weisdorf, Brent R. Logan, Hai-Lin Wang, Steven M. Devine, Marcos de Lima, Donald W. Bunjes, and Mei-Jie Zhang. 2015. "Survival of Patients with Acute Myeloid Leukemia Relapsing after Allogeneic Hematopoietic Cell Transplantation: A Center for International Blood and Marrow Transplant Research Study." *Biology of Blood and Marrow Transplantation: Journal of the American Society for Blood and Marrow Transplantation* 21 (3): 454–59. https://doi.org/10.1016/j.bbmt.2014.11.007.

Bellman, Richard, and Richard Ernest Bellman. 1957. *Dynamic Programming*. Princeton University Press.

Bleakley, Marie, and Stanley R. Riddell. 2004. "Molecules and Mechanisms of the Graft-versus-Leukaemia Effect." *Nature Reviews. Cancer* 4 (5): 371–80. https://doi.org/10.1038/nrc1365.

Borcherding, Nicholas, Nicholas L. Bormann, and Gloria Kraus. 2020. "scRepertoire: An R-Based Toolkit for Single-Cell Immune Receptor Analysis." *F1000Research* 9 (June): 47. https://doi.org/10.12688/f1000research.22139.2.

Bouland, Gerard A., Ahmed Mahfouz, and Marcel J. T. Reinders. 2023. "Consequences and Opportunities Arising Due to Sparser Single-Cell RNA-Seq Datasets." *Genome Biology* 24 (1): 86. https://doi.org/10.1186/s13059-023-02933-w.

Brennecke, Philip, Simon Anders, Jong Kyoung Kim, Aleksandra A. Kołodziejczyk, Xiuwei Zhang, Valentina Proserpio, Bianka Baying, et al. 2013. "Accounting for Technical Noise in Single-Cell RNA-Seq Experiments." *Nature Methods* 10 (11): 1093–95. https://doi.org/10.1038/nmeth.2645.

Bryder, David, Derrick J. Rossi, and Irving L. Weissman. 2006. "Hematopoietic Stem Cells: The Paradigmatic Tissue-Specific Stem Cell." *The American Journal of Pathology* 169 (2): 338–46. https://doi.org/10.2353/ajpath.2006.060312.

Cano-Gamez, Eddie, Blagoje Soskic, Theodoros I. Roumeliotis, Ernest So, Deborah J. Smyth, Marta Baldrighi, David Willé, et al. 2020. "Single-Cell Transcriptomics Identifies an Effectorness Gradient Shaping the Response of CD4+ T Cells to Cytokines." *Nature Communications* 11 (1): 1801. https://doi.org/10.1038/s41467-020-15543-y.

Carey, Alyssa, David K. Edwards, Christopher A. Eide, Laura Newell, Elie Traer, Bruno C. Medeiros, Daniel A. Pollyea, et al. 2017. "Identification of Interleukin-1 by Functional Screening as a Key Mediator of Cellular Expansion and Disease Progression in Acute Myeloid Leukemia." *Cell Reports* 18 (13): 3204–18. https://doi.org/10.1016/j.celrep.2017.03.018.

Casey, Stephanie C., Ling Tong, Yulin Li, Rachel Do, Susanne Walz, Kelly N. Fitzgerald, Arvin M. Gouw, et al. 2016. "MYC Regulates the Antitumor Immune Response through CD47 and PD-L1." *Science (New York, N.Y.)* 352 (6282): 227–31. https://doi.org/10.1126/science.aac9935.

Chang, Chih-Hao, Jing Qiu, David O'Sullivan, Michael D. Buck, Takuro Noguchi, Jonathan D. Curtis, Qiongyu Chen, et al. 2015. "Metabolic Competition in the Tumor Microenvironment Is a Driver of Cancer Progression." *Cell* 162 (6): 1229–41. https://doi.org/10.1016/j.cell.2015.08.016.

Chang, Ying-Jun, Xiang-Yu Zhao, and Xiao-Jun Huang. 2018. “Strategies for Enhancing and Preserving Anti-Leukemia Effects Without Aggravating Graft-Versus-Host Disease.” *Frontiers in Immunology* 9. https://www.frontiersin.org/article/10.3389/fimmu.2018.03041.

Chazarra-Gil, Ruben, Stijn van Dongen, Vladimir Yu Kiselev, and Martin Hemberg. 2021. “Flexible Comparison of Batch Correction Methods for Single-Cell RNA-Seq Using BatchBench.” *Nucleic Acids Research* 49 (7): e42. https://doi.org/10.1093/nar/gkab004.

Chen, Binbin, Michael S. Khodadoust, Chih Long Liu, Aaron M. Newman, and Ash A. Alizadeh. 2018. “Profiling Tumor Infiltrating Immune Cells with CIBERSORT.” *Methods in Molecular Biology (Clifton, N.J.)* 1711: 243–59. https://doi.org/10.1007/978-1-4939-7493-1_12.

Cheuk, Daniel KL. 2013. “Optimal Stem Cell Source for Allogeneic Stem Cell Transplantation for Hematological Malignancies.” *World Journal of Transplantation* 3 (4): 99–112. https://doi.org/10.5500/wjt.v3.i4.99.

Christopher, Matthew J., Allegra A. Petti, Michael P. Rettig, Christopher A. Miller, Ezhilarasi Chendamarai, Eric J. Duncavage, Jeffery M. Klco, et al. 2018a. “Immune Escape of Relapsed AML Cells after Allogeneic Transplantation.” *New England Journal of Medicine* 379 (24): 2330–41. https://doi.org/10.1056/NEJMoa1808777.

———. 2018b. “Immune Escape of Relapsed AML Cells after Allogeneic Transplantation.” *New England Journal of Medicine* 379 (24): 2330–41. https://doi.org/10.1056/NEJMoa1808777.

Cole, Michael B., Davide Risso, Allon Wagner, David DeTomaso, John Ngai, Elizabeth Purdom, Sandrine Dudoit, and Nir Yosef. 2019. “Performance Assessment and Selection of Normalization Procedures for Single-Cell RNA-Seq.” *Cell Systems* 8 (4): 315-328.e8. https://doi.org/10.1016/j.cels.2019.03.010.

Collins, R. H., O. Shpilberg, W. R. Drobyski, D. L. Porter, S. Giralt, R. Champlin, S. A. Goodman, et al. 1997. “Donor Leukocyte Infusions in 140 Patients with Relapsed Malignancy after Allogeneic Bone Marrow Transplantation.” *Journal of Clinical Oncology: Official Journal of the American Society of Clinical Oncology* 15 (2): 433–44. https://doi.org/10.1200/JCO.1997.15.2.433.

Cooper, Megan A, Todd A Fehniger, and Michael A Caligiuri. 2001. “The Biology of Human Natural Killer-Cell Subsets.” *Trends in Immunology* 22 (11): 633–40. https://doi.org/10.1016/S1471-4906(01)02060-9.

Copelan, Edward A. 2006. “Hematopoietic Stem-Cell Transplantation.” *New England Journal of Medicine* 354 (17): 1813–26. https://doi.org/10.1056/NEJMra052638.

Crinier, Adeline, Pierre-Yves Dumas, Bertrand Escalière, Christelle Piperoglou, Laurine Gil, Arnaud Villacreces, Frédéric Vély, et al. 2021. “Single-Cell Profiling Reveals the Trajectories of Natural Killer Cell Differentiation in Bone Marrow and a Stress Signature Induced by Acute Myeloid Leukemia.” *Cellular & Molecular Immunology* 18 (5): 1290–1304. https://doi.org/10.1038/s41423-020-00574-8.

Crucitti, L, R Crocchiolo, C Toffalori, B Mazzi, R Greco, A Signori, F Sizzano, et al. 2015. “Incidence, Risk Factors and Clinical Outcome of Leukemia Relapses with Loss of the Mismatched HLA after Partially Incompatible Hematopoietic Stem Cell Transplantation.” *Leukemia* 29 (5): 1143–52. https://doi.org/10.1038/leu.2014.314.

Cutler, Corey, Satyendra Giri, Suriya Jeyapalan, David Paniagua, Akila Viswanathan, and Joseph H. Antin. 2001. “Acute and Chronic Graft-Versus-Host Disease After Allogeneic Peripheral-Blood Stem-Cell and Bone Marrow Transplantation: A Meta-Analysis.” *Journal of Clinical Oncology* 19 (16): 3685–91. https://doi.org/10.1200/JCO.2001.19.16.3685.

Dal Molin, Alessandra, Giacomo Baruzzo, and Barbara Di Camillo. 2017. “Single-Cell RNA-Sequencing: Assessment of Differential Expression Analysis Methods.” *Frontiers in Genetics* 8 (May): 62. https://doi.org/10.3389/fgene.2017.00062.

Darmanis, Spyros, Steven A. Sloan, Derek Croote, Marco Mignardi, Sophia Chernikova, Peyman Samghababi, Ye Zhang, et al. 2017. “Single-Cell RNA-Seq Analysis of Infiltrating Neoplastic Cells at the Migrating Front of Human Glioblastoma.” *Cell Reports* 21 (5): 1399–1410. https://doi.org/10.1016/j.celrep.2017.10.030.

Deeg, H. Joachim. 2021. “Chimerism, the Microenvironment and Control of Leukemia.” *Frontiers in Immunology* 12 (April): 652105. https://doi.org/10.3389/fimmu.2021.652105.

Dekker, Linde, Coco de Koning, Caroline Lindemans, and Stefan Nierkens. 2020. “Reconstitution of T Cell Subsets Following Allogeneic Hematopoietic Cell Transplantation.” *Cancers* 12 (7): 1974. https://doi.org/10.3390/cancers12071974.

Depil, S., E. Deconinck, N. Milpied, L. Sutton, F. Witz, J. P. Jouet, G. Damaj, I. Yakoub-Agha, and Société Française de Greffe de Moelle et Thérapie cellulaire. 2004. “Donor Lymphocyte Infusion to Treat Relapse after Allogeneic Bone Marrow Transplantation for Myelodysplastic Syndrome.” *Bone Marrow Transplantation* 33 (5): 531–34. https://doi.org/10.1038/sj.bmt.1704381.

Dickinson, Anne M., Jean Norden, Shuang Li, Ilona Hromadnikova, Christoph Schmid, Helga Schmetzer, and Hans Jochem-Kolb. 2017. “Graft-versus-Leukemia Effect Following Hematopoietic Stem Cell Transplantation for Leukemia.” *Frontiers in Immunology* 8: 496. https://doi.org/10.3389/fimmu.2017.00496.

DiLillo, D. J., J. B. Weinberg, A. Yoshizaki, M. Horikawa, J. M. Bryant, Y. Iwata, T. Matsushita, et al. 2013. “Chronic Lymphocytic Leukemia and Regulatory B Cells Share IL-10 Competence and Immunosuppressive Function.” *Leukemia* 27 (1): 170–82. https://doi.org/10.1038/leu.2012.165.

Du, Jun, Dandan Yu, Xinle Han, Lijun Zhu, and Zoufang Huang. 2021. “Comparison of Allogeneic Stem Cell Transplant and Autologous Stem Cell Transplant in Refractory or Relapsed Peripheral T-Cell Lymphoma: A Systematic Review and Meta-Analysis.” *JAMA Network Open* 4 (5): e219807. https://doi.org/10.1001/jamanetworkopen.2021.9807.

Duarte, Rafael F., Myriam Labopin, Peter Bader, Grzegorz W. Basak, Chiara Bonini, Christian Chabannon, Selim Corbacioglu, et al. 2019. “Indications for Haematopoietic Stem Cell Transplantation for Haematological Diseases, Solid Tumours and Immune Disorders: Current Practice in Europe, 2019.” Report. Nature Publishing Group. https://doi.org/10.1038/s41409-019-0516-2.

Duault, Caroline, Anil Kumar, Adeleh Taghi Khani, Sung June Lee, Lu Yang, Min Huang, Christian Hurtz, et al. 2021. “Activated Natural Killer Cells Predict Poor Clinical Prognosis in High-Risk B- and T-Cell Acute Lymphoblastic Leukemia.” *Blood* 138 (16): 1465–80. https://doi.org/10.1182/blood.2020009871.

Dulphy, Nicolas, Guylaine Henry, Patrice Hemon, Zena Khaznadar, Hervé Dombret, Nicolas Boissel, Armand Bensussan, and Antoine Toubert. 2014. “Contribution of CD39 to the Immunosuppressive Microenvironment of Acute Myeloid Leukaemia at Diagnosis.” *British Journal of Haematology* 165 (5): 722–25. https://doi.org/10.1111/bjh.12774.

Duò, Angelo, Mark D. Robinson, and Charlotte Soneson. 2020. “A Systematic Performance Evaluation of Clustering Methods for Single-Cell RNA-Seq Data.” F1000Research. https://doi.org/10.12688/f1000research.15666.3.

Dvir Aran, Aaron Lun, Daniel Bunis, Jared Andrews, Friederike Dündar. n.d. “SingleR.” Bioconductor. Accessed October 11, 2023. https://doi.org/10.18129/B9.BIOC.SINGLER.

Eagle, Kenneth, Taku Harada, Jérémie Kalfon, Monika W. Perez, Yaser Heshmati, Jazmin Ewers, Jošt Vrabič Koren, et al. 2022. “Transcriptional Plasticity Drives Leukemia Immune

Escape." *Blood Cancer Discovery* 3 (5): 394–409. https://doi.org/10.1158/2643-3230.BCD-21-0207.

Ennishi, Daisuke, Katsuyoshi Takata, Wendy Béguelin, Gerben Duns, Anja Mottok, Pedro Farinha, Ali Bashashati, et al. 2019. "Molecular and Genetic Characterization of MHC Deficiency Identifies EZH2 as Therapeutic Target for Enhancing Immune Recognition." *Cancer Discovery* 9 (4): 546–63. https://doi.org/10.1158/2159-8290.CD-18-1090.

Falkenburg, J. H. Frederik, Lisette van de Corput, Erik W. A. Marijt, and Roel Willemze. 2003. "Minor Histocompatibility Antigens in Human Stem Cell Transplantation." *Experimental Hematology* 31 (9): 743–51.

Ferrara, James L. M., John E. Levine, Pavan Reddy, and Ernst Holler. 2009. "Graft-versus-Host Disease." *Lancet (London, England)* 373 (9674): 1550–61. https://doi.org/10.1016/S0140-6736(09)60237-3.

Ferrara, James LM, John E Levine, Pavan Reddy, and Ernst Holler. 2009. "Graft-versus-Host Disease." *The Lancet* 373 (9674): 1550–61. https://doi.org/10.1016/S0140-6736(09)60237-3.

Finak, Greg, Andrew McDavid, Masanao Yajima, Jingyuan Deng, Vivian Gersuk, Alex K. Shalek, Chloe K. Slichter, et al. 2015. "MAST: A Flexible Statistical Framework for Assessing Transcriptional Changes and Characterizing Heterogeneity in Single-Cell RNA Sequencing Data." *Genome Biology* 16 (1): 278. https://doi.org/10.1186/s13059-015-0844-5.

Fischer, Karin, Petra Hoffmann, Simon Voelkl, Norbert Meidenbauer, Julia Ammer, Matthias Edinger, Eva Gottfried, et al. 2007. "Inhibitory Effect of Tumor Cell–Derived Lactic Acid on Human T Cells." *Blood* 109 (9): 3812–19. https://doi.org/10.1182/blood-2006-07-035972.

Freud, Aharon G., Jianhua Yu, and Michael A. Caligiuri. 2014. "Human Natural Killer Cell Development in Secondary Lymphoid Tissues." *Seminars in Immunology* 26 (2): 132–37. https://doi.org/10.1016/j.smim.2014.02.008.

Gale, R. P., M. M. Bortin, D. W. van Bekkum, J. C. Biggs, K. A. Dicke, E. Gluckman, R. A. Good, R. G. Hoffmann, H. E. Kay, and J. H. Kersey. 1987. "Risk Factors for Acute Graft-versus-Host Disease." *British Journal of Haematology* 67 (4): 397–406.

Galen, Peter van, Volker Hovestadt, Marc H. Wadsworth Ii, Travis K. Hughes, Gabriel K. Griffin, Sofia Battaglia, Julia A. Verga, et al. 2019. "Single-Cell RNA-Seq Reveals AML Hierarchies Relevant to Disease Progression and Immunity." *Cell* 176 (6): 1265-1281.e24. https://doi.org/10.1016/j.cell.2019.01.031.

Gambacorta, Valentina, Stefano Beretta, Martina Ciccimarra, Laura Zito, Kety Giannetti, Angela Andrisani, Daniela Gnani, et al. 2022. "Integrated Multiomic Profiling Identifies the Epigenetic Regulator PRC2 as a Therapeutic Target to Counteract Leukemia Immune Escape and Relapse." *Cancer Discovery* 12 (6): 1449–61. https://doi.org/10.1158/2159-8290.CD-21-0980.

Germain, Pierre-Luc, Aaron Lun, Will Macnair, and Mark D. Robinson. 2021. "Doublet Identification in Single-Cell Sequencing Data Using scDblFinder." *F1000Research* 10 (September): 979. https://doi.org/10.12688/f1000research.73600.1.

Germain, Pierre-Luc, Anthony Sonrel, and Mark D. Robinson. 2020. "pipeComp, a General Framework for the Evaluation of Computational Pipelines, Reveals Performant Single Cell RNA-Seq Preprocessing Tools." *Genome Biology* 21 (1): 227. https://doi.org/10.1186/s13059-020-02136-7.

Ghimire, Sakhila, Daniela Weber, Emily Mavin, Xiao nong Wang, Anne Mary Dickinson, and Ernst Holler. 2017. "Pathophysiology of GvHD and Other HSCT-Related Major Complications." *Frontiers in Immunology* 8 (March): 79. https://doi.org/10.3389/fimmu.2017.00079.

Gibson, Greg. 2022. “Perspectives on Rigor and Reproducibility in Single Cell Genomics.” *PLoS Genetics* 18 (5). https://doi.org/10.1371/journal.pgen.1010210.

Gottschalk, Sven, Nora Anderson, Carsten Hainz, S. Gail Eckhardt, and Natalie J. Serkova. 2004. “Imatinib (STI571)-Mediated Changes in Glucose Metabolism in Human Leukemia BCR-ABL-Positive Cells.” *Clinical Cancer Research* 10 (19): 6661–68. https://doi.org/10.1158/1078-0432.CCR-04-0039.

Gragert, Loren, Mary Eapen, Eric Williams, John Freeman, Stephen Spellman, Robert Baitty, Robert Hartzman, et al. 2014. “HLA Match Likelihoods for Hematopoietic Stem-Cell Grafts in the U.S. Registry.” *New England Journal of Medicine* 371 (4): 339–48. https://doi.org/10.1056/NEJMsa1311707.

Green, Michael R., Stefano Monti, Scott J. Rodig, Przemyslaw Juszczynski, Treeve Currie, Evan O’Donnell, Bjoern Chapuy, et al. 2010. “Integrative Analysis Reveals Selective 9p24.1 Amplification, Increased PD-1 Ligand Expression, and Further Induction via JAK2 in Nodular Sclerosing Hodgkin Lymphoma and Primary Mediastinal Large B-Cell Lymphoma.” *Blood* 116 (17): 3268–77. https://doi.org/10.1182/blood-2010-05-282780.

Greten, Florian R., and Sergei I. Grivennikov. 2019. “Inflammation and Cancer: Triggers, Mechanisms, and Consequences.” *Immunity* 51 (1): 27–41. https://doi.org/10.1016/j.immuni.2019.06.025.

Griffiths, Jonathan A, Antonio Scialdone, and John C Marioni. 2018. “Using Single-cell Genomics to Understand Developmental Processes and Cell Fate Decisions.” *Molecular Systems Biology* 14 (4): e8046. https://doi.org/10.15252/msb.20178046.

Grosso, D, E Johnson, B Colombe, O Alpdogan, M Carabasi, J Filicko-O’Hara, S Gaballa, et al. 2017. “Acquired Uniparental Disomy in Chromosome 6p as a Feature of Relapse after T-Cell Replete Haploidentical Hematopoietic Stem Cell Transplantation Using Cyclophosphamide Tolerization.” *Bone Marrow Transplantation* 52 (4): 615–19. https://doi.org/10.1038/bmt.2016.324.

Han, Arnold, Jacob Glanville, Leo Hansmann, and Mark M Davis. 2014. “Linking T-Cell Receptor Sequence to Functional Phenotype at the Single-Cell Level.” *Nature Biotechnology* 32 (7): 684–92. https://doi.org/10.1038/nbt.2938.

Hanahan, Douglas, and Robert A. Weinberg. 2011. “Hallmarks of Cancer: The next Generation.” *Cell* 144 (5): 646–74. https://doi.org/10.1016/j.cell.2011.02.013.

Hao, Yuhan, Stephanie Hao, Erica Andersen-Nissen, William M. Mauck, Shiwei Zheng, Andrew Butler, Maddie J. Lee, et al. 2021a. “Integrated Analysis of Multimodal Single-Cell Data.” *Cell* 184 (13): 3573-3587.e29. https://doi.org/10.1016/j.cell.2021.04.048.

———. 2021b. “Integrated Analysis of Multimodal Single-Cell Data.” *Cell* 184 (13): 3573-3587.e29. https://doi.org/10.1016/j.cell.2021.04.048.

Heaton, Haynes, Arthur M. Talman, Andrew Knights, Maria Imaz, Daniel J. Gaffney, Richard Durbin, Martin Hemberg, and Mara K. N. Lawniczak. 2020. “Souporcell: Robust Clustering of Single-Cell RNA-Seq Data by Genotype without Reference Genotypes.” *Nature Methods* 17 (6): 615–20. https://doi.org/10.1038/s41592-020-0820-1.

Hemmati, Philipp G., Theis H. Terwey, Philipp le Coutre, Lam G. Vuong, Gero Massenkeil, Bernd Dörken, and Renate Arnold. 2011. “A Modified EBMT Risk Score Predicts the Outcome of Patients with Acute Myeloid Leukemia Receiving Allogeneic Stem Cell Transplants.” *European Journal of Haematology* 86 (4): 305–16. https://doi.org/10.1111/j.1600-0609.2011.01580.x.

Heumos, Lukas, Anna C. Schaar, Christopher Lance, Anastasia Litinetskaya, Felix Drost, Luke Zappia, Malte D. Lücken, et al. 2023. “Best Practices for Single-Cell Analysis across Modalities.” *Nature Reviews Genetics*, March. https://doi.org/10.1038/s41576-023-00586-w.

Ho, Ping-Chih, and Pu-Ste Liu. 2016. “Metabolic Communication in Tumors: A New Layer of Immunoregulation for Immune Evasion.” *Journal for ImmunoTherapy of Cancer* 4 (1): 4. https://doi.org/10.1186/s40425-016-0109-1.

Horowitz, M. M., R. P. Gale, P. M. Sondel, J. M. Goldman, J. Kersey, H. J. Kolb, A. A. Rimm, O. Ringdén, C. Rozman, and B. Speck. 1990. “Graft-versus-Leukemia Reactions after Bone Marrow Transplantation.” *Blood* 75 (3): 555–62.

Horowitz, M., H. Schreiber, A. Elder, O. Heidenreich, J. Vormoor, C. Toffalori, L. Vago, and N. Kröger. 2018. “Epidemiology and Biology of Relapse after Stem Cell Transplantation.” *Bone Marrow Transplantation* 53 (11): 1379–89. https://doi.org/10.1038/s41409-018-0171-z.

Horowitz, Mary, Hans Schreiber, Alex Elder, Olaf Heidenreich, Josef Vormoor, Christina Toffalori, Luca Vago, and Nicolaus Kröger. 2018. “Epidemiology and Biology of Relapse after Stem Cell Transplantation.” *Bone Marrow Transplantation* 53 (11): 1379–89. https://doi.org/10.1038/s41409-018-0171-z.

Huber, Wolfgang, Vincent J. Carey, Robert Gentleman, Simon Anders, Marc Carlson, Benilton S. Carvalho, Hector Corrada Bravo, et al. 2015. “Orchestrating High-Throughput Genomic Analysis with Bioconductor.” *Nature Methods* 12 (2): 115–21. https://doi.org/10.1038/nmeth.3252.

Jain, Prachi, Xin Tian, Stefan Cordes, Jinguo Chen, Caroline R. Cantilena, Christian Bradley, Reema Panjwani, et al. 2019. “Over-Expression of PD-1 Does Not Predict Leukemic Relapse after Allogeneic Stem Cell Transplantation.” *Biology of Blood and Marrow Transplantation* 25 (2): 216–22. https://doi.org/10.1016/j.bbmt.2018.09.037.

Jerby-Arnon, Livnat, Cyril Neftel, Marni E. Shore, Hannah R. Weisman, Nathan D. Mathewson, Matthew J. McBride, Brian Haas, et al. 2021. “Opposing Immune and Genetic Mechanisms Shape Oncogenic Programs in Synovial Sarcoma.” *Nature Medicine* 27 (2): 289–300. https://doi.org/10.1038/s41591-020-01212-6.

Kashima, Yukie, Yoshitaka Sakamoto, Keiya Kaneko, Masahide Seki, Yutaka Suzuki, and Ayako Suzuki. 2020. “Single-Cell Sequencing Techniques from Individual to Multiomics Analyses.” *Experimental & Molecular Medicine* 52 (9): 1419–27. https://doi.org/10.1038/s12276-020-00499-2.

Kawase, Takakazu, Keitaro Matsuo, Koichi Kashiwase, Hidetoshi Inoko, Hiroh Saji, Seishi Ogawa, Shunichi Kato, et al. 2009. “HLA Mismatch Combinations Associated with Decreased Risk of Relapse: Implications for the Molecular Mechanism.” *Blood* 113 (12): 2851–58. https://doi.org/10.1182/blood-2008-08-171934.

Keren-Shaul, Hadas, Ephraim Kenigsberg, Diego Adhemar Jaitin, Eyal David, Franziska Paul, Amos Tanay, and Ido Amit. 2019. “MARS-Seq2.0: An Experimental and Analytical Pipeline for Indexed Sorting Combined with Single-Cell RNA Sequencing.” *Nature Protocols* 14 (6): 1841–62. https://doi.org/10.1038/s41596-019-0164-4.

Klein, Jan, and Akie Sato. 2000. “The HLA System.” *New England Journal of Medicine* 343 (10): 702–9. https://doi.org/10.1056/NEJM200009073431006.

Klepin, Heidi D., Arati V. Rao, and Timothy S. Pardee. 2014. “Acute Myeloid Leukemia and Myelodysplastic Syndromes in Older Adults.” *Journal of Clinical Oncology: Official Journal of the American Society of Clinical Oncology* 32 (24): 2541–52. https://doi.org/10.1200/JCO.2014.55.1564.

Köhler, Natalie, Dietrich Alexander Ruess, Rebecca Kesselring, and Robert Zeiser. 2021. “The Role of Immune Checkpoint Molecules for Relapse After Allogeneic Hematopoietic Cell Transplantation.” *Frontiers in Immunology* 12 (March): 634435. https://doi.org/10.3389/fimmu.2021.634435.

Kolb, Hans-Jochem, Christoph Schmid, A. John Barrett, and Dolores J. Schendel. 2004. "Graft-versus-Leukemia Reactions in Allogeneic Chimeras." *Blood* 103 (3): 767–76. https://doi.org/10.1182/blood-2003-02-0342.

Kong, Hyewon, and Navdeep S. Chandel. 2018. "Regulation of Redox Balance in Cancer and T Cells." *Journal of Biological Chemistry* 293 (20): 7499–7507. https://doi.org/10.1074/jbc.TM117.000257.

Kong, Y., J. Zhang, D. F. Claxton, W. C. Ehmann, W. B. Rybka, L. Zhu, H. Zeng, T. D. Schell, and H. Zheng. 2015. "PD-1(Hi)TIM-3(+) T Cells Associate with and Predict Leukemia Relapse in AML Patients Post Allogeneic Stem Cell Transplantation." *Blood Cancer Journal* 5 (7): e330. https://doi.org/10.1038/bcj.2015.58.

Korsunsky, Ilya, Nghia Millard, Jean Fan, Kamil Slowikowski, Fan Zhang, Kevin Wei, Yuriy Baglaenko, Michael Brenner, Po-ru Loh, and Soumya Raychaudhuri. 2019. "Fast, Sensitive and Accurate Integration of Single-Cell Data with Harmony." *Nature Methods* 16 (12): 1289–96. https://doi.org/10.1038/s41592-019-0619-0.

Kurts, Christian, Bruce W. S. Robinson, and Percy A. Knolle. 2010. "Cross-Priming in Health and Disease." *Nature Reviews Immunology* 10 (6): 403–14. https://doi.org/10.1038/nri2780.

Lähnemann, David, Johannes Köster, Ewa Szczurek, Davis J. McCarthy, Stephanie C. Hicks, Mark D. Robinson, Catalina A. Vallejos, et al. 2020. "Eleven Grand Challenges in Single-Cell Data Science." *Genome Biology* 21 (1): 31. https://doi.org/10.1186/s13059-020-1926-6.

Larsson, Ludvig, Jonas Frisén, and Joakim Lundeberg. 2021. "Spatially Resolved Transcriptomics Adds a New Dimension to Genomics." *Nature Methods* 18 (1): 15–18. https://doi.org/10.1038/s41592-020-01038-7.

Lasry, Audrey, Bettina Nadorp, Maarten Fornerod, Deedra Nicolet, Huiyun Wu, Christopher J. Walker, Zhengxi Sun, et al. 2023. "An Inflammatory State Remodels the Immune Microenvironment and Improves Risk Stratification in Acute Myeloid Leukemia." *Nature Cancer* 4 (1): 27–42. https://doi.org/10.1038/s43018-022-00480-0.

Li, Chia-Wei, Seung-Oe Lim, Weiya Xia, Heng-Huan Lee, Li-Chuan Chan, Chu-Wei Kuo, Kay-Hooi Khoo, et al. 2016. "Glycosylation and Stabilization of Programmed Death Ligand-1 Suppresses T-Cell Activity." *Nature Communications* 7 (August): 12632. https://doi.org/10.1038/ncomms12632.

Li, Li, Vakul Mohanty, Jinzhuang Dou, Yuefan Huang, Pinaki P. Banerjee, Qi Miao, Jens G. Lohr, et al. 2023. "Loss of Metabolic Fitness Drives Tumor Resistance after CAR-NK Cell Therapy and Can Be Overcome by Cytokine Engineering." *Science Advances* 9 (30): eadd6997. https://doi.org/10.1126/sciadv.add6997.

Lindahl, Hannes, Sofie Vonlanthen, Davide Valentini, Andreas T. Björklund, Mikael Sundin, Stephan Mielke, and Dan Hauzenberger. 2022. "Lineage-Specific Early Complete Donor Chimerism and Risk of Relapse after Allogeneic Hematopoietic Stem Cell Transplantation for Acute Myeloid Leukemia." *Bone Marrow Transplantation* 57 (5): 753–59. https://doi.org/10.1038/s41409-022-01615-8.

Luecken, Malte D, and Fabian J Theis. 2019. "Current Best Practices in Single-cell RNA-seq Analysis: A Tutorial." *Molecular Systems Biology* 15 (6): e8746. https://doi.org/10.15252/msb.20188746.

Lv, Ying, Hongtao Wang, and Zhuogang Liu. 2019. "The Role of Regulatory B Cells in Patients with Acute Myeloid Leukemia." *Medical Science Monitor : International Medical Journal of Experimental and Clinical Research* 25 (April): 3026–31. https://doi.org/10.12659/MSM.915556.

Mabbott, Neil A, J Baillie, Helen Brown, Tom C Freeman, and David A Hume. 2013. "An Expression Atlas of Human Primary Cells: Inference of Gene Function from

Coexpression Networks." *BMC Genomics* 14 (1): 632. https://doi.org/10.1186/1471-2164-14-632.

Mace, Emily M. 2023. "Human Natural Killer Cells: Form, Function, and Development." *Journal of Allergy and Clinical Immunology* 151 (2): 371–85. https://doi.org/10.1016/j.jaci.2022.09.022.

Macosko, Evan Z., Anindita Basu, Rahul Satija, James Nemesh, Karthik Shekhar, Melissa Goldman, Itay Tirosh, et al. 2015. "Highly Parallel Genome-Wide Expression Profiling of Individual Cells Using Nanoliter Droplets." *Cell* 161 (5): 1202–14. https://doi.org/10.1016/j.cell.2015.05.002.

Maechler, Martin, Peter Rousseeuw (Qn and Sn), Christophe Croux (Qn and Sn), Valentin Todorov (most robust Cov), Andreas Ruckstuhl (nlrob, anova, glmrob), et al. 2023. "Robustbase: Basic Robust Statistics." https://cran.r-project.org/web/packages/robustbase/index.html.

Marmont, A. M., M. M. Horowitz, R. P. Gale, K. Sobocinski, R. C. Ash, D. W. van Bekkum, R. E. Champlin, K. A. Dicke, J. M. Goldman, and R. A. Good. 1991. "T-Cell Depletion of HLA-Identical Transplants in Leukemia." *Blood* 78 (8): 2120–30.

Martens, J. H. A., and H. G. Stunnenberg. 2013. "BLUEPRINT: Mapping Human Blood Cell Epigenomes." *Haematologica* 98 (10): 1487–89. https://doi.org/10.3324/haematol.2013.094243.

Martin, P. J., G. Schoch, L. Fisher, V. Byers, C. Anasetti, F. R. Appelbaum, P. G. Beatty, K. Doney, G. B. McDonald, and J. E. Sanders. 1990. "A Retrospective Analysis of Therapy for Acute Graft-versus-Host Disease: Initial Treatment." *Blood* 76 (8): 1464–72.

McCarthy, Davis J, Kieran R Campbell, Aaron T L Lun, and Quin F Wills. 2017. "Scater: Pre-Processing, Quality Control, Normalization and Visualization of Single-Cell RNA-Seq Data in R." Edited by Ivo Hofacker. *Bioinformatics* 33 (8): 1179–86. https://doi.org/10.1093/bioinformatics/btw777.

McCurdy, S R, B S Iglehart, D A Batista, C D Gocke, Y Ning, H A Knaus, A M Jackson, M S Leffell, L Luznik, and I Gojo. 2016. "Loss of the Mismatched Human Leukocyte Antigen Haplotype in Two Acute Myelogenous Leukemia Relapses after Haploidentical Bone Marrow Transplantation with Post-Transplantation Cyclophosphamide." *Leukemia* 30 (10): 2102–6. https://doi.org/10.1038/leu.2016.144.

Michelis, Fotios V., Hans A. Messner, Jieun Uhm, Naheed Alam, Anna Lambie, Laura McGillis, Matthew D. Seftel, et al. 2015. "Modified EBMT Pretransplant Risk Score Can Identify Favorable-Risk Patients Undergoing Allogeneic Hematopoietic Cell Transplantation for AML, Not Identified by the HCT-CI Score." *Clinical Lymphoma Myeloma and Leukemia* 15 (5): e73–81. https://doi.org/10.1016/j.clml.2014.09.014.

Mishra, Sushanta Kumar, Scott E. Millman, and Lingbo Zhang. 2023. "Metabolism in Acute Myeloid Leukemia: Mechanistic Insights and Therapeutic Targets." *Blood* 141 (10): 1119–35. https://doi.org/10.1182/blood.2022018092.

Monaco, Gianni, Bernett Lee, Weili Xu, Seri Mustafah, You Yi Hwang, Christophe Carré, Nicolas Burdin, et al. 2019. "RNA-Seq Signatures Normalized by mRNA Abundance Allow Absolute Deconvolution of Human Immune Cell Types." *Cell Reports* 26 (6): 1627-1640.e7. https://doi.org/10.1016/j.celrep.2019.01.041.

Moras, Martina, Sophie D. Lefevre, and Mariano A. Ostuni. 2017. "From Erythroblasts to Mature Red Blood Cells: Organelle Clearance in Mammals." *Frontiers in Physiology* 8 (December): 1076. https://doi.org/10.3389/fphys.2017.01076.

Morrison, Sean J., and David T. Scadden. 2014. "The Bone Marrow Niche for Haematopoietic Stem Cells." *Nature* 505 (7483): 327–34. https://doi.org/10.1038/nature12984.

Munn, David H., Madhav D. Sharma, Babak Baban, Heather P. Harding, Yuhong Zhang, David Ron, and Andrew L. Mellor. 2005. "GCN2 Kinase in T Cells Mediates Proliferative Arrest

and Anergy Induction in Response to Indoleamine 2,3-Dioxygenase." *Immunity* 22 (5): 633–42. https://doi.org/10.1016/j.immuni.2005.03.013.
Mussai, Francis, Carmela De Santo, Issa Abu-Dayyeh, Sarah Booth, Lynn Quek, Rosanna M. McEwen-Smith, Amrana Qureshi, Francesco Dazzi, Paresh Vyas, and Vincenzo Cerundolo. 2013. "Acute Myeloid Leukemia Creates an Arginase-Dependent Immunosuppressive Microenvironment." *Blood* 122 (5): 749–58. https://doi.org/10.1182/blood-2013-01-480129.
Nash, R. A., M. S. Pepe, R. Storb, G. Longton, M. Pettinger, C. Anasetti, F. R. Appelbaum, R. A. Bowden, H. J. Deeg, and K. Doney. 1992. "Acute Graft-versus-Host Disease: Analysis of Risk Factors after Allogeneic Marrow Transplantation and Prophylaxis with Cyclosporine and Methotrexate." *Blood* 80 (7): 1838–45.
Nayak-Kapoor, Asha, Zhonglin Hao, Ramses Sadek, Robin Dobbins, Lisa Marshall, Nicholas N. Vahanian, W. Jay Ramsey, et al. 2018. "Phase Ia Study of the Indoleamine 2,3-Dioxygenase 1 (IDO1) Inhibitor Navoximod (GDC-0919) in Patients with Recurrent Advanced Solid Tumors." *Journal for ImmunoTherapy of Cancer* 6 (1): 61. https://doi.org/10.1186/s40425-018-0351-9.
Neefjes, Jacques, Marlieke L. M. Jongsma, Petra Paul, and Oddmund Bakke. 2011. "Towards a Systems Understanding of MHC Class I and MHC Class II Antigen Presentation." *Nature Reviews Immunology* 11 (12): 823–36. https://doi.org/10.1038/nri3084.
Newell, Laura F., and Rachel J. Cook. 2021. "Advances in Acute Myeloid Leukemia." *BMJ* 375 (October): n2026. https://doi.org/10.1136/bmj.n2026.
Ng, Stanley W. K., Amanda Mitchell, James A. Kennedy, Weihsu C. Chen, Jessica McLeod, Narmin Ibrahimova, Andrea Arruda, et al. 2016. "A 17-Gene Stemness Score for Rapid Determination of Risk in Acute Leukaemia." *Nature* 540 (7633): 433–37. https://doi.org/10.1038/nature20598.
Nguyen, Stephanie, Nathalie Dhedin, Jean-Paul Vernant, Mathieu Kuentz, Ahmad Al Jijakli, Nathalie Rouas-Freiss, Edgardo D. Carosella, Ali Boudifa, Patrice Debré, and Vincent Vieillard. 2005. "NK-Cell Reconstitution after Haploidentical Hematopoietic Stem-Cell Transplantations: Immaturity of NK Cells and Inhibitory Effect of NKG2A Override GvL Effect." *Blood* 105 (10): 4135–42. https://doi.org/10.1182/blood-2004-10-4113.
Ni, Jing, Xi Wang, Ana Stojanovic, Qin Zhang, Marian Wincher, Lea Bühler, Annette Arnold, et al. 2020. "Single-Cell RNA Sequencing of Tumor-Infiltrating NK Cells Reveals That Inhibition of Transcription Factor HIF-1α Unleashes NK Cell Activity." *Immunity* 52 (6): 1075-1087.e8. https://doi.org/10.1016/j.immuni.2020.05.001.
Novershtern, Noa, Aravind Subramanian, Lee N. Lawton, Raymond H. Mak, W. Nicholas Haining, Marie E. McConkey, Naomi Habib, et al. 2011. "Densely Interconnected Transcriptional Circuits Control Cell States in Human Hematopoiesis." *Cell* 144 (2): 296–309. https://doi.org/10.1016/j.cell.2011.01.004.
Noviello, Maddalena, Francesco Manfredi, Eliana Ruggiero, Tommaso Perini, Giacomo Oliveira, Filippo Cortesi, Pantaleo De Simone, et al. 2019a. "Bone Marrow Central Memory and Memory Stem T-Cell Exhaustion in AML Patients Relapsing after HSCT." *Nature Communications* 10 (1): 1065. https://doi.org/10.1038/s41467-019-08871-1.
———. 2019b. "Bone Marrow Central Memory and Memory Stem T-Cell Exhaustion in AML Patients Relapsing after HSCT." *Nature Communications* 10 (1): 1065. https://doi.org/10.1038/s41467-019-08871-1.
O'Keefe, Christine, Michael A. McDevitt, and Jaroslaw P. Maciejewski. 2010. "Copy Neutral Loss of Heterozygosity: A Novel Chromosomal Lesion in Myeloid Malignancies." *Blood* 115 (14): 2731–39. https://doi.org/10.1182/blood-2009-10-201848.
Pasquini, Giovanni, Jesus Eduardo Rojo Arias, Patrick Schäfer, and Volker Busskamp. 2021. "Automated Methods for Cell Type Annotation on scRNA-Seq Data." *Computational*

and Structural Biotechnology Journal 19: 961–69. https://doi.org/10.1016/j.csbj.2021.01.015.

Passweg, J. R., H. Baldomero, P. Bader, C. Bonini, R. F. Duarte, C. Dufour, A. Gennery, et al. 2017. "Use of Haploidentical Stem Cell Transplantation Continues to Increase: The 2015 European Society for Blood and Marrow Transplant Activity Survey Report." *Bone Marrow Transplantation* 52 (6): 811–17. https://doi.org/10.1038/bmt.2017.34.

Picelli, Simone, Omid R Faridani, Åsa K Björklund, Gösta Winberg, Sven Sagasser, and Rickard Sandberg. 2014. "Full-Length RNA-Seq from Single Cells Using Smart-Seq2." *Nature Protocols* 9 (1): 171–81. https://doi.org/10.1038/nprot.2014.006.

Prestipino, Alessandro, Alica J. Emhardt, Konrad Aumann, David O'Sullivan, Sivahari P. Gorantla, Sandra Duquesne, Wolfgang Melchinger, et al. 2018. "Oncogenic JAK2V617F Causes PD-L1 Expression, Mediating Immune Escape in Myeloproliferative Neoplasms." *Science Translational Medicine* 10 (429): eaam7729. https://doi.org/10.1126/scitranslmed.aam7729.

Pruszczyk, Katarzyna, Kamila Skwierawska, Małgorzata Król, Albert Moskowicz, Dariusz Jabłoński, Tigran Torosian, Iwona Piotrowska, Elżbieta Urbanowska, Wiesław Wiktor-Jędrzejczak, and Emilian Snarski. 2017. "Bone Marrow Harvest from Unrelated Donors—up-to-Date Methodology." *European Journal of Haematology* 99 (4): 357–65. https://doi.org/10.1111/ejh.12929.

Regev, Aviv, Sarah A. Teichmann, Eric S. Lander, Ido Amit, Christophe Benoist, Ewan Birney, Bernd Bodenmiller, et al. 2017. "The Human Cell Atlas." *eLife* 6 (December): e27041. https://doi.org/10.7554/eLife.27041.

Risdon, Grant, Jay Gaddy, Frederick B. Stehman, and Hal E. Broxmeyer. 1994. "Proliferative and Cytotoxic Responses of Human Cord Blood T Lymphocytes Following Allogeneic Stimulation." *Cellular Immunology* 154 (1): 14–24. https://doi.org/10.1006/cimm.1994.1053.

Saber, Wael, Shaun Opie, J. Douglas Rizzo, Mei-Jie Zhang, Mary M. Horowitz, and Jeff Schriber. 2012. "Outcomes after Matched Unrelated Donor versus Identical Sibling Hematopoietic Cell Transplantation in Adults with Acute Myelogenous Leukemia." *Blood* 119 (17): 3908–16. https://doi.org/10.1182/blood-2011-09-381699.

Sabuncuoğlu, S, B Kuşkonmaz, D Uckun Çetinkaya, and H Özgüneş. 2012. "Evaluation of Oxidative and Antioxidative Parameters in Pediatric Hematopoietic SCT Patients." *Bone Marrow Transplantation* 47 (5): 651–56. https://doi.org/10.1038/bmt.2011.145.

Sari, Ismail, Aysun Cetin, Leylagul Kaynar, Recep Saraymen, Sibel Kabukcu Hacioglu, Ahmet Ozturk, Ismail Kocyigit, Fevzi Altuntas, and Bulent Eser. 2008. "Disturbance of Pro-Oxidative/Antioxidative Balance in Allogeneic Peripheral Blood Stem Cell Transplantation." *Annals of Clinical and Laboratory Science* 38 (2): 120–25.

Sasagawa, Yohei, Itoshi Nikaido, Tetsutaro Hayashi, Hiroki Danno, Kenichiro D. Uno, Takeshi Imai, and Hiroki R. Ueda. 2013. "Quartz-Seq: A Highly Reproducible and Sensitive Single-Cell RNA Sequencing Method, Reveals Non-Genetic Gene-Expression Heterogeneity." *Genome Biology* 14 (4): 3097. https://doi.org/10.1186/gb-2013-14-4-r31.

Serra, Sara, Alberto L. Horenstein, Tiziana Vaisitti, Davide Brusa, Davide Rossi, Luca Laurenti, Giovanni D'Arena, et al. 2011. "CD73-Generated Extracellular Adenosine in Chronic Lymphocytic Leukemia Creates Local Conditions Counteracting Drug-Induced Cell Death." *Blood* 118 (23): 6141–52. https://doi.org/10.1182/blood-2011-08-374728.

Shaw, B. E., D. L. Confer, W. Hwang, and M. A. Pulsipher. 2015. "A Review of the Genetic and Long-Term Effects of G-CSF Injections in Healthy Donors: A Reassuring Lack of Evidence for the Development of Haematological Malignancies." *Bone Marrow Transplantation* 50 (3): 334–40. https://doi.org/10.1038/bmt.2014.278.

Shlush, Liran I., Amanda Mitchell, Lawrence Heisler, Sagi Abelson, Stanley W. K. Ng, Aaron Trotman-Grant, Jessie J. F. Medeiros, et al. 2017. “Tracing the Origins of Relapse in Acute Myeloid Leukaemia to Stem Cells.” *Nature* 547 (7661): 104–8. https://doi.org/10.1038/nature22993.

Sikkema, Lisa, Ciro Ramírez-Suástegui, Daniel C. Strobl, Tessa E. Gillett, Luke Zappia, Elo Madissoon, Nikolay S. Markov, et al. 2023. “An Integrated Cell Atlas of the Lung in Health and Disease.” *Nature Medicine* 29 (6): 1563–77. https://doi.org/10.1038/s41591-023-02327-2.

Singh, Mandeep, Ghamdan Al-Eryani, Shaun Carswell, James M. Ferguson, James Blackburn, Kirston Barton, Daniel Roden, et al. 2019. “High-Throughput Targeted Long-Read Single Cell Sequencing Reveals the Clonal and Transcriptional Landscape of Lymphocytes.” *Nature Communications* 10 (1): 3120. https://doi.org/10.1038/s41467-019-11049-4.

Snyder, Michael P., Shin Lin, Amanda Posgai, Mark Atkinson, Aviv Regev, Jennifer Rood, Orit Rozenblatt-Rosen, et al. 2019. “The Human Body at Cellular Resolution: The NIH Human Biomolecular Atlas Program.” *Nature* 574 (7777): 187–92. https://doi.org/10.1038/s41586-019-1629-x.

Soneson, Charlotte, and Mark D Robinson. 2018. “Bias, Robustness and Scalability in Single-Cell Differential Expression Analysis.” *Nature Methods* 15 (4): 255–61. https://doi.org/10.1038/nmeth.4612.

Sorror, M. L. 2005. “Hematopoietic Cell Transplantation (HCT)-Specific Comorbidity Index: A New Tool for Risk Assessment before Allogeneic HCT.” *Blood* 106 (8): 2912–19. https://doi.org/10.1182/blood-2005-05-2004.

Soumillon, Magali, Davide Cacchiarelli, Stefan Semrau, Alexander van Oudenaarden, and Tarjei S. Mikkelsen. 2014. “Characterization of Directed Differentiation by High-Throughput Single-Cell RNA-Seq.” bioRxiv. https://doi.org/10.1101/003236.

Staron, Matthew M., Simon M. Gray, Heather D. Marshall, Ian A. Parish, Jonathan H. Chen, Curtis J. Perry, Guoliang Cui, Ming O. Li, and Susan M. Kaech. 2014. “The Transcription Factor FoxO1 Sustains Expression of the Inhibitory Receptor PD-1 and Survival of Antiviral CD8+ T Cells during Chronic Infection.” *Immunity* 41 (5): 802–14. https://doi.org/10.1016/j.immuni.2014.10.013.

Steidl, Christian, Sohrab P. Shah, Bruce W. Woolcock, Lixin Rui, Masahiro Kawahara, Pedro Farinha, Nathalie A. Johnson, et al. 2011. “MHC Class II Transactivator CIITA Is a Recurrent Gene Fusion Partner in Lymphoid Cancers.” *Nature* 471 (7338): 377–81. https://doi.org/10.1038/nature09754.

Stoeckius, Marlon, Christoph Hafemeister, William Stephenson, Brian Houck-Loomis, Pratip K Chattopadhyay, Harold Swerdlow, Rahul Satija, and Peter Smibert. 2017. “Simultaneous Epitope and Transcriptome Measurement in Single Cells.” *Nature Methods* 14 (9): 865–68. https://doi.org/10.1038/nmeth.4380.

Stölzel, Friedrich, Karl Hackmann, Friederike Kuithan, Brigitte Mohr, Monika Füssel, Uta Oelschlägel, Christian Thiede, et al. 2012. “Clonal Evolution Including Partial Loss of Human Leukocyte Antigen Genes Favoring Extramedullary Acute Myeloid Leukemia Relapse after Matched Related Allogeneic Hematopoietic Stem Cell Transplantation.” *Transplantation* 93 (7): 744–49. https://doi.org/10.1097/TP.0b013e3182481113.

Stratmann, Svea, Sara A. Yones, Mateusz Garbulowski, Jitong Sun, Aron Skaftason, Markus Mayrhofer, Nina Norgren, et al. 2022. “Transcriptomic Analysis Reveals Proinflammatory Signatures Associated with Acute Myeloid Leukemia Progression.” *Blood Advances* 6 (1): 152–64. https://doi.org/10.1182/bloodadvances.2021004962.

Sullivan, K. M., M. Mori, J. Sanders, M. Siadak, R. P. Witherspoon, C. Anasetti, F. R. Appelbaum, W. Bensinger, R. Bowden, and C. D. Buckner. 1992. “Late Complications of Allogeneic

and Autologous Marrow Transplantation." *Bone Marrow Transplantation* 10 Suppl 1: 127–34.

Tang, Fuchou, Catalin Barbacioru, Yangzhou Wang, Ellen Nordman, Clarence Lee, Nanlan Xu, Xiaohui Wang, et al. 2009. "mRNA-Seq Whole-Transcriptome Analysis of a Single Cell." *Nature Methods* 6 (5): 377–82. https://doi.org/10.1038/nmeth.1315.

The ENCODE Project Consortium. 2012. "An Integrated Encyclopedia of DNA Elements in the Human Genome." *Nature* 489 (7414): 57–74. https://doi.org/10.1038/nature11247.

Timothy Tickle and Itay Tirosh. n.d. "inferCNV of the Trinity CTAT Project." Klarman Cell Observatory, Broad Institute of MIT and Harvard. https://github.com/broadinstitute/inferCNV.

Toffalori, Cristina, Irene Cavattoni, Sara Deola, Sara Mastaglio, Fabio Giglio, Benedetta Mazzi, Andrea Assanelli, et al. 2012. "Genomic Loss of Patient-Specific HLA in Acute Myeloid Leukemia Relapse after Well-Matched Unrelated Donor HSCT." *Blood* 119 (20): 4813–15. https://doi.org/10.1182/blood-2012-02-411686.

Toffalori, Cristina, Laura Zito, Valentina Gambacorta, Michela Riba, Giacomo Oliveira, Gabriele Bucci, Matteo Barcella, et al. 2019a. "Immune Signature Drives Leukemia Escape and Relapse after Hematopoietic Cell Transplantation." *Nature Medicine* 25 (4): 603–11. https://doi.org/10.1038/s41591-019-0400-z.

———. 2019b. "Immune Signature Drives Leukemia Escape and Relapse after Hematopoietic Cell Transplantation." *Nature Medicine* 25 (4): 603–11. https://doi.org/10.1038/s41591-019-0400-z.

———. 2019c. "Immune Signature Drives Leukemia Escape and Relapse after Hematopoietic Cell Transplantation." *Nature Medicine* 25 (4): 603–11. https://doi.org/10.1038/s41591-019-0400-z.

Traag, V. A., L. Waltman, and N. J. van Eck. 2019. "From Louvain to Leiden: Guaranteeing Well-Connected Communities." *Scientific Reports* 9 (1): 5233. https://doi.org/10.1038/s41598-019-41695-z.

Tran, Hoa Thi Nhu, Kok Siong Ang, Marion Chevrier, Xiaomeng Zhang, Nicole Yee Shin Lee, Michelle Goh, and Jinmiao Chen. 2020. "A Benchmark of Batch-Effect Correction Methods for Single-Cell RNA Sequencing Data." *Genome Biology* 21 (1): 12. https://doi.org/10.1186/s13059-019-1850-9.

Tsirigotis, P, M Byrne, C Schmid, F Baron, F Ciceri, J Esteve, N C Gorin, et al. 2016a. "Relapse of AML after Hematopoietic Stem Cell Transplantation: Methods of Monitoring and Preventive Strategies. A Review from the ALWP of the EBMT." *Bone Marrow Transplantation* 51 (11): 1431–38. https://doi.org/10.1038/bmt.2016.167.

Tsirigotis, P., M. Byrne, C. Schmid, F. Baron, F. Ciceri, J. Esteve, N. C. Gorin, et al. 2016b. "Relapse of AML after Hematopoietic Stem Cell Transplantation: Methods of Monitoring and Preventive Strategies. A Review from the ALWP of the EBMT." *Bone Marrow Transplantation* 51 (11): 1431–38. https://doi.org/10.1038/bmt.2016.167.

Tuna, Musaffe, Sakari Knuutila, and Gordon B. Mills. 2009. "Uniparental Disomy in Cancer." *Trends in Molecular Medicine* 15 (3): 120–28. https://doi.org/10.1016/j.molmed.2009.01.005.

Uhl, Franziska M., Sophia Chen, David O'Sullivan, Joy Edwards-Hicks, Gesa Richter, Eileen Haring, Geoffroy Andrieux, et al. 2020. "Metabolic Reprogramming of Donor T Cells Enhances Graft-versus-Leukemia Effects in Mice and Humans." *Science Translational Medicine* 12 (567): eabb8969. https://doi.org/10.1126/scitranslmed.abb8969.

Vadakekolathu, Jayakumar, Mark D. Minden, Tressa Hood, Sarah E. Church, Stephen Reeder, Heidi Altmann, Amy H. Sullivan, et al. 2020. "Immune Landscapes Predict Chemotherapy Resistance and Immunotherapy Response in Acute Myeloid Leukemia."

Science Translational Medicine 12 (546): eaaz0463. https://doi.org/10.1126/scitranslmed.aaz0463.

Vago, Luca. 2019. "Clonal Evolution and Immune Evasion in Posttransplantation Relapses." *Hematology. American Society of Hematology. Education Program* 2019 (1): 610–16. https://doi.org/10.1182/hematology.2019000005.

Vago, Luca, Barbara Forno, Maria Pia Sormani, Roberto Crocchiolo, Elisabetta Zino, Simona Di Terlizzi, Maria Teresa Lupo Stanghellini, et al. 2008. "Temporal, Quantitative, and Functional Characteristics of Single-KIR–Positive Alloreactive Natural Killer Cell Recovery Account for Impaired Graft-versus-Leukemia Activity after Haploidentical Hematopoietic Stem Cell Transplantation." *Blood* 112 (8): 3488–99. https://doi.org/10.1182/blood-2007-07-103325.

Vago, Luca, Serena Kimi Perna, Monica Zanussi, Benedetta Mazzi, Cristina Barlassina, Maria Teresa Lupo Stanghellini, Nicola Flavio Perrelli, et al. 2009a. "Loss of Mismatched HLA in Leukemia after Stem-Cell Transplantation." *New England Journal of Medicine* 361 (5): 478–88. https://doi.org/10.1056/NEJMoa0811036.

———. 2009b. "Loss of Mismatched HLA in Leukemia after Stem-Cell Transplantation." *The New England Journal of Medicine* 361 (5): 478–88. https://doi.org/10.1056/NEJMoa0811036.

Vallet, Nicolas, Sophie Le Grand, Louise Bondeelle, Bénédicte Hoareau, Aurélien Corneau, Delphine Bouteiller, Simon Tournier, et al. 2022. "Azithromycin Promotes Relapse by Disrupting Immune and Metabolic Networks after Allogeneic Stem Cell Transplantation." *Blood* 140 (23): 2500–2513. https://doi.org/10.1182/blood.2022016926.

Vieth, Beate, Swati Parekh, Christoph Ziegenhain, Wolfgang Enard, and Ines Hellmann. 2019. "A Systematic Evaluation of Single Cell RNA-Seq Analysis Pipelines." *Nature Communications* 10 (1): 4667. https://doi.org/10.1038/s41467-019-12266-7.

Villalobos, I. B., Y. Takahashi, Y. Akatsuka, H. Muramatsu, N. Nishio, A. Hama, H. Yagasaki, et al. 2010. "Relapse of Leukemia with Loss of Mismatched HLA Resulting from Uniparental Disomy after Haploidentical Hematopoietic Stem Cell Transplantation." *Blood* 115 (15): 3158–61. https://doi.org/10.1182/blood-2009-11-254284.

Villalobos, Itzel Bustos, Yoshiyuki Takahashi, Yoshiki Akatsuka, Hideki Muramatsu, Nobuhiro Nishio, Asahito Hama, Hiroshi Yagasaki, et al. 2010. "Relapse of Leukemia with Loss of Mismatched HLA Resulting from Uniparental Disomy after Haploidentical Hematopoietic Stem Cell Transplantation." *Blood* 115 (15): 3158–61. https://doi.org/10.1182/blood-2009-11-254284.

Virshup, Isaac, Danila Bredikhin, Lukas Heumos, Giovanni Palla, Gregor Sturm, Adam Gayoso, Ilia Kats, et al. 2023. "The Scverse Project Provides a Computational Ecosystem for Single-Cell Omics Data Analysis." *Nature Biotechnology* 41 (5): 604–6. https://doi.org/10.1038/s41587-023-01733-8.

Wang, Xi, Jinge Li, Ke Dong, Fang Lin, Min Long, Yongri Ouyang, Junxia Wei, et al. 2015. "Tumor Suppressor miR-34a Targets PD-L1 and Functions as a Potential Immunotherapeutic Target in Acute Myeloid Leukemia." *Cellular Signalling* 27 (3): 443–52. https://doi.org/10.1016/j.cellsig.2014.12.003.

Wang, Zi-Hao, Wen-Bei Peng, Pei Zhang, Xiang-Ping Yang, and Qiong Zhou. 2021. "Lactate in the Tumour Microenvironment: From Immune Modulation to Therapy." *EBioMedicine* 73 (November): 103627. https://doi.org/10.1016/j.ebiom.2021.103627.

Waterhouse, Miguel, Dietmar Pfeifer, Milena Pantic, Florian Emmerich, Hartmut Bertz, and Jürgen Finke. 2011. "Genome-Wide Profiling in AML Patients Relapsing after Allogeneic Hematopoietic Cell Transplantation." *Biology of Blood and Marrow Transplantation:*

Journal of the American Society for Blood and Marrow Transplantation 17 (10): 1450-1459.e1. https://doi.org/10.1016/j.bbmt.2011.07.012.

Webster, Jonathan A., Leo Luznik, and Ivana Gojo. 2021. "Treatment of AML Relapse After Allo-HCT." *Frontiers in Oncology* 11 (December): 812207. https://doi.org/10.3389/fonc.2021.812207.

Williams, Patrick, Sreyashi Basu, Guillermo Garcia-Manero, Christopher S. Hourigan, Karolyn A. Oetjen, Jorge E. Cortes, Farhad Ravandi, et al. 2019. "The Distribution of T-cell Subsets and the Expression of Immune Checkpoint Receptors and Ligands in Patients with Newly Diagnosed and Relapsed Acute Myeloid Leukemia." *Cancer* 125 (9): 1470–81. https://doi.org/10.1002/cncr.31896.

Witkowski, Matthew T., Igor Dolgalev, Nikki A. Evensen, Chao Ma, Tiffany Chambers, Kathryn G. Roberts, Sheetal Sreeram, et al. 2020. "Extensive Remodeling of the Immune Microenvironment in B Cell Acute Lymphoblastic Leukemia." *Cancer Cell* 37 (6): 867-882.e12. https://doi.org/10.1016/j.ccell.2020.04.015.

Yakoub-Agha, Ibrahim. 2016. "Transplantations from HLA-Identical Siblings versus 10/10 HLA-Matched Unrelated Donors." *Seminars in Hematology* 53 (2): 74–76. https://doi.org/10.1053/j.seminhematol.2016.01.013.

Yang, Chao, Jason R. Siebert, Robert Burns, Zachary J. Gerbec, Benedetta Bonacci, Amy Rymaszewski, Mary Rau, et al. 2019. "Heterogeneity of Human Bone Marrow and Blood Natural Killer Cells Defined by Single-Cell Transcriptome." *Nature Communications* 10 (1): 3931. https://doi.org/10.1038/s41467-019-11947-7.

Yang, Wei, Yibing Bai, Ying Xiong, Jin Zhang, Shuokai Chen, Xiaojun Zheng, Xiangbo Meng, et al. 2016. "Potentiating the Antitumour Response of CD8+ T Cells by Modulating Cholesterol Metabolism." *Nature* 531 (7596): 651–55. https://doi.org/10.1038/nature17412.

Young, Matthew D, and Sam Behjati. 2020. "SoupX Removes Ambient RNA Contamination from Droplet-Based Single-Cell RNA Sequencing Data." *GigaScience* 9 (12): giaa151. https://doi.org/10.1093/gigascience/giaa151.

Zappia, Luke, Belinda Phipson, and Alicia Oshlack. 2018. "Exploring the Single-Cell RNA-Seq Analysis Landscape with the scRNA-Tools Database." *PLOS Computational Biology* 14 (6): e1006245. https://doi.org/10.1371/journal.pcbi.1006245.

Zappia, Luke, and Fabian J. Theis. 2021. "Over 1000 Tools Reveal Trends in the Single-Cell RNA-Seq Analysis Landscape." *Genome Biology* 22 (1): 301. https://doi.org/10.1186/s13059-021-02519-4.

Zeiser, Robert, and Bruce R. Blazar. 2017. "Pathophysiology of Chronic Graft-versus-Host Disease and Therapeutic Targets." *New England Journal of Medicine* 377 (26): 2565–79. https://doi.org/10.1056/NEJMra1703472.

Zeiser, Robert, and Luca Vago. 2019. "Mechanisms of Immune Escape after Allogeneic Hematopoietic Cell Transplantation." *Blood* 133 (12): 1290–97. https://doi.org/10.1182/blood-2018-10-846824.

Zheng, Grace X. Y., Jessica M. Terry, Phillip Belgrader, Paul Ryvkin, Zachary W. Bent, Ryan Wilson, Solongo B. Ziraldo, et al. 2017. "Massively Parallel Digital Transcriptional Profiling of Single Cells." *Nature Communications* 8 (1): 14049. https://doi.org/10.1038/ncomms14049.

7 Appendix

7.1 Tables

Table 1. Patient Characteristics

Table summarizes clinical data collected for each patient. Data for AML patients was collected at the time of relapse, data for HC was obtained at BM collection, and data for CR patients was retrieved at both +90 (3mo) and +365 (1y) days following allo-HCT.

Characteristic	N = 41[1]
Patient sex	
F	14 (34%)
M	27 (66%)
Donor sex	
F	15 (43%)
M	20 (57%)
Type of allo-HCT	
Haploidentical	25 (71%)
HLA identical	6 (17%)
MUD	4 (11%)
Allele mismatches (12 alleles)	
0	6 (17%)
1	1 (2.9%)
2	2 (5.7%)
3	2 (5.7%)

Table 1. Patient Characteristics

Table summarizes clinical data collected for each patient. Data for AML patients was collected at the time of relapse, data for HC was obtained at BM collection, and data for CR patients was retrieved at both +90 (3mo) and +365 (1y) days following allo-HCT.

Characteristic	N = 41[1]
4	5 (14%)
5	4 (11%)
6	15 (43%)
aGvHD at sampling	6 (17%)
cGvHD at sampling	6 (17%)
IST at sampling	18 (51%)
Altered cytogenetic	13 (72%)
Age at sampling	54 (46, 63)
Time from allo-HCT to sampling	198 (91, 612)

[1] *Median (IQR) or Frequency (%)*

Table 2. Cell Ranger Outputs

	Intronic Reads Retention		
Variable	No, N = 51[1]	Yes, N = 51[1]	p-value[2]
Estimated Number of Cells	7,442 (437-20,364)	7,648 (438-25,480)	0.83
Mean Reads per Cell	43,874 (16,673-298,978)	42,630 (14,893-279,683)	0.87
Median Genes per Cell	1,441 (418-3,226)	1,667 (480-4,423)	0.007
Number of Reads	407,075,690 (63,704,583-648,990,308)	407,075,690 (63,704,583-648,990,308)	>0.99
Valid Barcodes	91.7 (85.6-97.9)	91.7 (85.6-97.9)	>0.99
Sequencing Saturation	67 (41-89)	67 (41-89)	0.95
Q30 Bases in Barcode	96.00 (94.60-98.00)	96.00 (94.60-98.00)	>0.99
Q30 Bases in RNA Read	92.80 (84.70-95.60)	92.80 (84.70-95.60)	>0.99
Q30 Bases in UMI	95.80 (94.20-97.90)	95.80 (94.20-97.90)	>0.99
Reads Mapped to Genome	92.50 (81.80-97.40)	92.50 (81.80-97.40)	>0.99
Reads Mapped Confidently to Genome	83 (48-94)	83 (48-94)	>0.99
Reads Mapped Confidently to Intergenic Regions	4.50 (2.20-7.60)	4.50 (2.20-7.60)	>0.99
Reads Mapped Confidently to Intronic Regions	10 (4-35)	10 (4-35)	>0.99
Reads Mapped Confidently to Exonic Regions	65 (33-81)	65 (33-81)	>0.99
Reads Mapped Confidently to Transcriptome	60 (30-74)	72 (40-82)	<0.001

Table 2. Cell Ranger Outputs

	Intronic Reads Retention		
Variable	No, N = 51[1]	Yes, N = 51[1]	p-value[2]
Reads Mapped Antisense to Gene	3.30 (0.70-5.80)	6.40 (3.70-10.10)	<0.001
Fraction Reads in Cells	88 (42-97)	87 (41-97)	0.90
Total Genes Detected	22,946 (18,132-25,803)	26,759 (22,224-29,355)	<0.001
Median UMI Counts per Cell	4,066 (1,286-13,083)	4,424 (1,749-16,409)	0.13

[1] *Median (Range)*

[2] *Wilcoxon rank sum test*

Table 3. Cytogenetic alterations in our AML patient cohort.

Patient code	Cytogenetics at relapse
PZ170168	46,XY [19] / 46XX [1]
PZ14000041	46,XX [20] / 46,XY [22]
PZ160065	45,XY, del(3)(q?), der(4)t(?1;4)(p?;p?), -11, -12, add(21)(q?), +mar1 [3] / 46,XY, idem, +mar2, +mar3 [10]
PZ170022	46, XY, add(15)(P10) [3] / 46, XY, i(17)(Q10) [9] / 46, XY [8]
PZ12000122	45, XY, -7 [13]
PZ15000085	46, XY, del(1)(q?), -2, add(4)(q?35),- 5, -7, -12, -14, -17, +18, +5mar [7] / 46, XX
PZ190333	46, XY, del(9)(P?13), del(11)(p?11.2), add(20)(q?13.3) [12]
PZ170161	47, XYY [16]
PZ190045	45, XY, -7 [20]
PZ160198	45,XY,-7 [11] / 46, XY [9]
PZ1000236	46,XY[22],40-43,XY[14],80-82,XY[2]
PZ11004972	46XX,[20] nuc ish (D13S319_D13S25,D12S1825) x2[278]
PZ200216	45,XY,-5,add(21)(q?22)[6]/46,XY,-5,add(21)(q?22),+mar[2]//46,XX[34]

Table 4. List of mAbs used in this study

mAb	Clone	Producer	Catalogue
Human Fc Block	Fc1	BD	564219
HuCD45 PerCP-Cy5.5	2S1	BD	340953
CD34 APC	8G12	BD	345804
CD117 PC7	104D2D1	Beckman Coulter	B49221
CD3 FITC	SK7	Biolegend	344804
CD235a FITC	GA-R2	BD	559943
CD19 FITC	HIB19	Biolegend	302206
Annexin V PB	n.a.	Biolegend	640918

7.2 Custom functions

The following function allows data scaling with cell cycle difference regression.

```
calculate_variance <- function(seu, nfeatures = 2000,
log_file = NULL){
  # calculate variance of genes in a seurat object

  assay = DefaultAssay(seu)

  # identify features that are outliers on a 'mean
variability plot'
  seu = FindVariableFeatures(seu,
                             assay = assay,
                             selection.method = "vst",
                             nfeatures = nfeatures,
                             verbose = TRUE)

  # calculate cell cycle score (potential source of
variation that we might want to regress later)
  cc.genes <- cc.genes.updated.2019
  s.genes <- cc.genes.updated.2019$s.genes
  g2m.genes <- cc.genes.updated.2019$g2m.genes
  seu <- CellCycleScoring(object = seu, s.features =
s.genes, g2m.features = g2m.genes, set.ident = TRUE)
  seu@meta.data$CC.Difference <- seu@meta.data$S.Score -
seu@meta.data$G2M.Score

  # regress out unwanted sources of variation
  # regressing uninteresting sources of variation can
improve dimensionality reduction and clustering
  # could include technical noise, batch effects,
biological sources of variation (cell cycle stage)
  # scaled z-scored residuals of these models are stored in
scale.data slot
  # used for dimensionality reduction and clustering
  # scale data in the assay
  seu = ScaleData(seu,
                  assay = assay,
                  vars.to.regress = c("CC.Difference",
"percent.mt", "nCount_RNA"),
                  verbose = TRUE)
  return(seu)
}
```

The following function was used to calculate gene set scores in cell annotation.

```
geneset_score_calc.default = function(module_tbl,
counts_raw, min_cpm = 0, limit_pct = 1) {
  # perform the cell type enrichment calculation based on
rescaled values
  module_list <- module_tbl %>%
    with(split(.$gene, celltype))

  if (!is.matrix(counts_raw)) { stop("expression matrix is
not a matrix") }
  if (max(counts_raw) < 100) { stop("expression values
appear to be log-scaled") }

  # filter matrix for expressed genes only
  # expression level equivalent to 1 CPM (1 for 1m, 0.01
for 10k)
  exp_cpm1 = (1 / 1000000) * median(colSums(counts_raw))
  # expression level equivalent to the requested CPM
  min_exp = exp_cpm1 * min_cpm
  # filtered expression matrix
  counts_raw = counts_raw[matrixStats::rowMaxs(counts_raw)
> min_exp, ]

  # rescale matrix for expressed genes only
  if (limit_pct > 1) { stop("percentile should be expressed
as a fraction") }
  if (!is(counts_raw, "matrix")) { stop("expression matrix
is not a matrix") }
  if (max(counts_raw) < 100) { stop("expression values
appear to be log-scaled") }

  rescale_vector = function(x, limit_pct = 1) {
    x / quantile(x, limit_pct)
  }
  counts_raw_subs = apply(subset(counts_raw,
rownames(counts_raw) %in% unlist(module_list)), MARGIN = 1,
FUN = rescale_vector, limit_pct = limit_pct)
  counts_raw_subs = t(counts_raw_subs)
  counts_raw_subs[counts_raw_subs > 1] = 1


  # check if enough genes pass filter
  if (min(lengths(module_list)) < 3) { stop("too few genes
per celltype") }

  # calculate average z-score per celltype
  celltype_scores_tbl = tibble()
  for (ct in names(module_list)) {
    celltype_scores_tbl =
```

```
      bind_rows(
        celltype_scores_tbl,
        tibble(
          cell = colnames(counts_raw_subs),
          celltype = ct,
          score = colMeans(subset(counts_raw_subs,
rownames(counts_raw_subs) %in% module_list[[ct]]))
        )
      )
    ct_scores = colnames(counts_raw_subs)
  }

  celltype_scores_tbl <- celltype_scores_tbl %>%
    spread(celltype, score) %>%
    rename_at(vars(-contains("cell")), list(~paste0(.,
".score")))

  return(celltype_scores_tbl)
}
```